



University of
Zurich^{UZH}

Noble liquid detectors, part two

SOUP2022: the second INFN school on underground physics
LNGS, June 22, 2022

Laura Baudis
University of Zurich



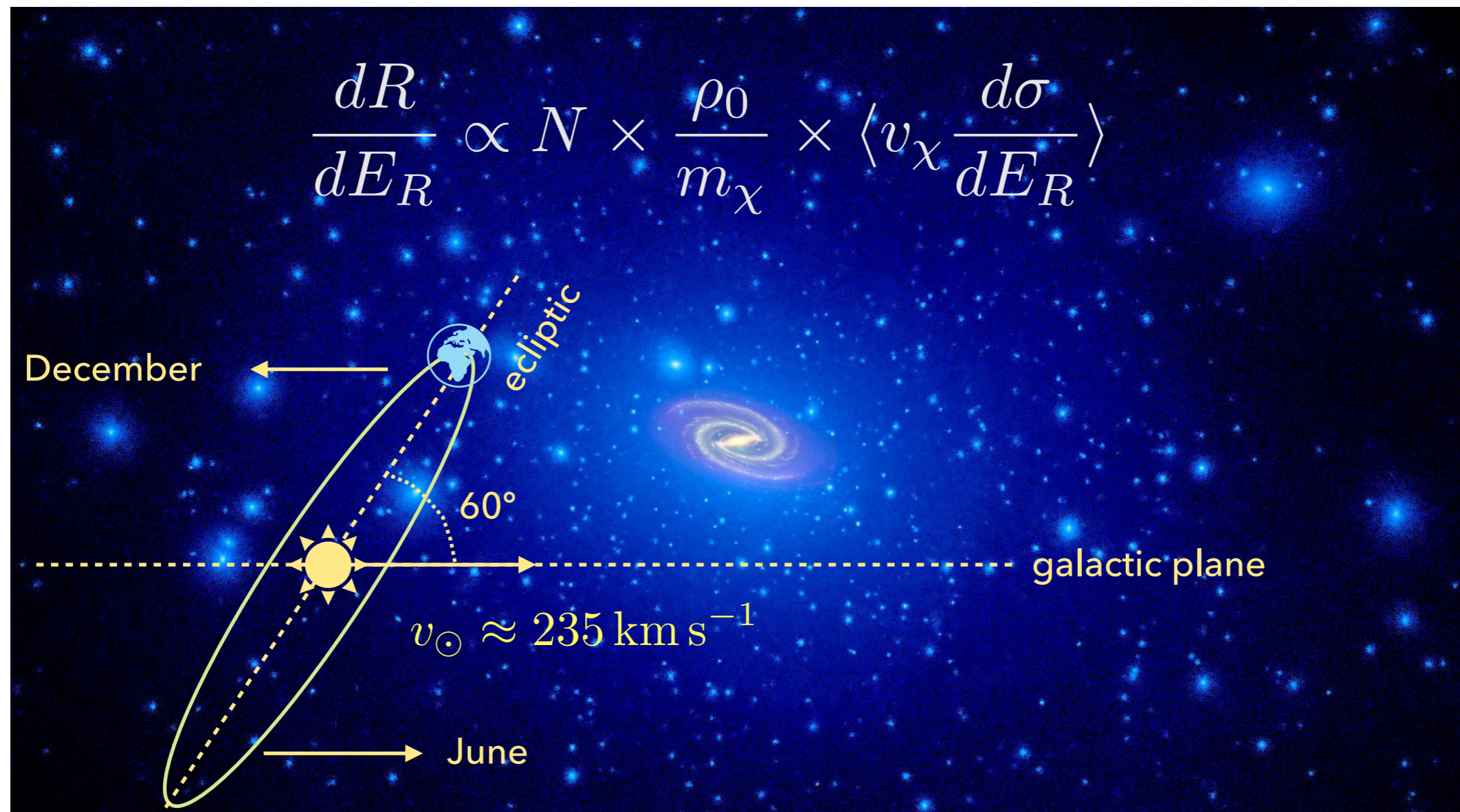
Content, second part

- Applications to direct dark matter detection and experiments
 - Brief review of direct detection principles
 - Single-phase: DEAP (LAr), XMASS (LXe)
 - Two-phase: DarkSide (LAr), ARGO; XENON, LZ, PandaX, DARWIN (all LXe)
- Applications to neutrino physics and experiments
 - Brief motivation and open questions in neutrino physics
 - EXO-200, nEXO (LXe)
 - DUNE (LAr)
- Summary

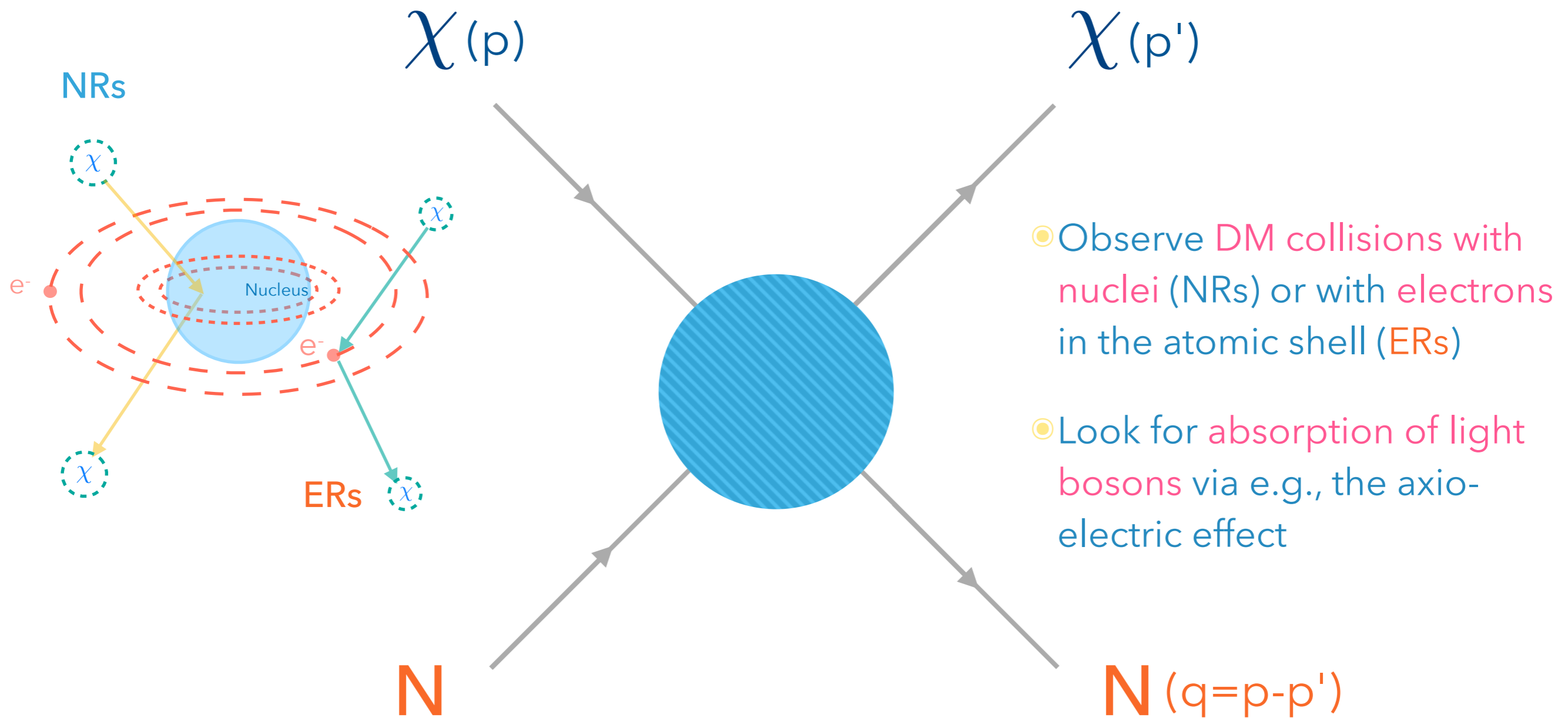
Direct detection principles

Direct dark matter detection

- Look for scatter of galactic particles in underground detectors

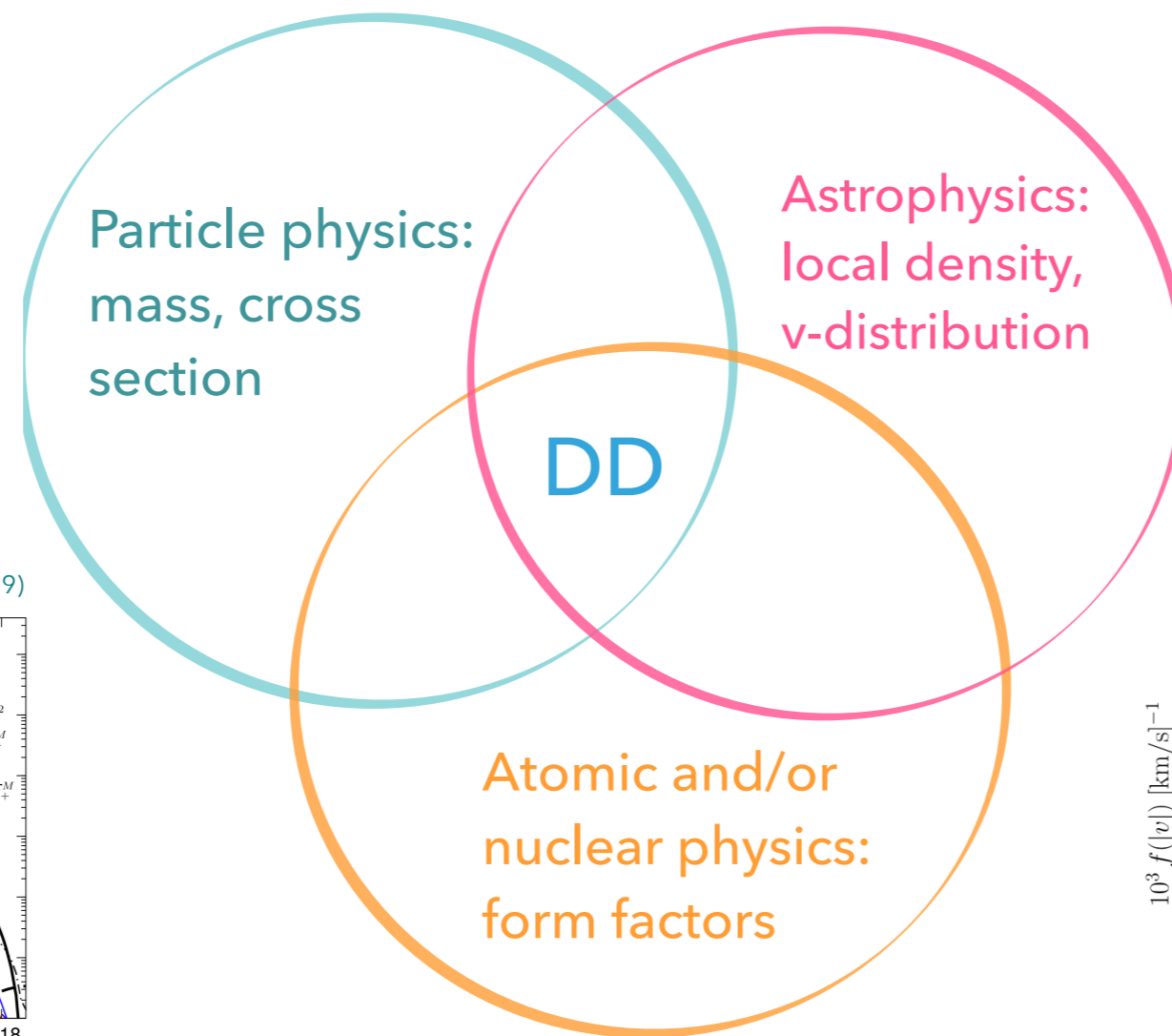


Direct dark matter detection

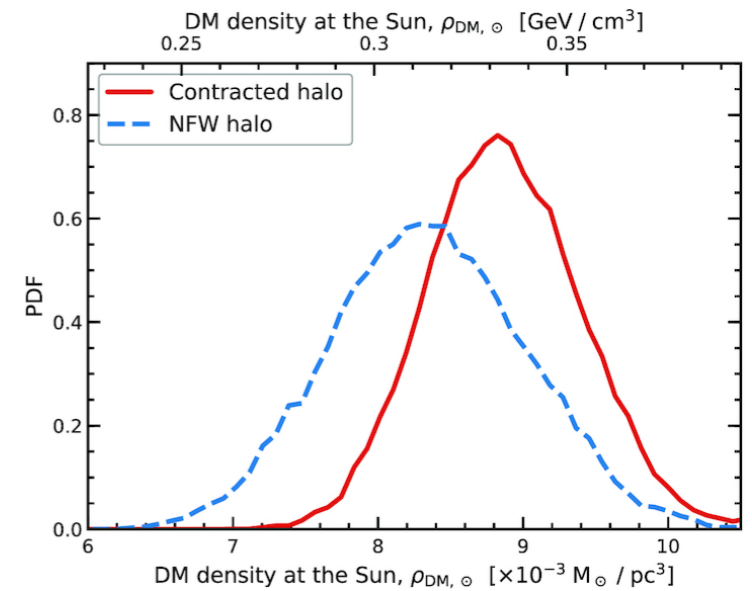


Direct dark matter detection

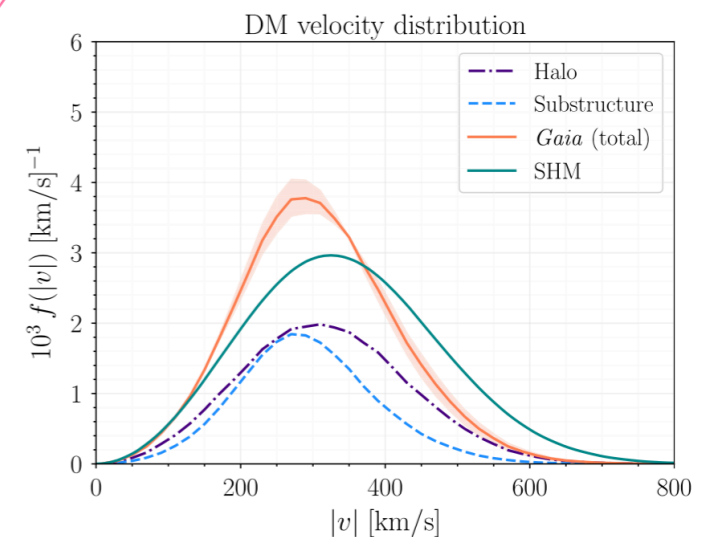
- Main physical observable: a differential recoil spectrum
 - ◉ its modelling relies on several phenomenological inputs



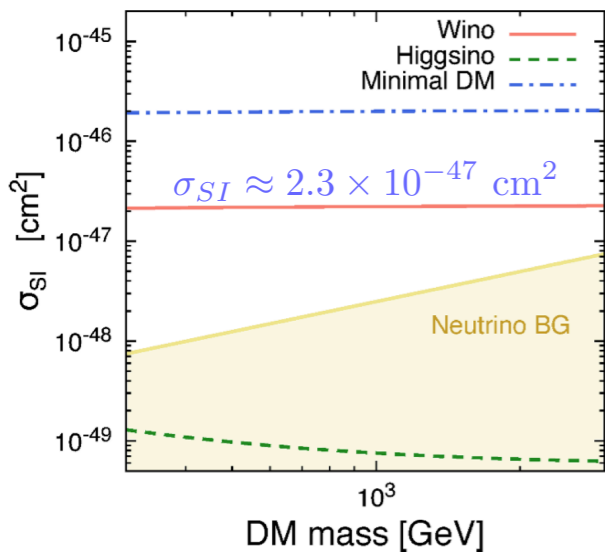
M. Cautun et al, MNRAS 2020



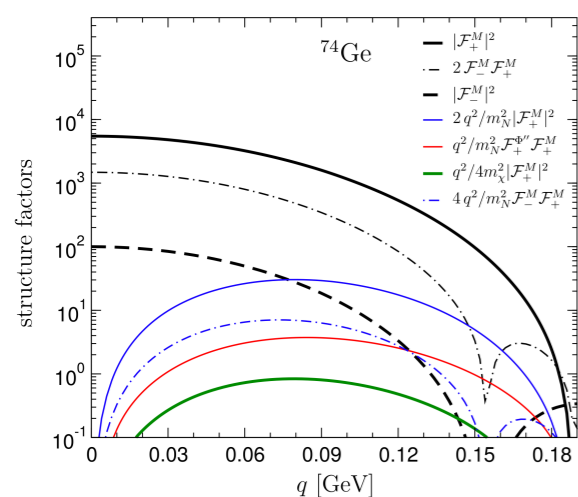
Buch et al, PRD101, 2020



Hisano et al., JHEP 06 (2015)



Hoferichter et al., PRD 99 (2019)



Kinematics: dark matter particle mass

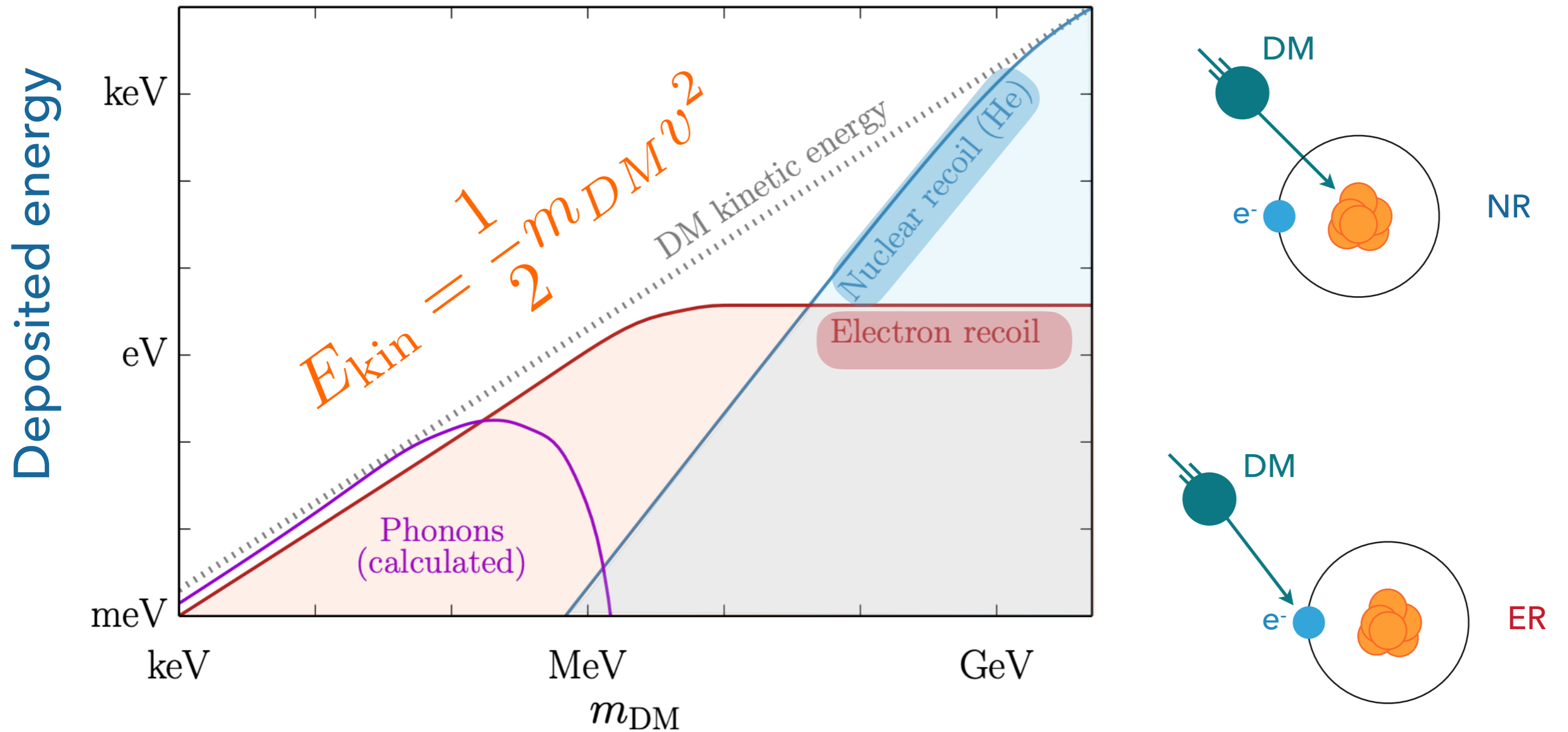
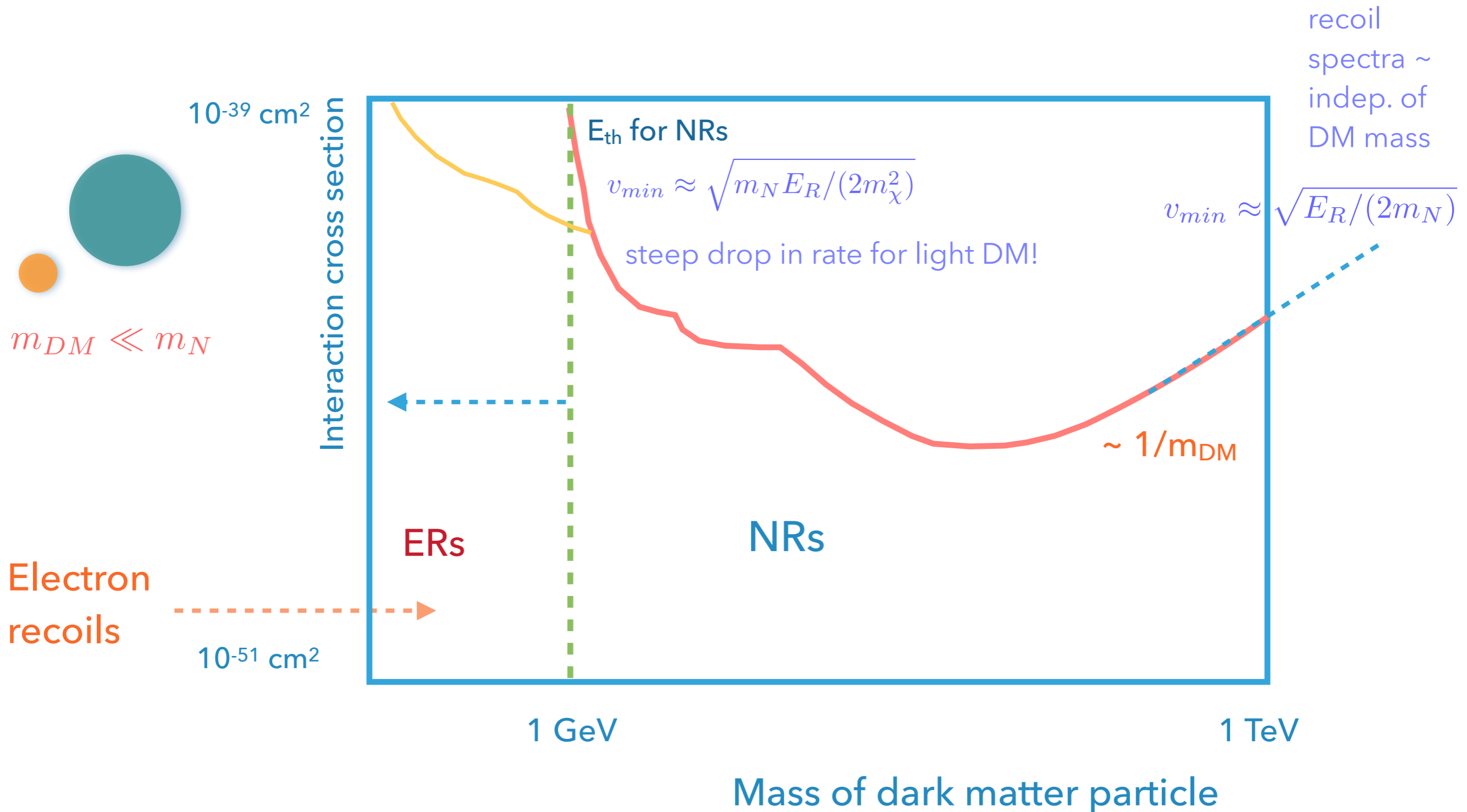


Figure: Tongyan Lin, TASI lectures on DM models and direct detection, arXiv:1904.07915

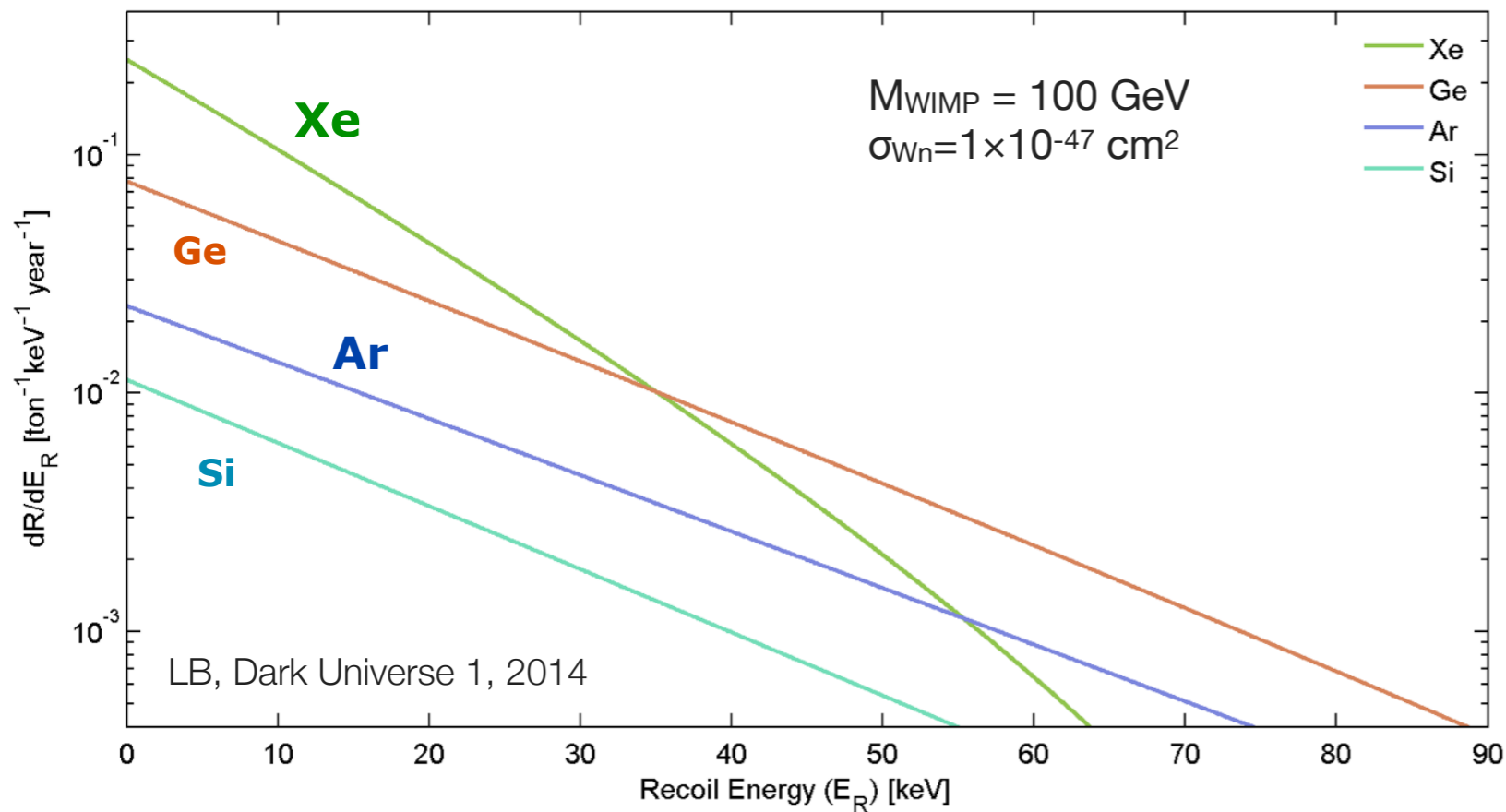
Dark matter particle mass

Interaction cross section versus mass



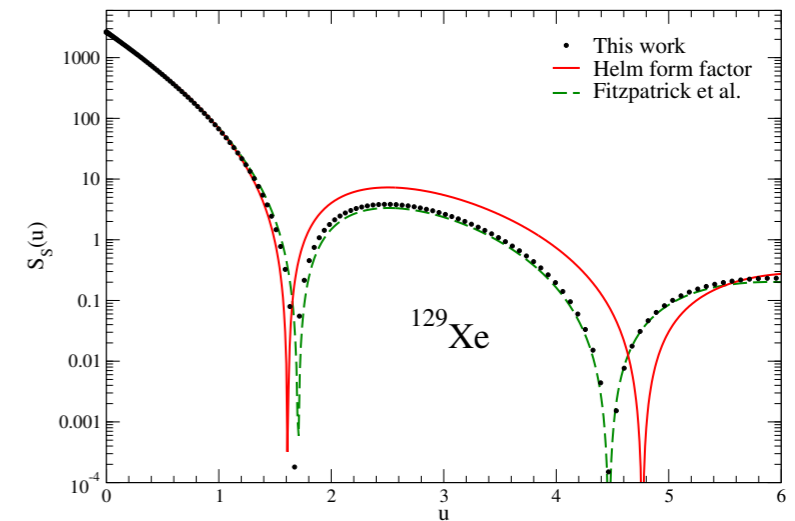
Interaction rates: DM-nucleus scattering

$$R \sim 0.13 \frac{\text{events}}{\text{kg year}} \left[\frac{A}{100} \times \frac{\sigma_{WN}}{10^{-38} \text{ cm}^2} \times \frac{\langle v \rangle}{220 \text{ km s}^{-1}} \times \frac{\rho_0}{0.3 \text{ GeV cm}^{-3}} \right]$$

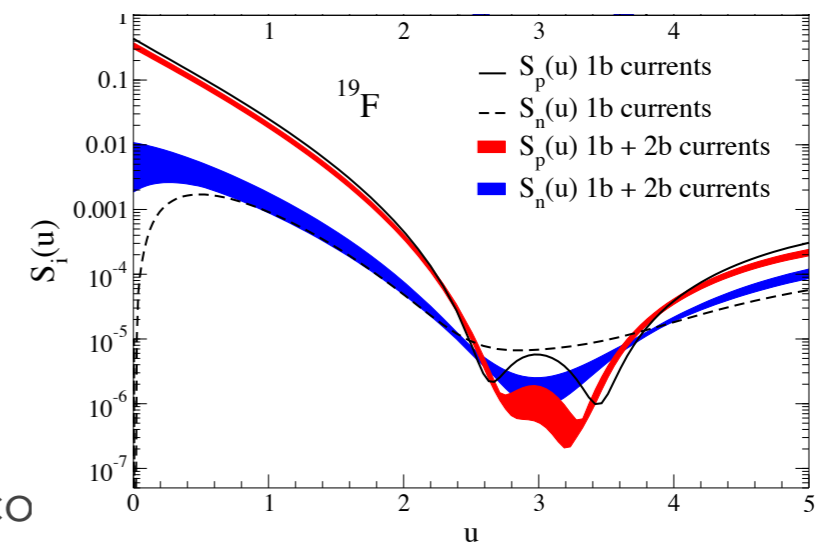


Spin-independent (SI) nuclear reco

L. Vietze, W. Haxton et al., Phys.Rev. D91 (2015)



SI



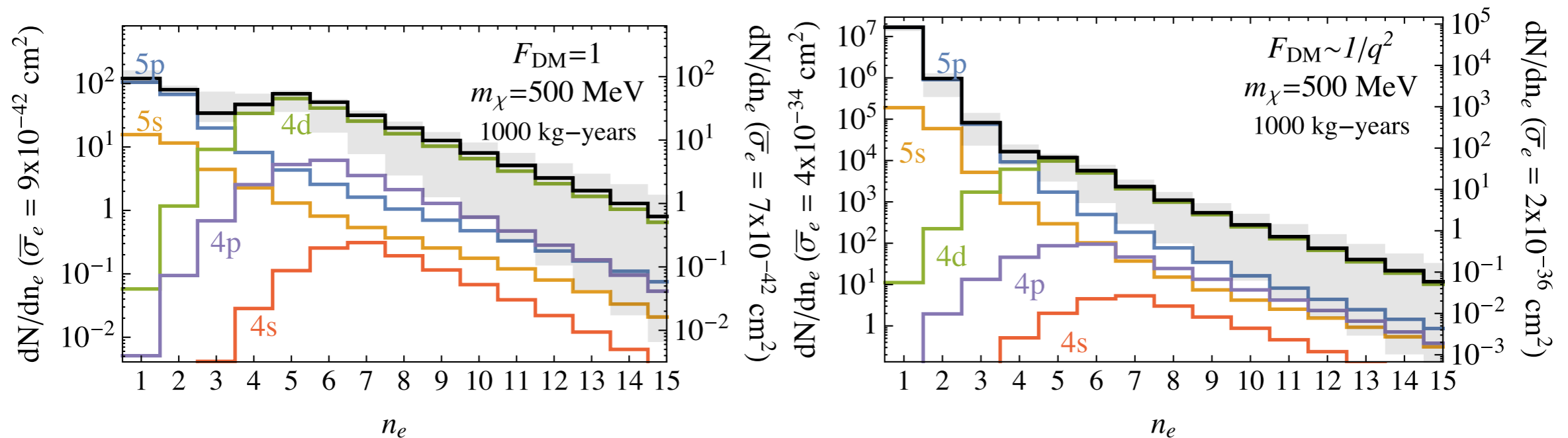
SD

P. Klos et al., PRD 88 (2013)

Interaction rates: DM-electron scattering

$$\frac{dR_{ion}}{d \ln E_R} = \frac{6.2}{A} \left(\frac{\rho_0}{0.4 \text{ GeV cm}^{-3}} \right) \left(\frac{\sigma_e}{10^{-40} \text{ cm}^2} \right) \left(\frac{10 \text{ MeV}}{m_{\text{DM}}} \right) \times \frac{d\langle \sigma_{ion} v \rangle / d \ln E_R}{10^{-3} \sigma_e} \frac{\text{events}}{\text{kg d}}$$

Example: expected number of events for a xenon detector with 1 tonne year exposure



$$F_{DM} = 1$$

Heavy dark photon A' mediator

$$F_{DM} = \alpha^2 \frac{m_e^2}{q^2}$$

Ultra-light dark photon A' mediator

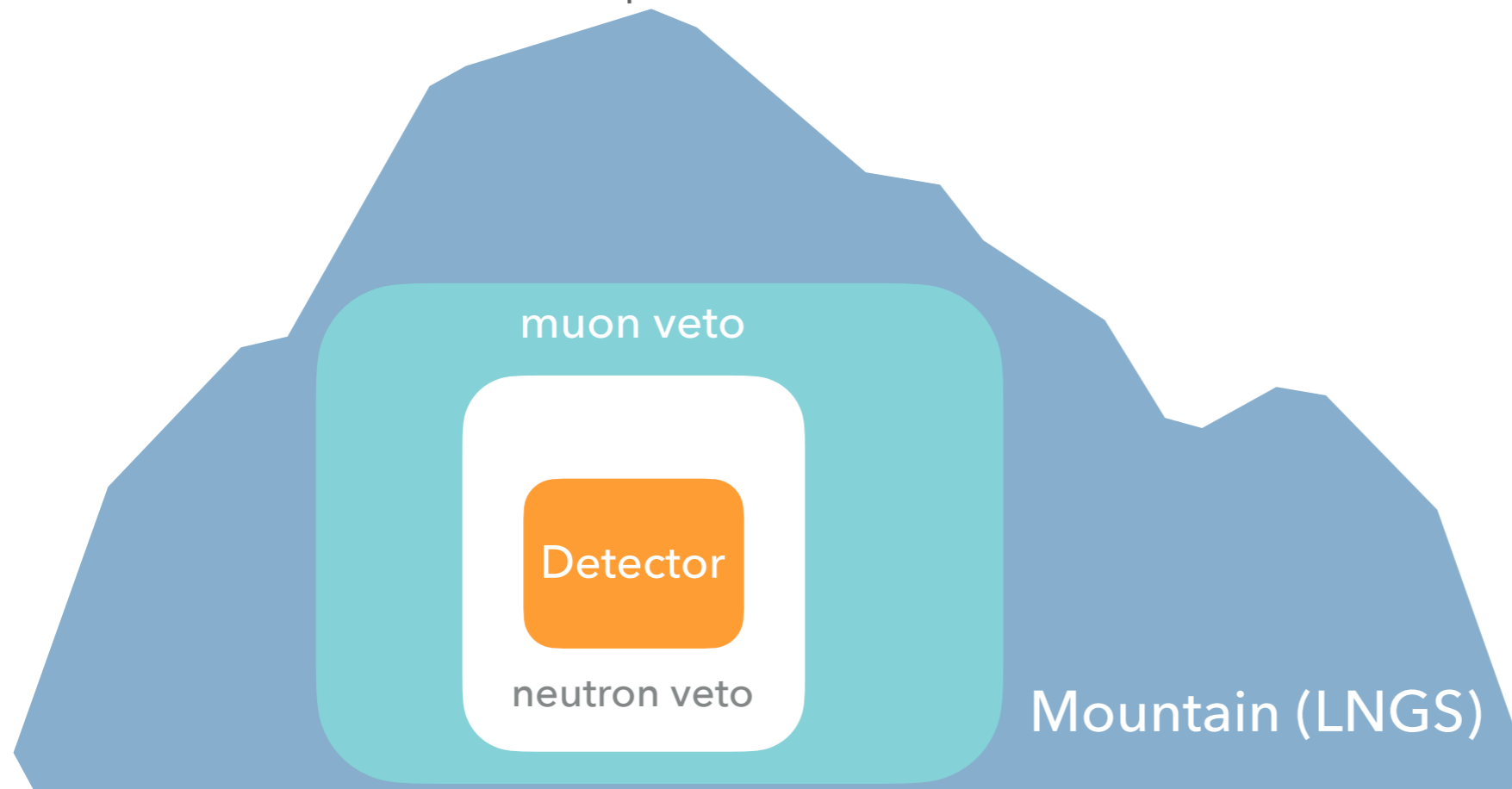
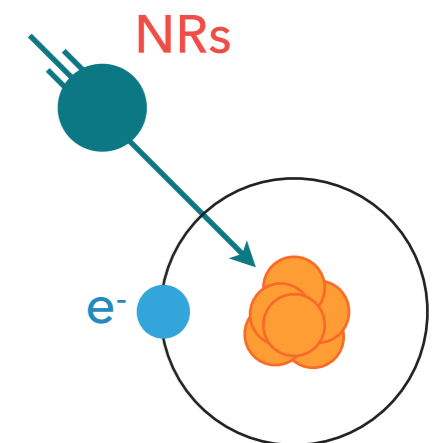
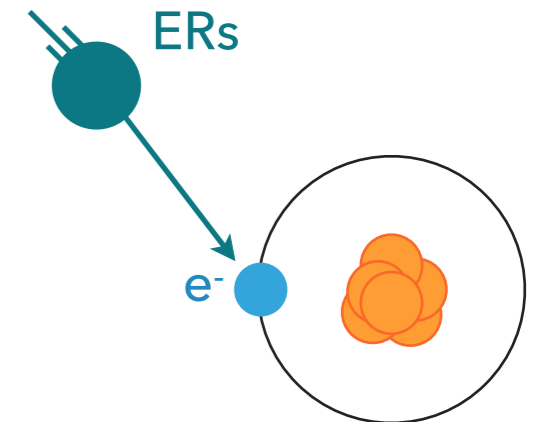
Main experimental challenges

- To observe a signal which is:
 - very small → low recoil energies: \sim eV to keV (perhaps even meV)
 - very rare → < 1 event/(kg y) at low masses and < 1 event/(t y) at high masses
 - buried in backgrounds with $> 10^6$ x higher rates → deep underground & low-radioactivity materials



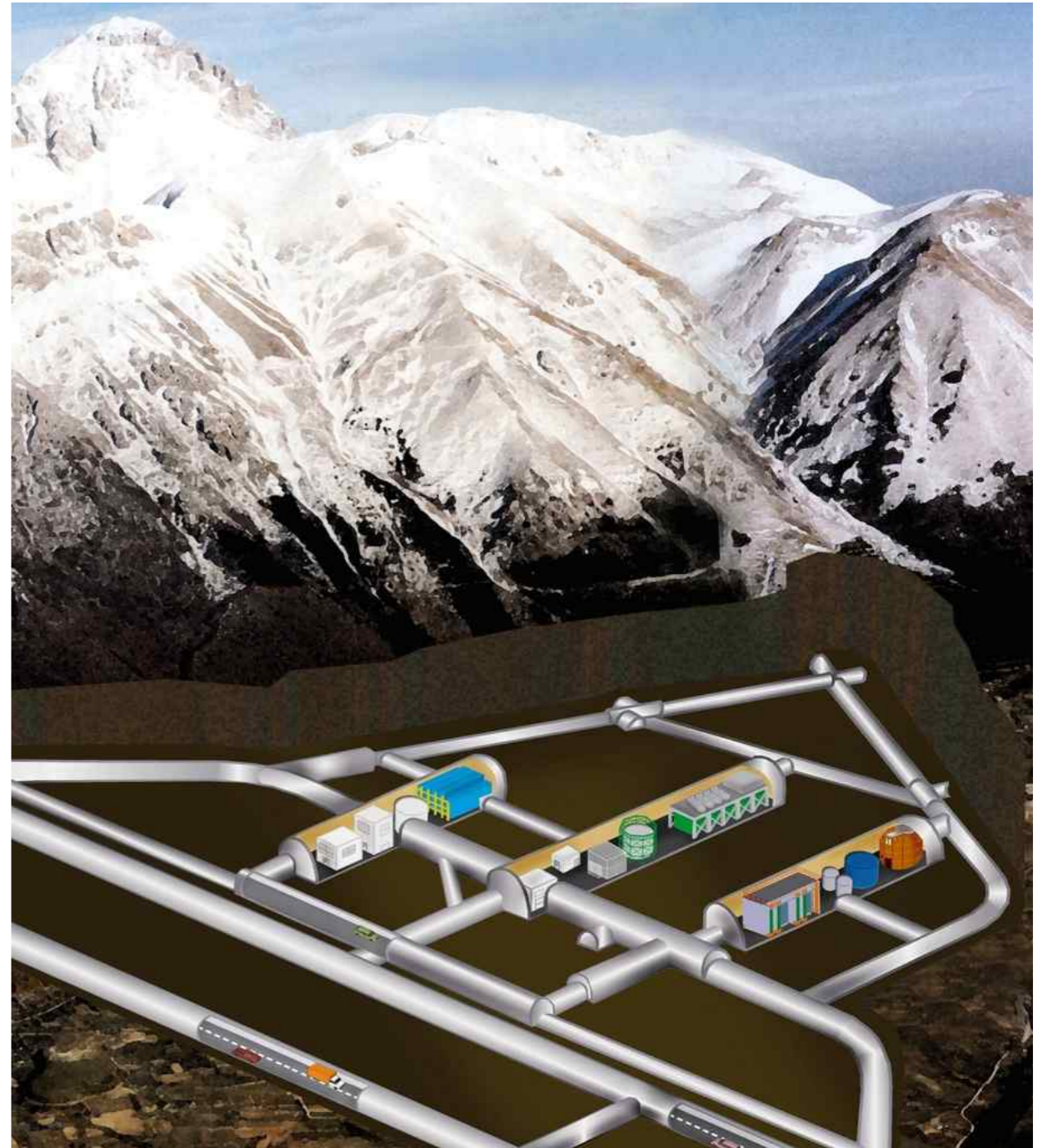
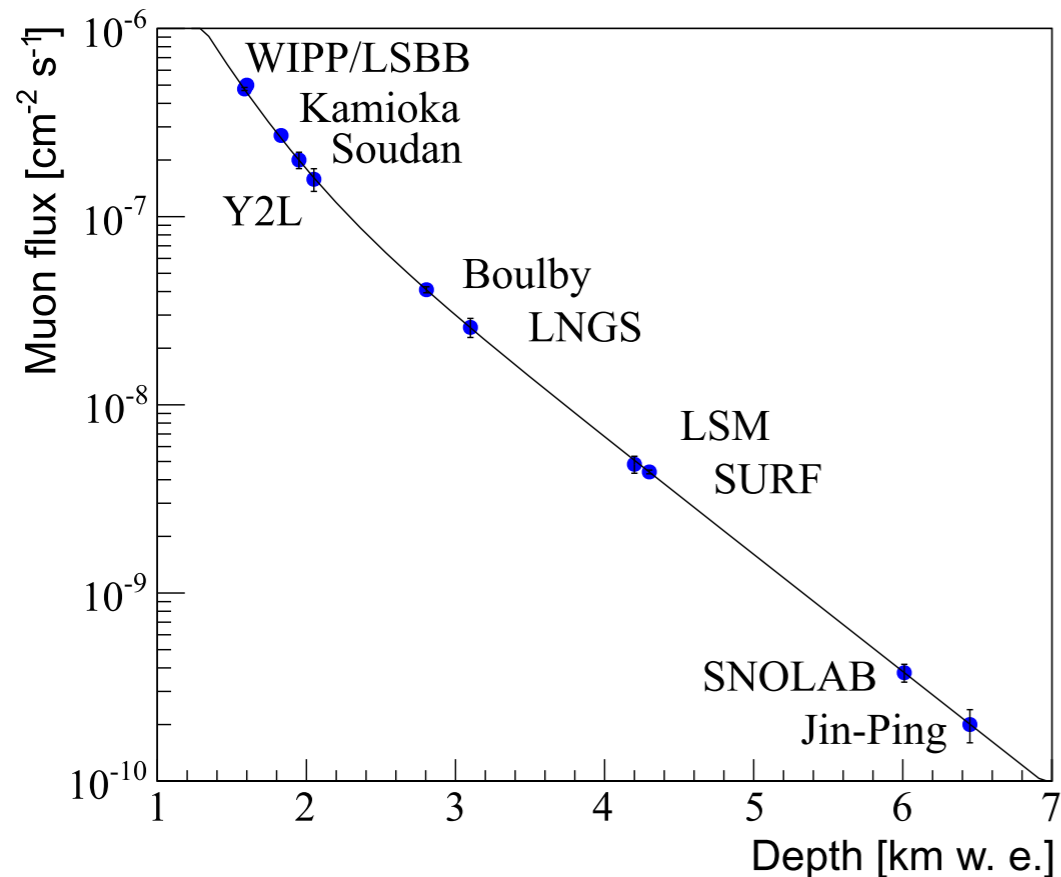
Backgrounds: overview

- Muon-induced neutrons: **NRs**
- Cosmogenic activation of materials/targets (^3H , ^{32}Si , ^{60}Co , ^{39}Ar): **ERs**
- Radioactivity of detector materials (n , γ , α , e^-): **NRs** and **ERs**
- Target intrinsic isotopes (^{85}Kr , ^{222}Rn , ^{136}Xe , ^{39}Ar , ^{124}Xe , ^{42}Ar , etc): **ERs**
- Neutrinos (solar, atmospheric, DSNB): **NRs** and **ERs**



Backgrounds and shields

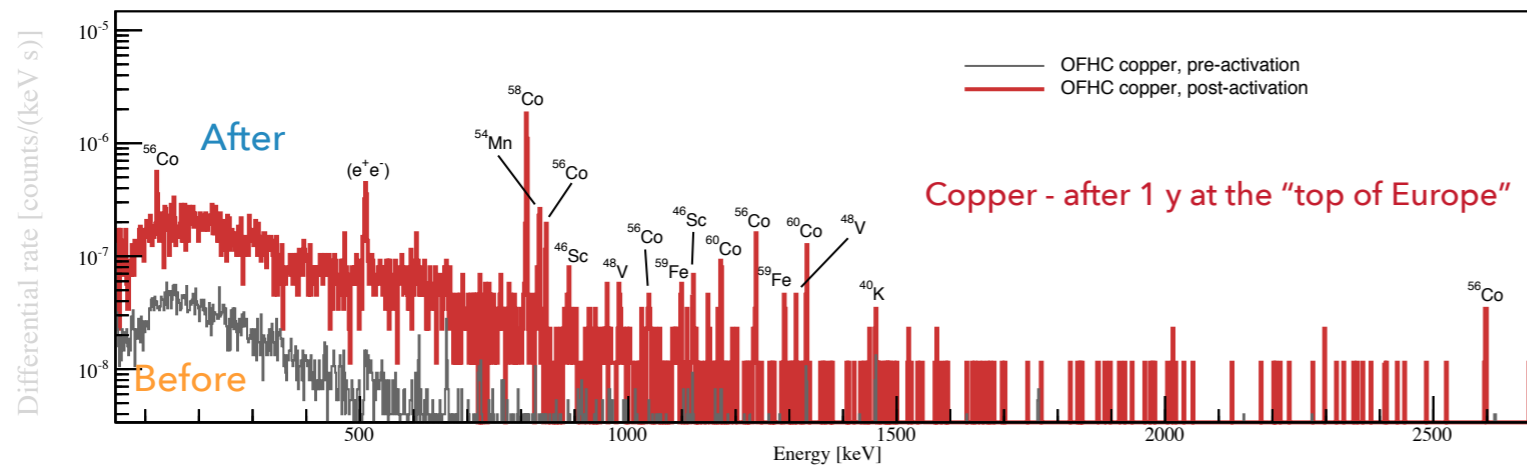
- Go deep underground
 - However, can't shield neutrinos
 - On the bright side: possible signals (pp, ${}^7\text{Be}$, ${}^8\text{B}$, SN,...)



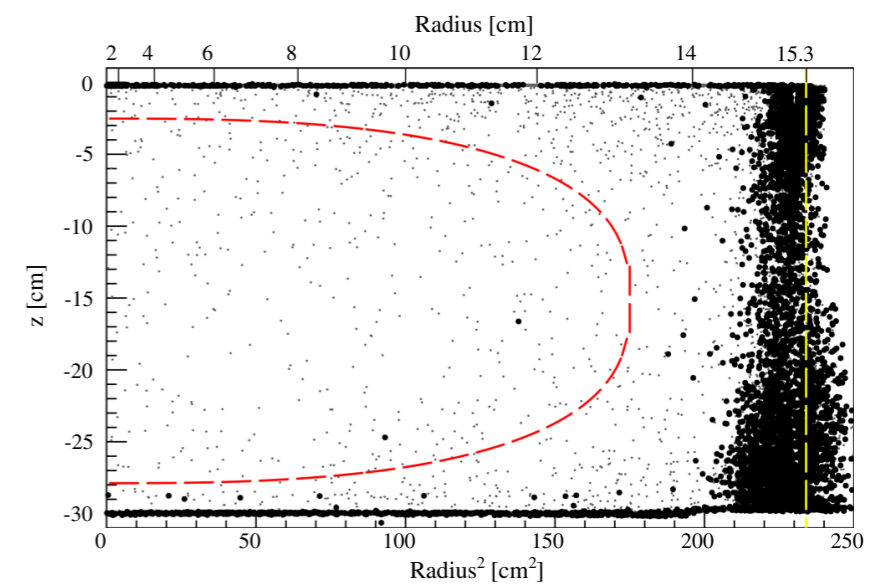
Further background reduction

● Avoid cosmic activation

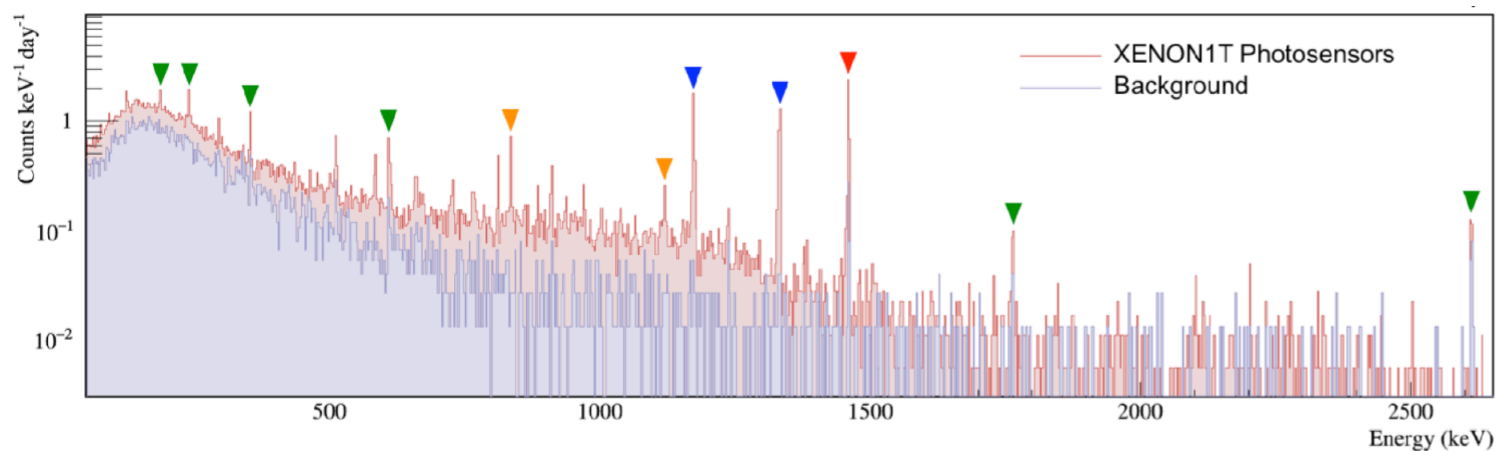
LB et al., Eur. Phys. J. C75 2015



● Fiducialise



● Select low-radioactivity materials



XENON collaboration, EPJ-C 75 (2015) 11

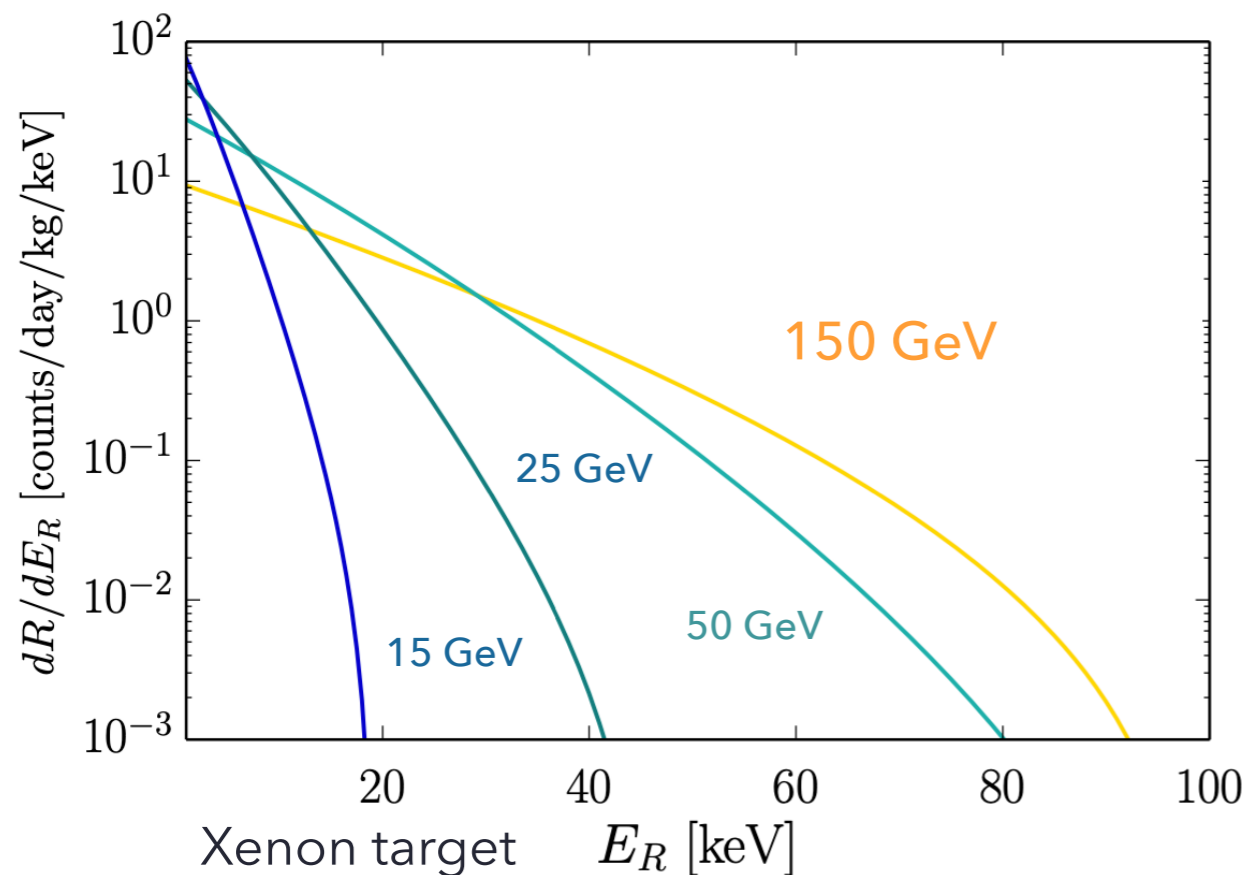
● Use active shields



Dark matter signatures

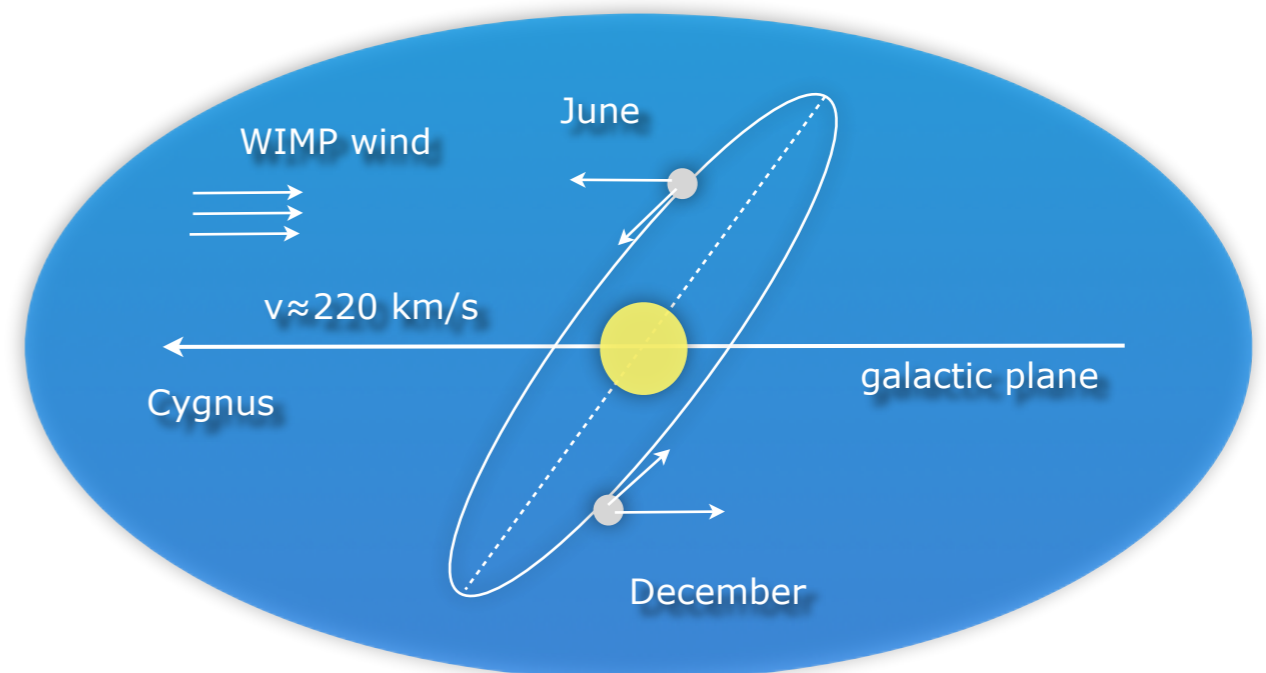
Rate % shape of recoil spectrum depend on:

- DM particle mass
- Target material (hence different target materials are required to constrain the DM mass in case of a positive signal)

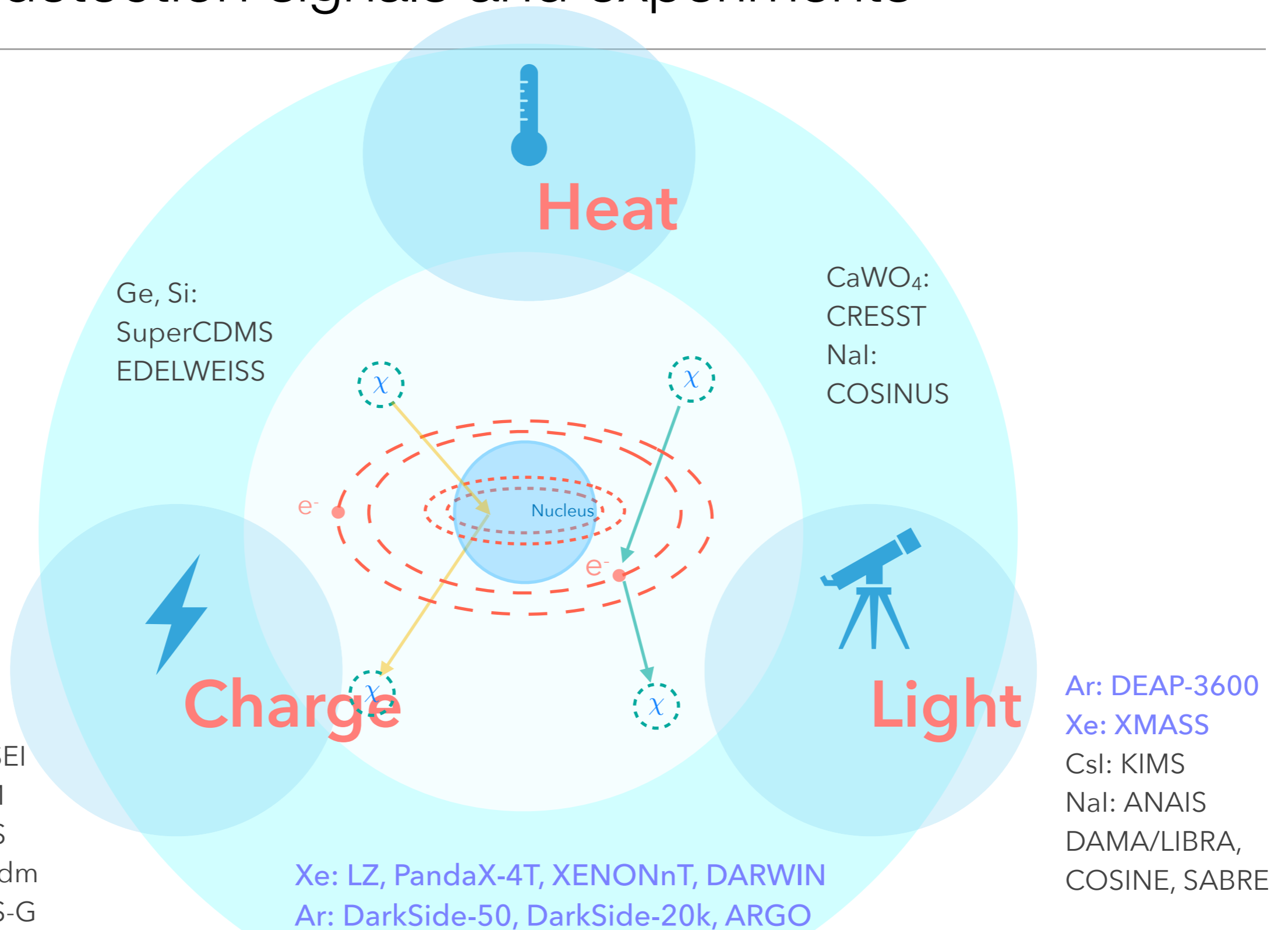


Motion of Earth causes:

- Annual event rate modulation: June - December asymmetry $\sim 2-10\%$
- Sidereal directional modulation: asymmetry $\sim 20-100\%$ in forward-backward event rate

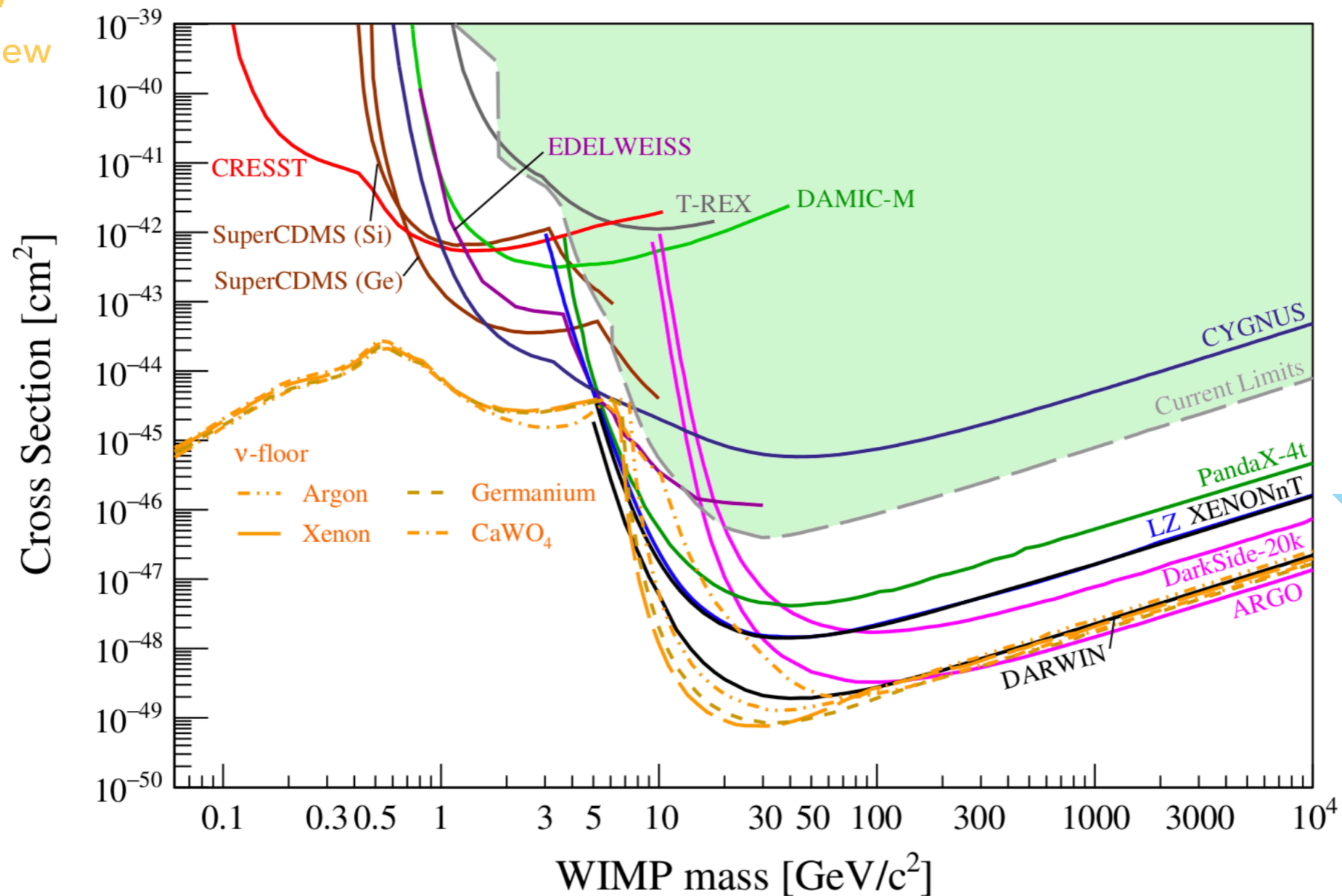


Direct detection signals and experiments

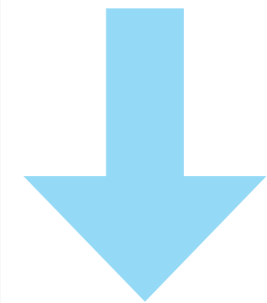


The direct detection landscape

Bolometers,
CCDs (plus new
technologies)



Noble
liquids



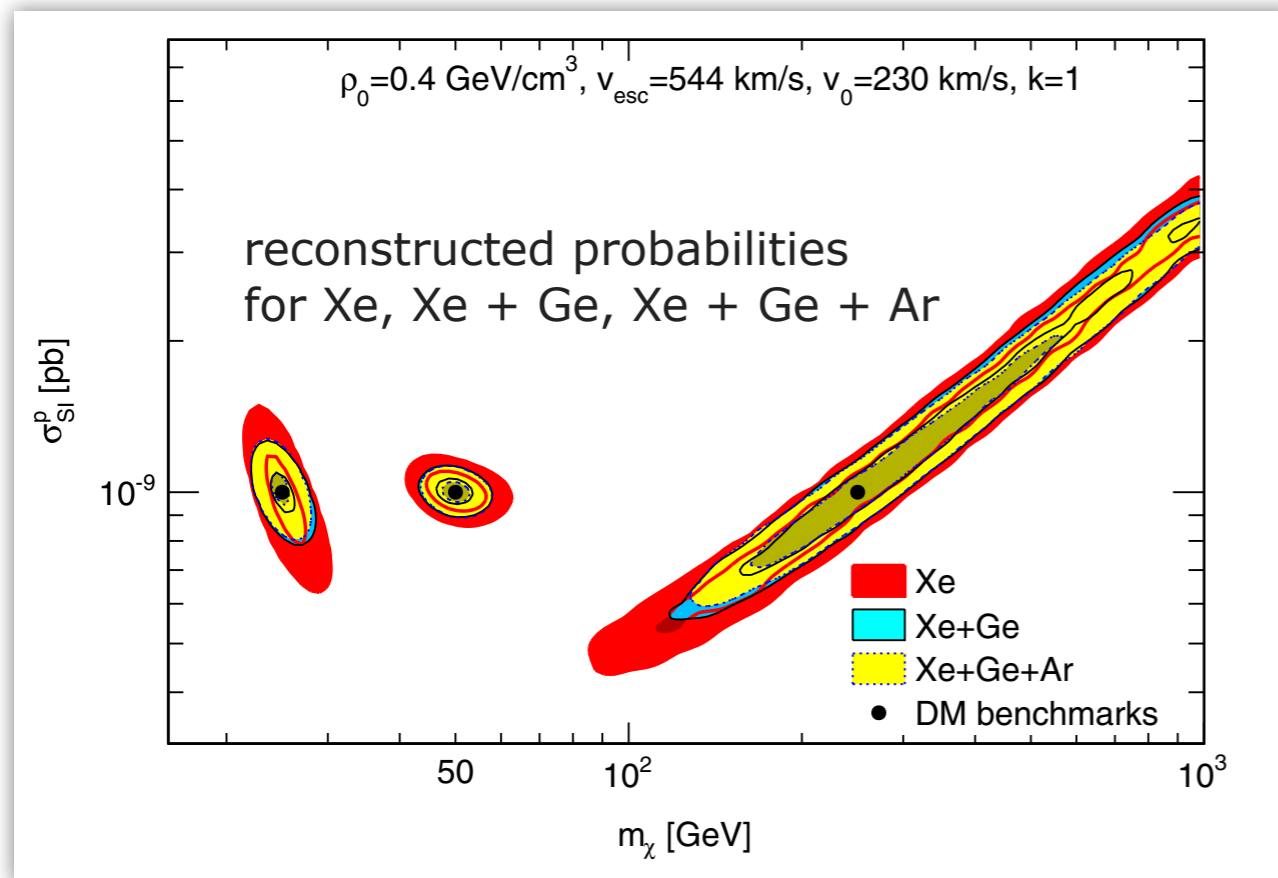
Scattering off nuclei

Complementarity: argon and xenon detectors

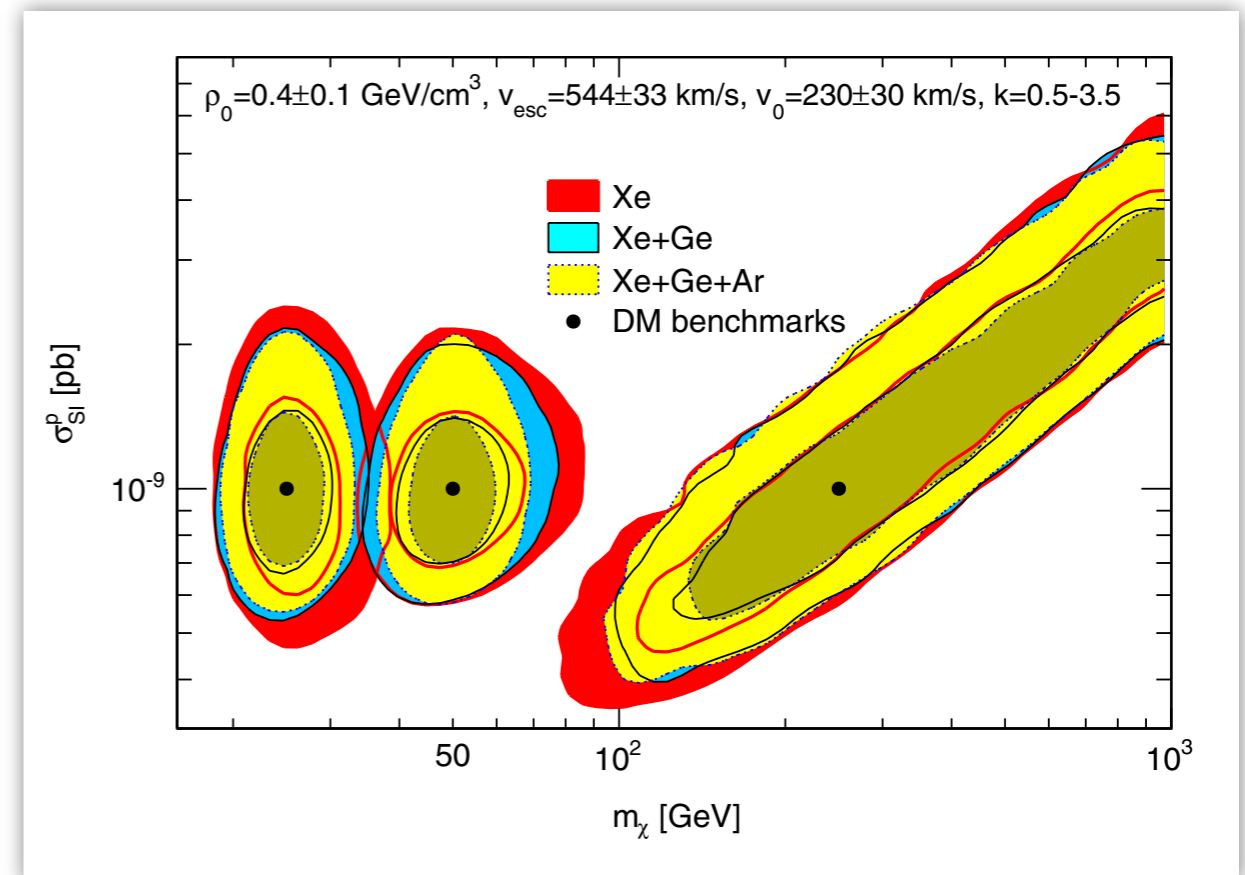
- Different targets are sensitive to different directions in the m_χ - σ_{SI} plane

Xe: 2.0 t x yr, $E_{th} = 10$ keV
 Ge: 2.2 t x yr, $E_{th} = 10$ keV
 Ar: 6.4 t x yr, $E_{th} = 30$ keV

fixed galactic model



including galactic uncertainties



Pato, Baudis, Bertone, Ruiz de Austri, Strigari, Trotta: Phys. Rev. D 83, 2011

Single-phase LAr and LXe detectors

Single-phase detectors

- Challenge: ultra-low absolute backgrounds
- LAr: pulse shape discrimination, factor $\sim 10^9$ for gammas/betas



DEAP at SNOLab:

3300 kg LAr (1t fiducial)

255 PMTs

data taking since fall 2016

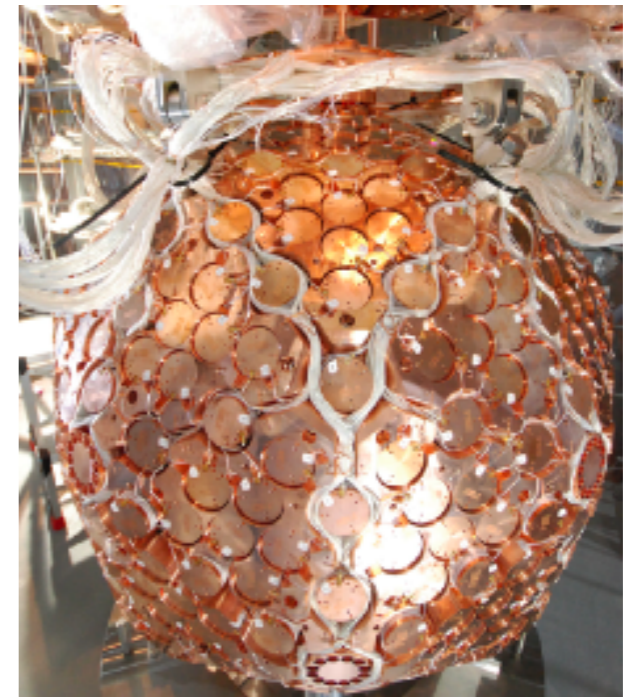


MiniCLEAN at SNOLab:

500 kg LAr (150 kg fiducial)

single-phase open volume, 92
PMTs

operated from 2013-2019

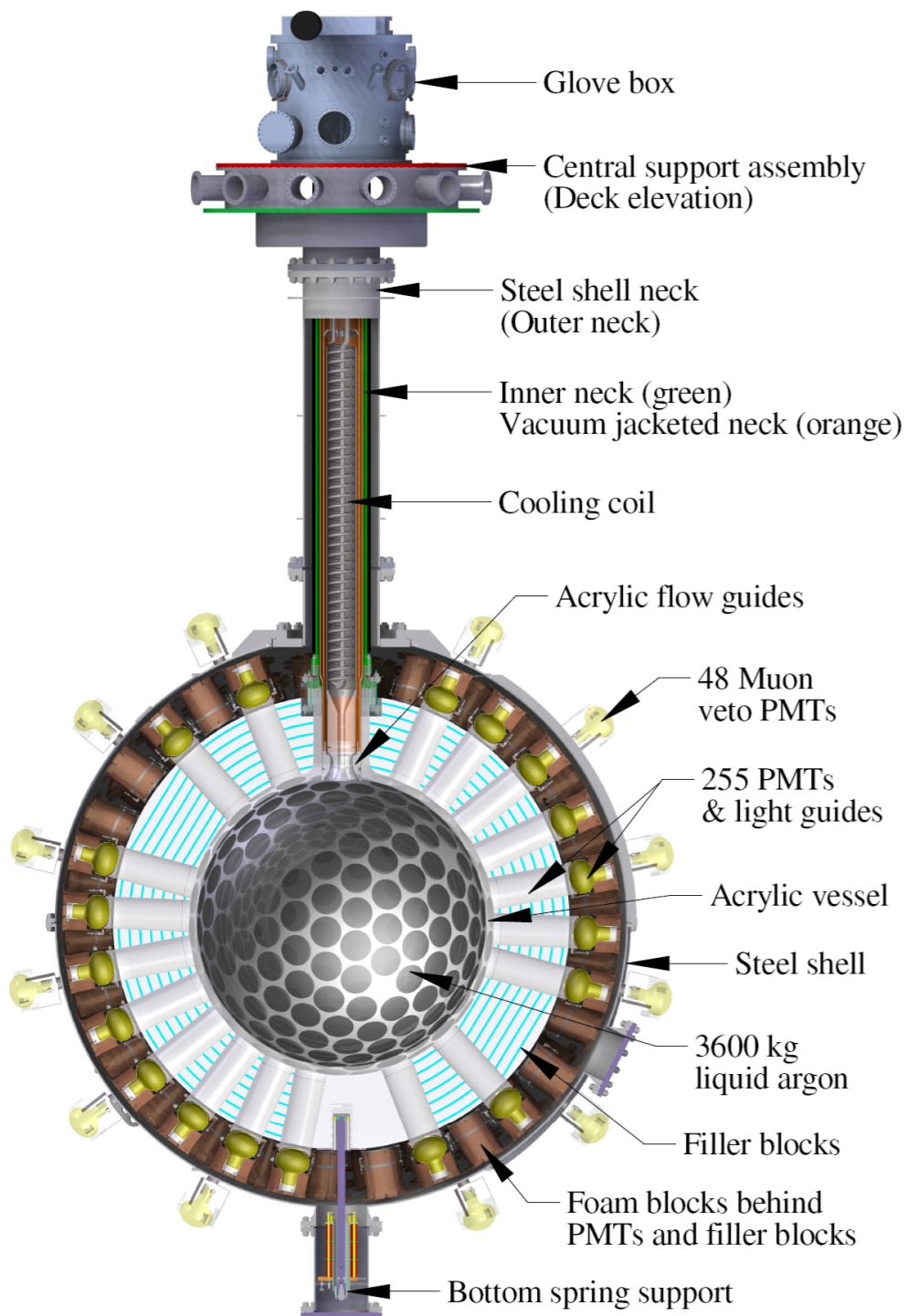


XMASS at Kamioka:

832 kg LXe (100 kg
fiducial), single-phase, 642
2-inch PMTs

operated from 2013-2019

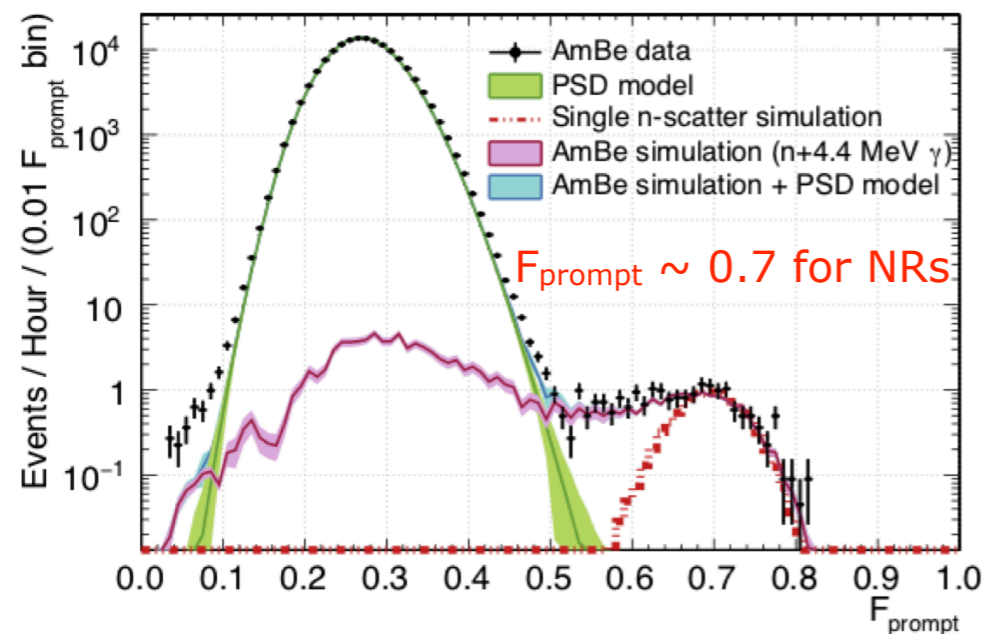
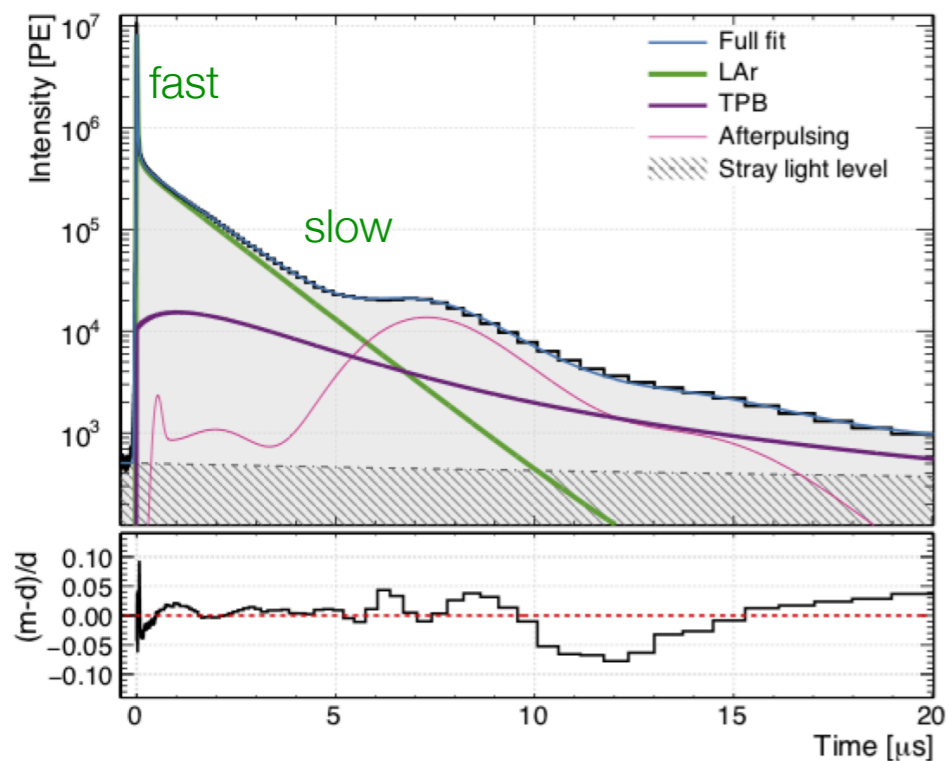
Liquid argon: the DEAP-3600 Experiment



Single-phase LAr detector, located 2 km underground at SNOLAB

- 3.3 t target (1 t fiducial) in sealed ultra-clean acrylic vessel
- vessel is resurfaced in-situ to remove deposited Rn daughters after construction
- in-situ vacuum evaporated *tetra-phenyl butadiene* (TPB) wavelength shifter (128 nm → 420 nm) with ~10 m² surface
- bonded 50 cm long light guides + PE shield against neutrons
- 255 8-inch PMTs (32% QE, 75% coverage)
- detector immersed in 8 m water shield, instrumented with PMTs to veto muons

Liquid argon: the DEAP-3600 Experiment



Pulse-shape discrimination

- Short time constant (~ 8 ns) from the prompt de-excitation of the Ar_2^* dimer singlet state (combined with the TPB prompt decay times)
- Long time constant (~ 1.4 μs) from the de-excitation of the Ar_2^* dimer long-lived triplet state: dependent on the liquid argon purity
- NRs predominantly excite the singlet state of LAr, with larger relative amplitudes compared to ERs
- F_{prompt} : counts the fraction of photoelectrons (PE) detected in a prompt window around the event time, over the total number of PE detected

$$F_{\text{prompt}} = \frac{\sum_{t=-28 \text{ ns}}^{60 \text{ ns}} \text{PE}(t)}{\sum_{t=-28 \text{ ns}}^{10 \mu\text{s}} \text{PE}(t)}$$

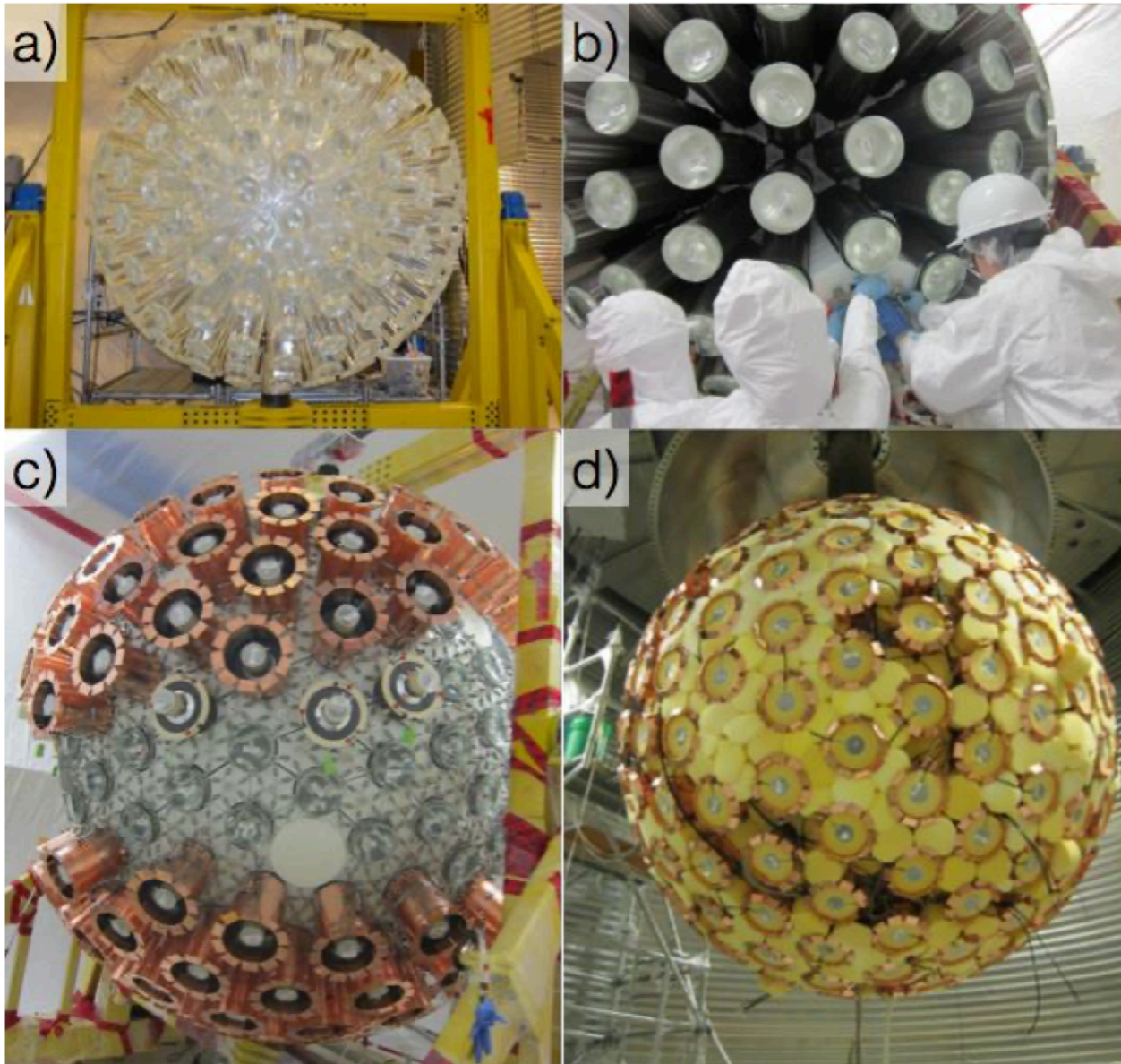
ER leakage probability:

$\sim 4 \times 10^{-9}$ with 90% NR acceptance in 15.6 - 32.9 keV_{ee} window

Liquid argon: the DEAP-3600 Experiment

Light guides on AV

Reflectors on light guides



PMT and inner detector installation Oct 2014

Source	N^{CR}	N^{ROI}
β/γ 's		
ERs	2.44×10^9	0.03 ± 0.01
Cherenkov	$< 3.3 \times 10^5$	< 0.14
n 's		
Radiogenic	6 ± 4	$0.10^{+0.10}_{-0.09}$
Cosmogenic	< 0.2	< 0.11
α 's		
AV surface	< 3600	< 0.08
Neck FG	28^{+13}_{-10}	$0.49^{+0.27}_{-0.26}$
Total	N/A	$0.62^{+0.31}_{-0.28}$

Background rate is **LOW!**

$0.07 \pm 0.03 \text{ ev/t.y/keV}_{ee}$

(NR bkg in WIMP search ROI)

231 live-days with 824 kg fiducial mass

v. Low backgrounds: ^{222}Rn 0.2 microBq/kg

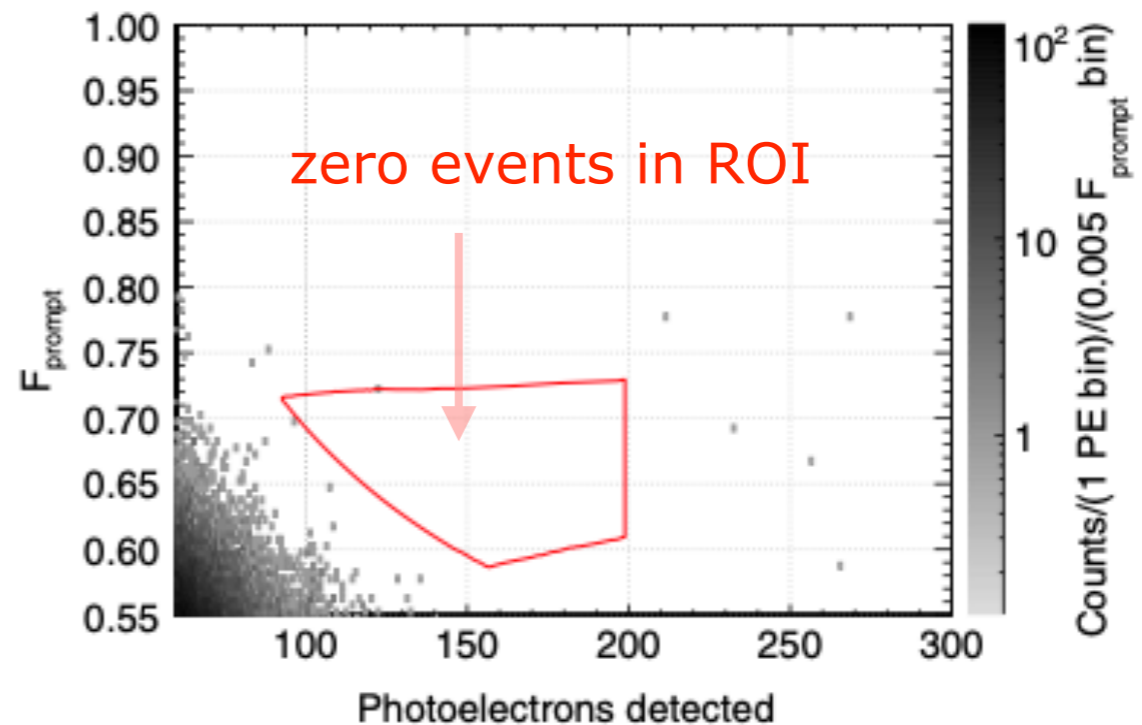
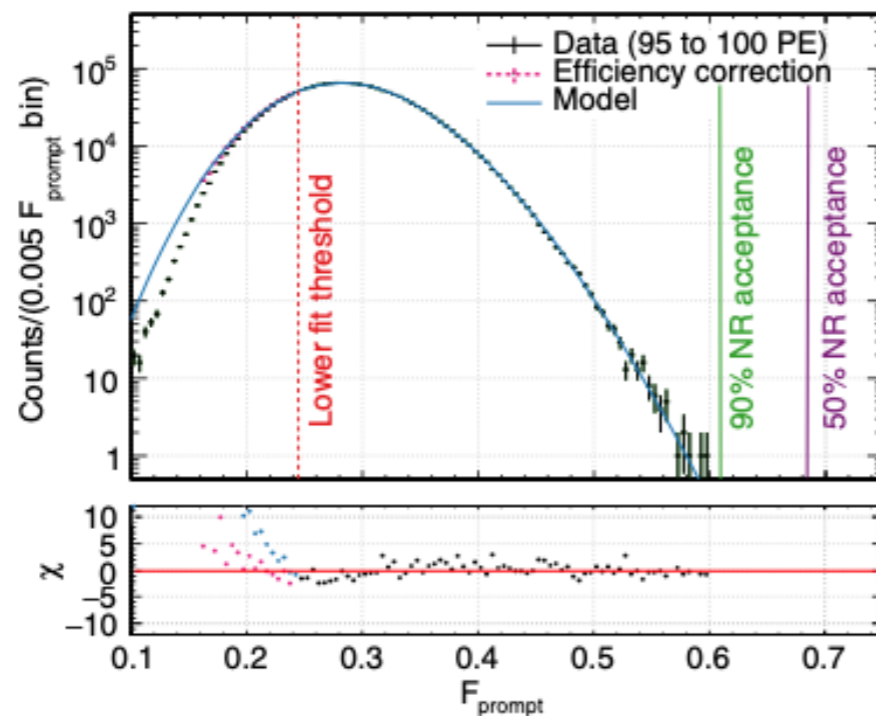
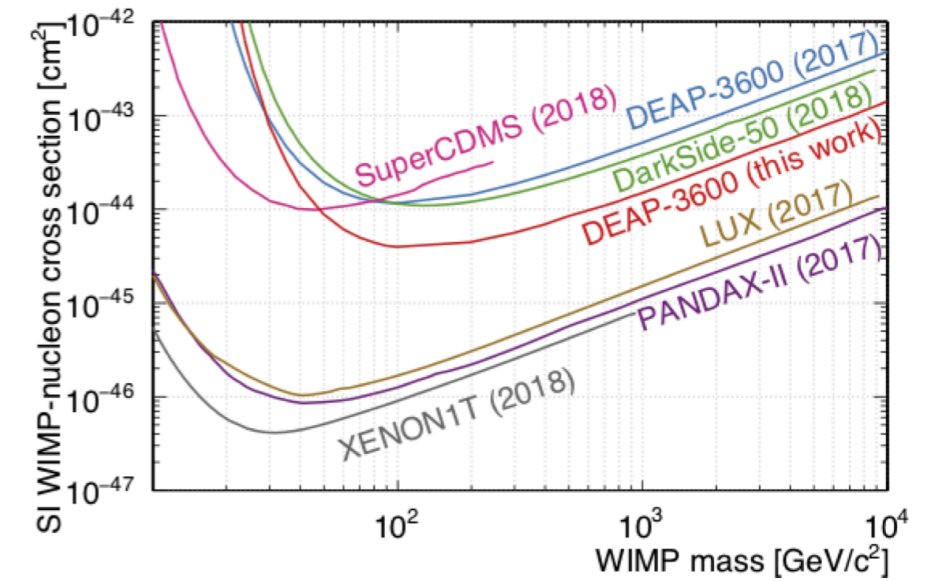
Dominant source: shadowed α decays from ^{210}Po on neck flowguides

ER backgrounds after argon-PSD

Experiment	Fid. Mass (tonnes, nominal)	^{39}Ar specific activity	Total ^{39}Ar rate (Bq)	ER Events in ROI
DEAP-3600	1	$\sim 1 \text{ Bq/kg}$	1,000	0.03 ± 0.01 in 231-days x 824 kg *
DS-20k	20	$< 1/1400 \text{ Bq/kg}$	< 14.3	
ARGO	300	$< 1/1400 \text{ Bq/kg}$	< 214.3	

Liquid argon: the DEAP-3600 Experiment

- Dark matter search with 231 live days
 - exposure: 758 tonne-day
 - light yield: ~ 6 PE/keV
- No events observed: $\sigma < 3.9 \times 10^{-44} \text{ cm}^2$ at 100 GeV
- 806 d data set under analysis; upgrades in progress, to restart 2023



Liquid xenon: the XMASS Experiment



Japan

Kamioka Mine



Tokyo



(c) 東京大学宇宙線研究所 神岡宇宙素粒子研究施設

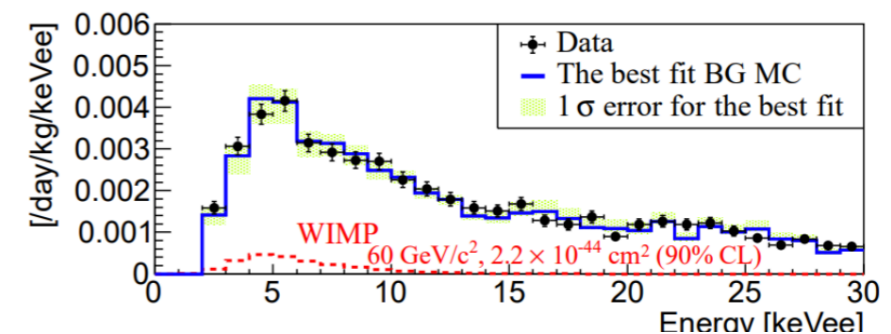
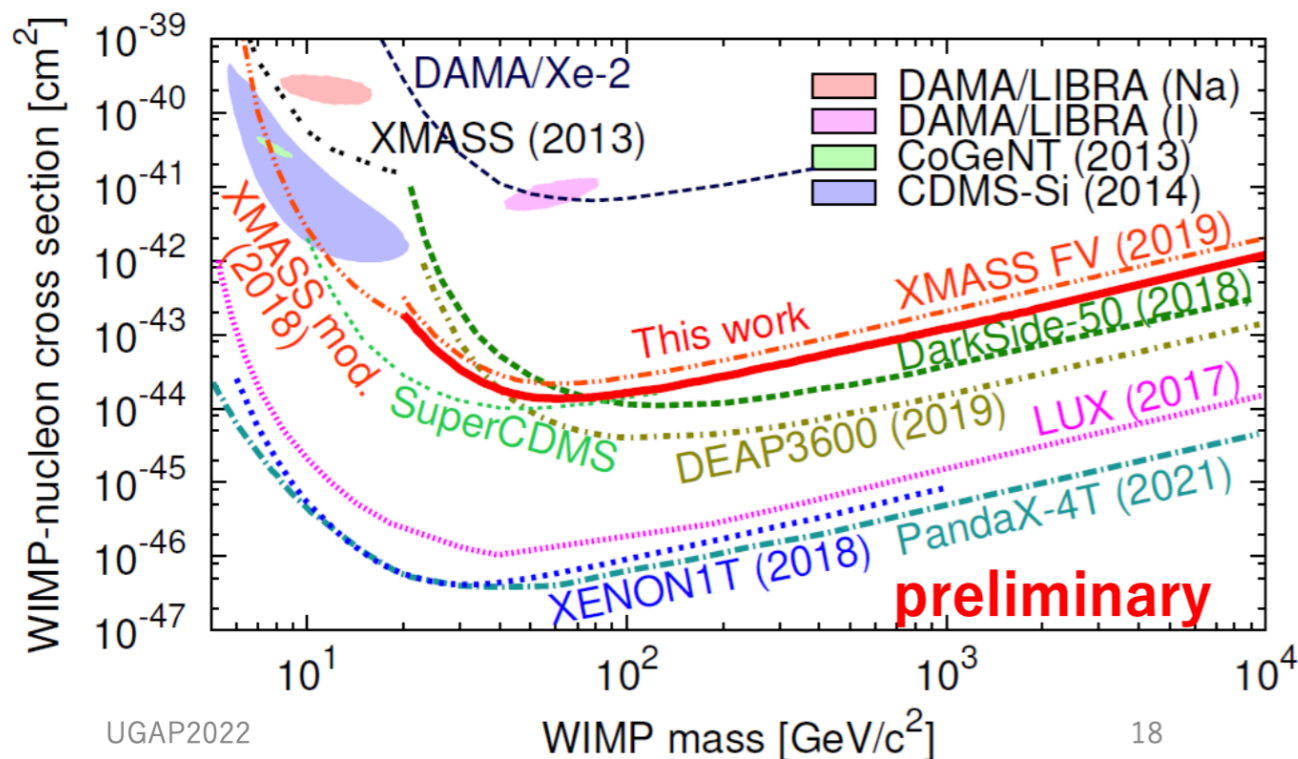
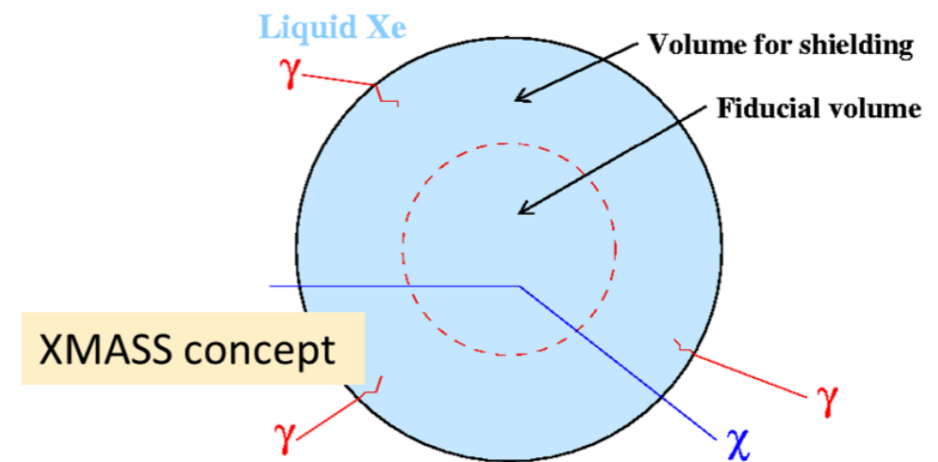
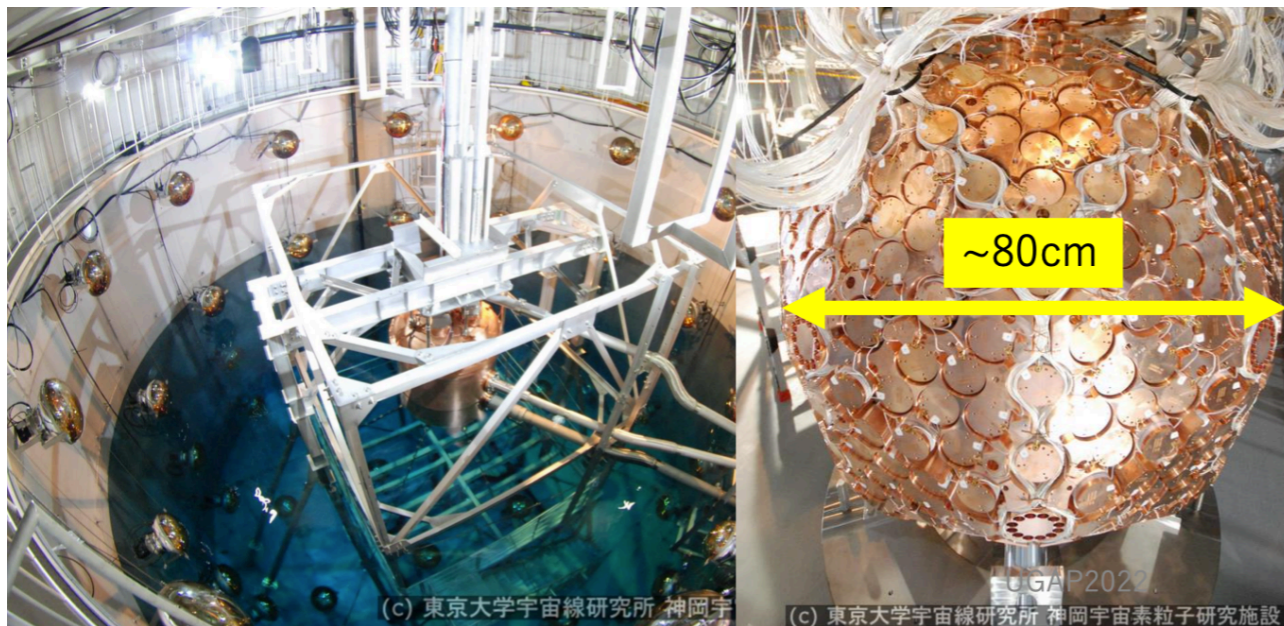


Hex shape PMT

Single-phase LXe detector, located underground at the Kamioka Observatory

- 832 kg target (100 kg fiducial) in ultra-low background Cu vessel
- 642 2-inch PMTs (62% photo-coverage)
- detector immersed in 10 m water shield, instrumented with 70 20-inch PMTs to veto muons
- Light yield: ~ 14 PE/keV
- Energy threshold: ~ 0.5 keVee
- Carried out a variety of rare-event searches (DM, solar axion, 2νECEC, etc)

Liquid xenon: the XMASS Experiment



Five years stable operation: 2013 - 2019

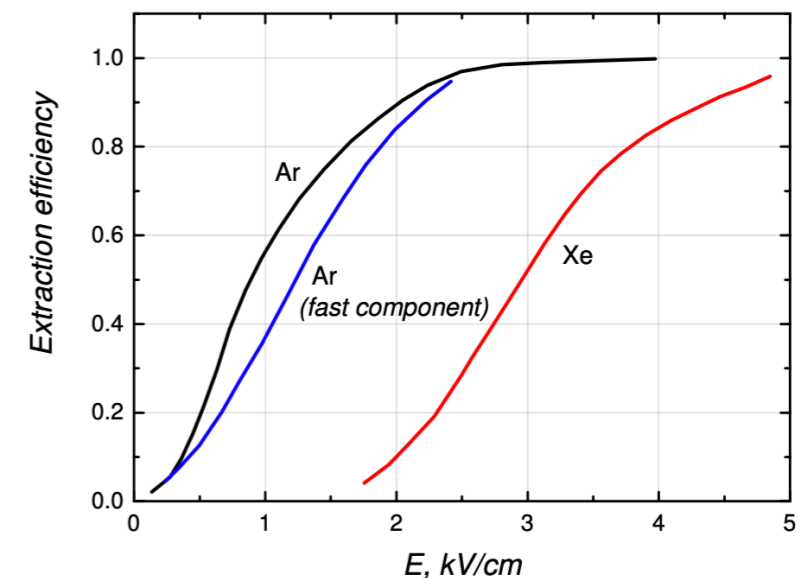
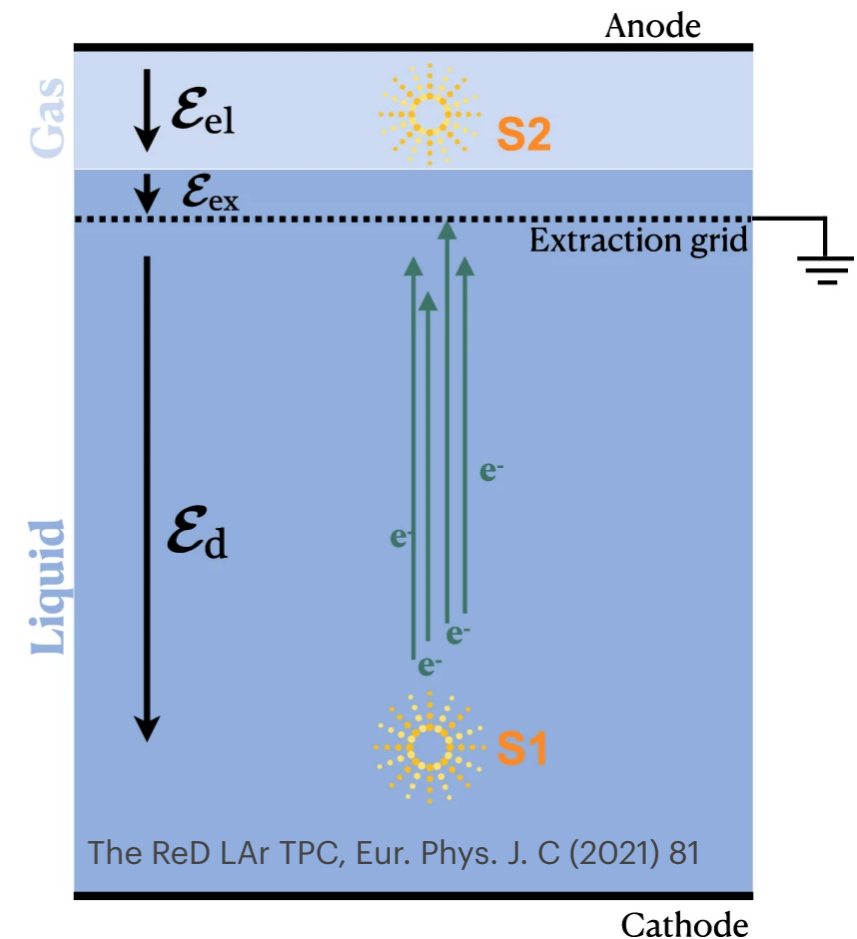
- Energy threshold with 4-fold (3-fold) coincidence: 1 keVee (0.5 keVee)
- Search for signal by fitting data with background + expected signal

Two-phase LAr and LXe detectors

Two-phase detection principle

- Time projection chambers

- Prompt scintillation light signal in the liquid from the direct excitation process (signal is called S1)
- Electrons drifted away from the interaction site via an electric drift field $\sim \mathcal{O}(100 \text{ V/cm})$
- Electrons extracted from the condensed liquid into the vapour phase by a stronger electric field $\sim \mathcal{O}(\text{few kV/cm})$, also called "extraction field" (e^- need sufficient momentum to overcome the potential barrier at the liquid/gas interface)
- Electrons in the gas phase are accelerated by the electric field and gain sufficient energy to excite atoms in collisions and create electroluminescence (EL; also called proportional scintillation), with similar emission spectra to those of direct scintillation (signal is called S2)



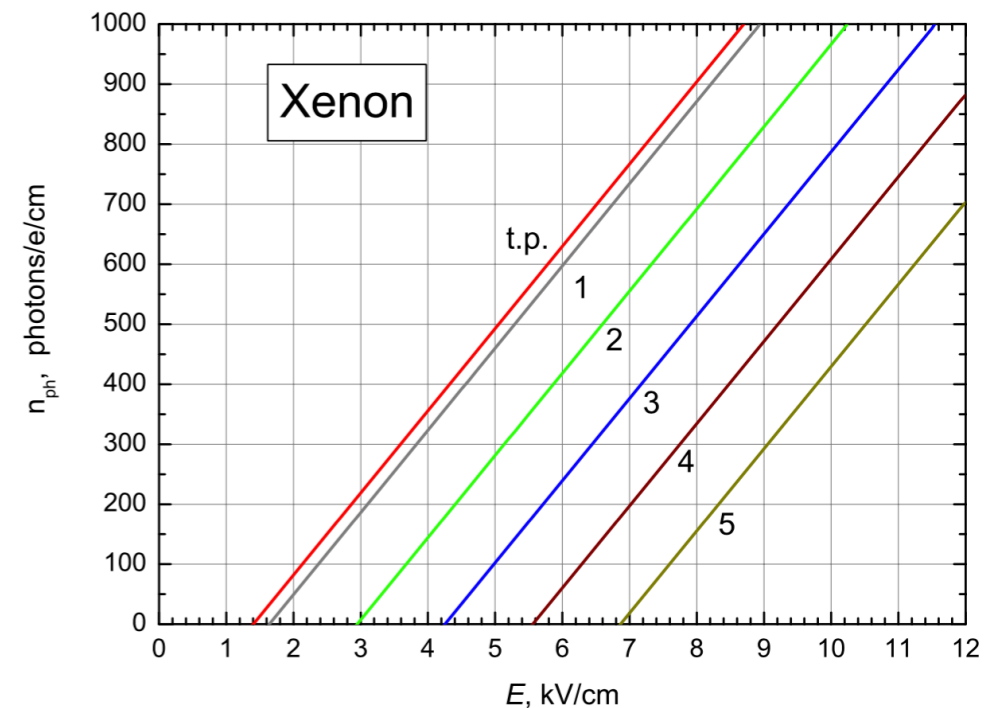
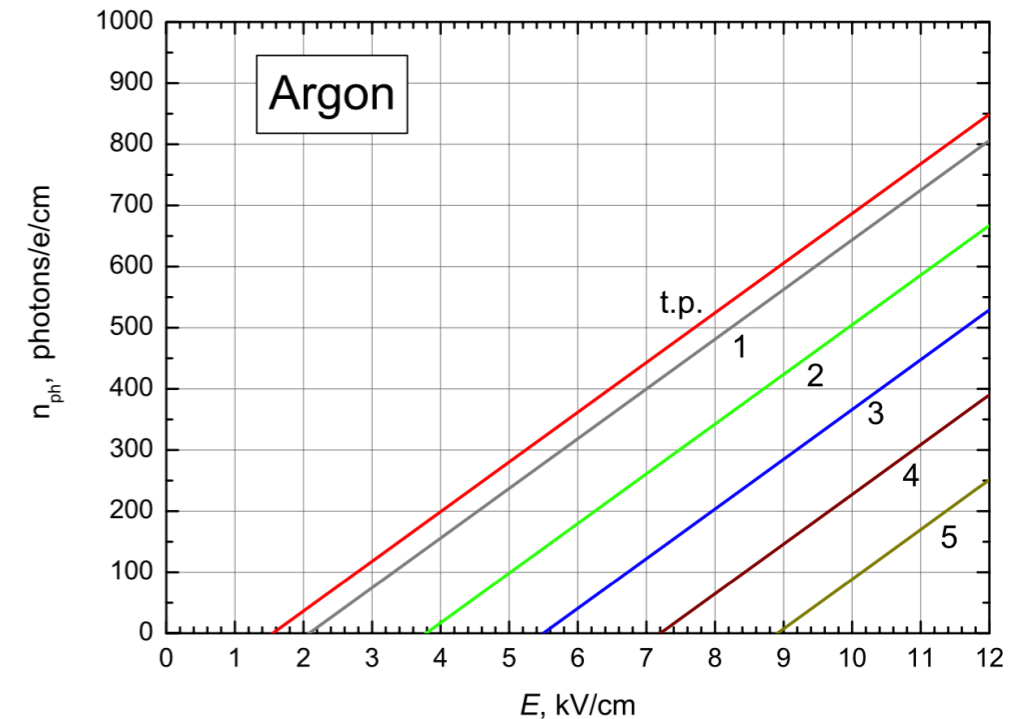
Two-phase detection principle

- Time projection chambers

- A single extracted e⁻ can produce ~ $\mathcal{O}(100)$ of photons, which then produce tens of photoelectrons in the photosensors
- The number of generated S2 photons will depend on the drift path, the field strength (in V/cm) and the gas density:

$$\frac{1}{n} \frac{dN_{ph}}{dx} = a \frac{E}{n} - b$$

- with $n = N_A \rho/A$, a and b being gas-specific empirical coefficients
- Important: the EL process is linear, since the energy of the drifting e⁻ is dissipated via photon emissions (and these do not participate further in the process)

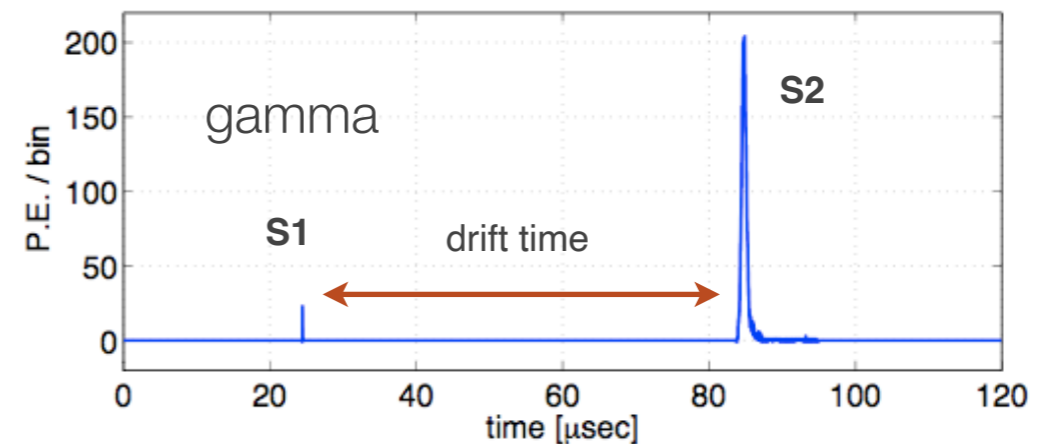
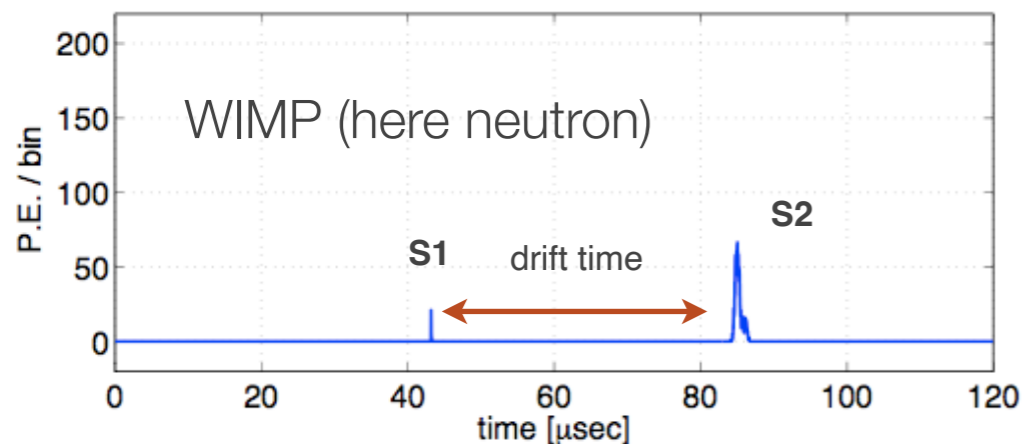
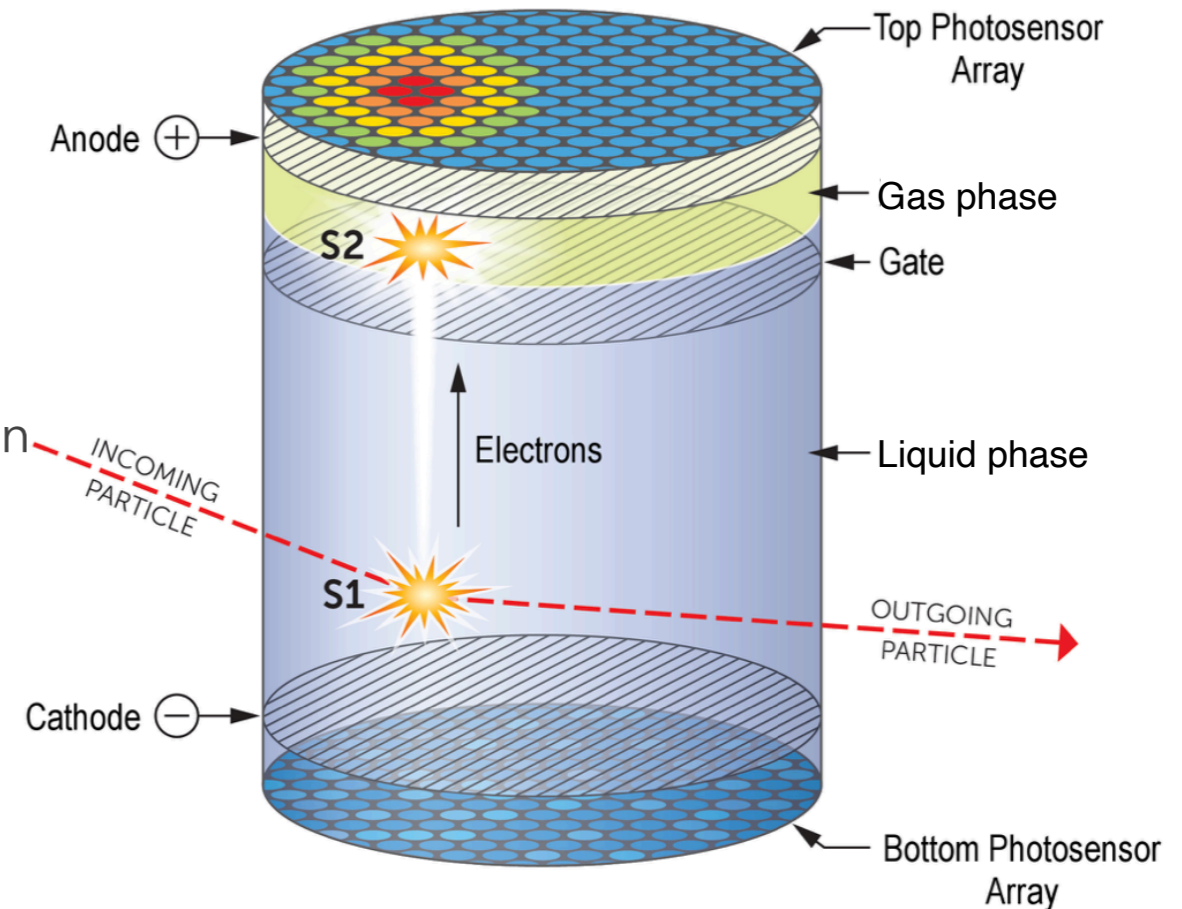


Number of photons generated in 1 cm of gas, as a function of field, from Chepel and Araujo, JINST 2013 ²⁹

Two-phase detection principle

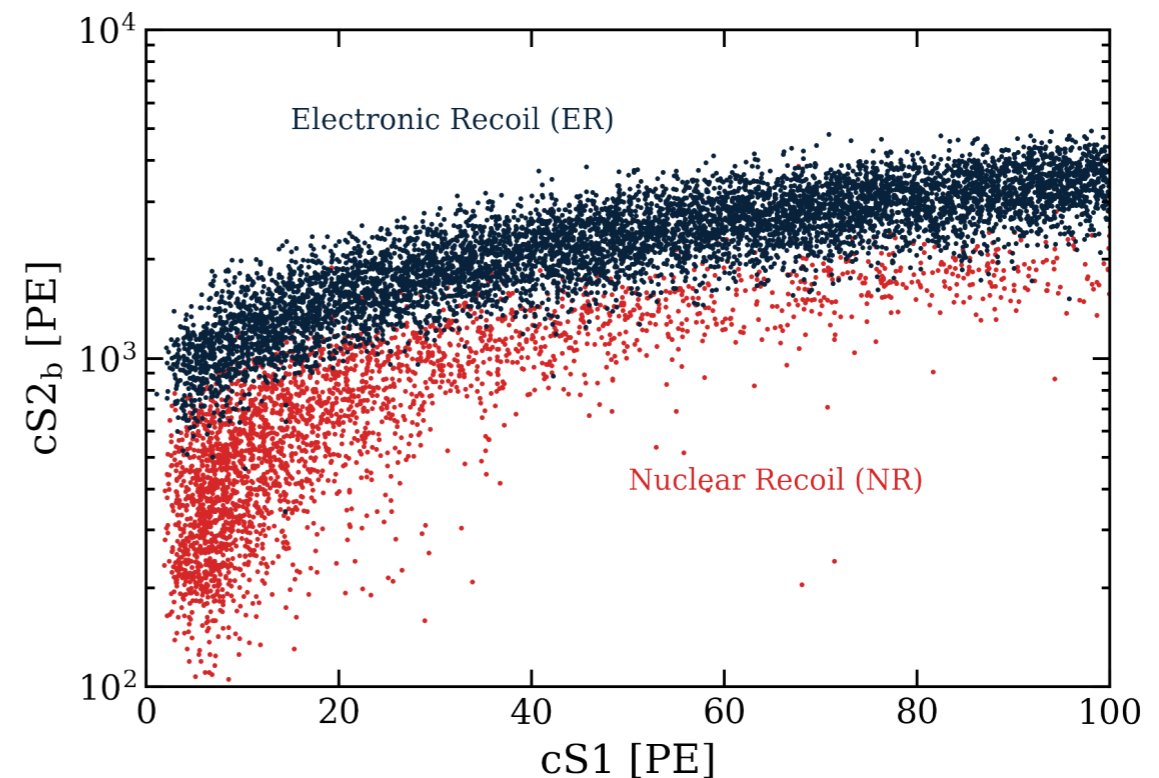
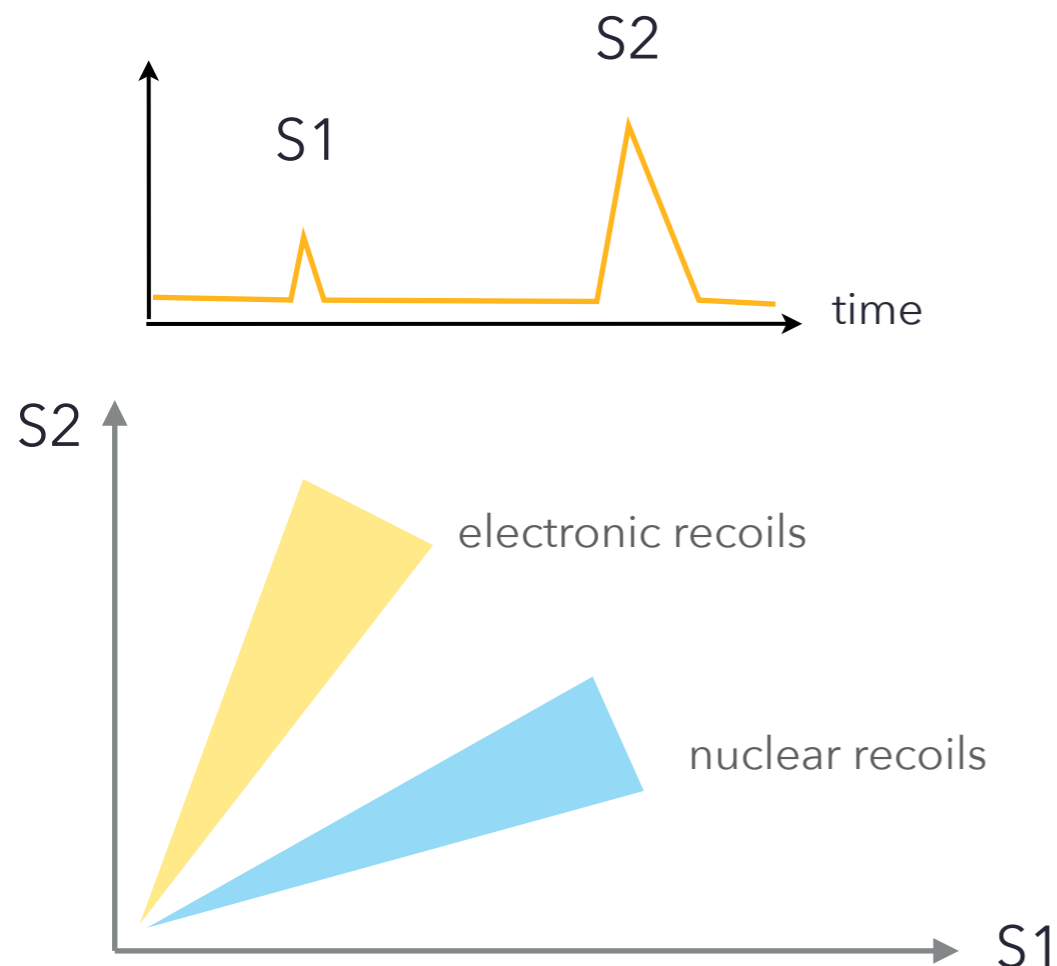
- Time projection chambers

- Signals detected with arrays of photosensors
- energy determination based on light (S1) & charge (S2) signals
- 3D position resolution, which allows for fiducialisation
- S2 over S1 \Rightarrow ER versus NR discrimination
- Identification of single versus multiple interactions
- Pulse shape information (LAr) \Rightarrow ER versus NR discrimination



NR versus ER discrimination

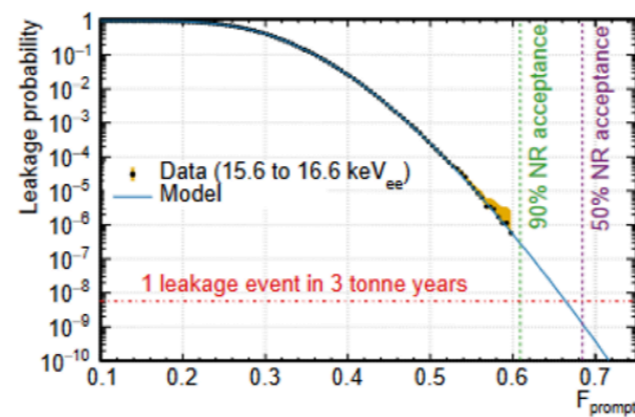
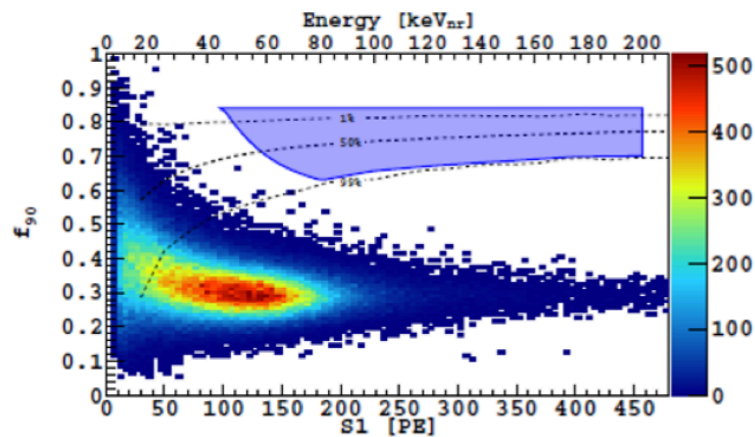
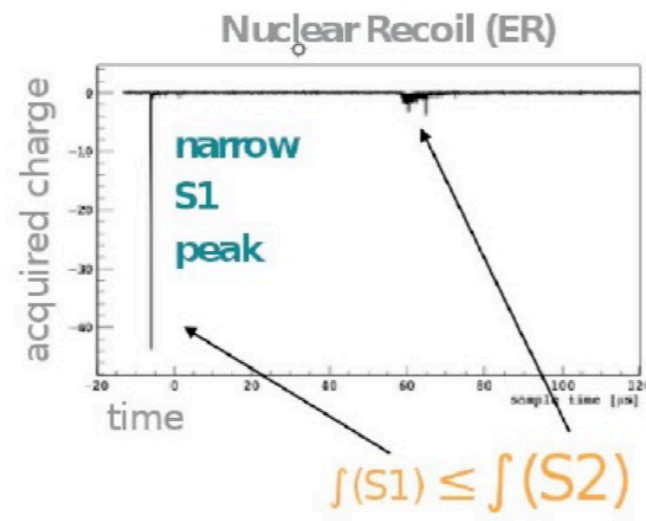
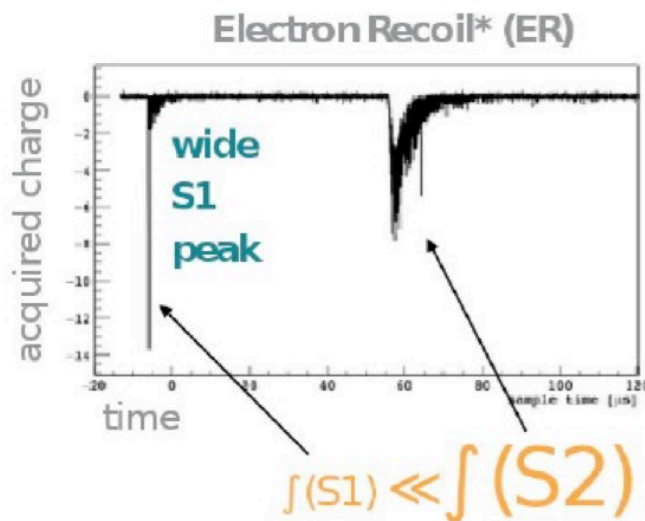
- S2 over S1 depends on the type of particle (LET); in particular, it is different for ERs versus NRs
- The ER rejection power depends on an interplay between the drift field (that changes the mean recombination fraction $\langle r \rangle$ and the recombination fluctuations Δr ; and the e-ion recombination factor for ERs is more significantly affected by the field) and total S1 light collection (higher field means less S1 light and thus larger statistical fluctuations)
- Typically 99.5 up to 99.99% ER rejection at 50% NR acceptance



NR versus ER discrimination in LAr TPCs

Nuclear recoil (NR) vs β - γ (ER) signal discrimination

Fraction of prompt and delayed light (f_{prompt}) + S2/S1 ratio

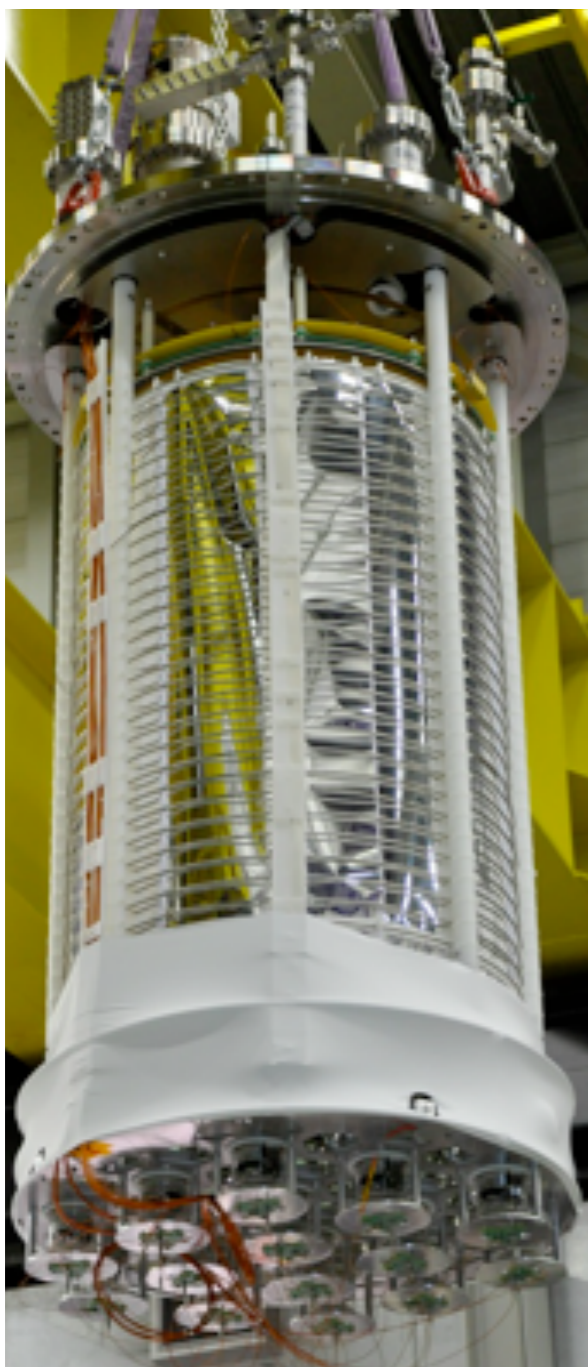


DS50 Coll, Phys Rev D 98 (2018) 102006

DEAP Coll, Euro Phys J C 81 (2021)

- NRs predominantly excite the singlet state of LAr, with larger relative amplitudes compared to ERs
- ERs: the low density of e-ion pairs results in less recombination, thus more free electrons, compared with NRs of the same S1
- f_{90} : defined as the integral over the S1 pulse in the first 90 ns over the pulse in 7 μ s
- typically f_{90} is 0.7 for NRs and 0.3 for ERs

Time projection chambers: argon



ArDM at Canfranc:

850 kg active LAr
(500 kg fiducial)

28 8-inch PMTs



DarkSide-50 at LNGS

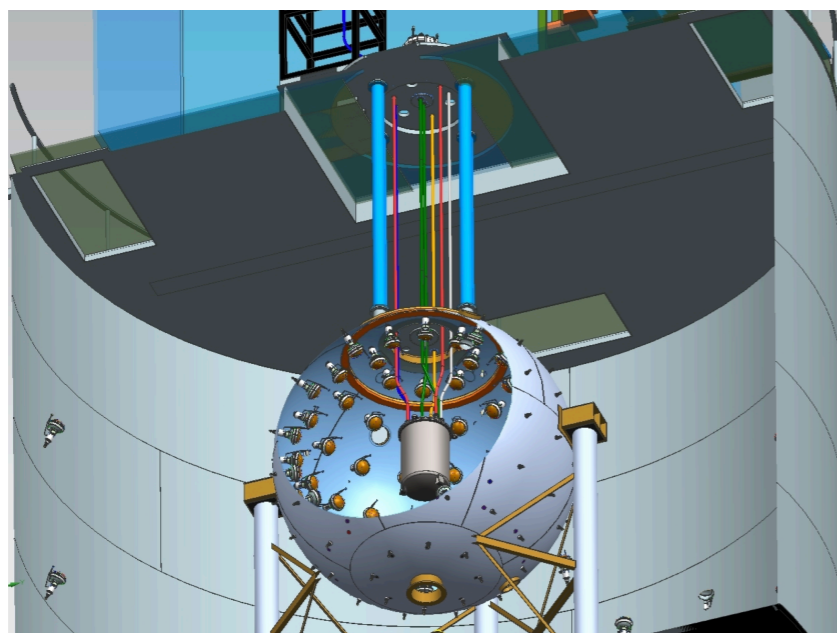
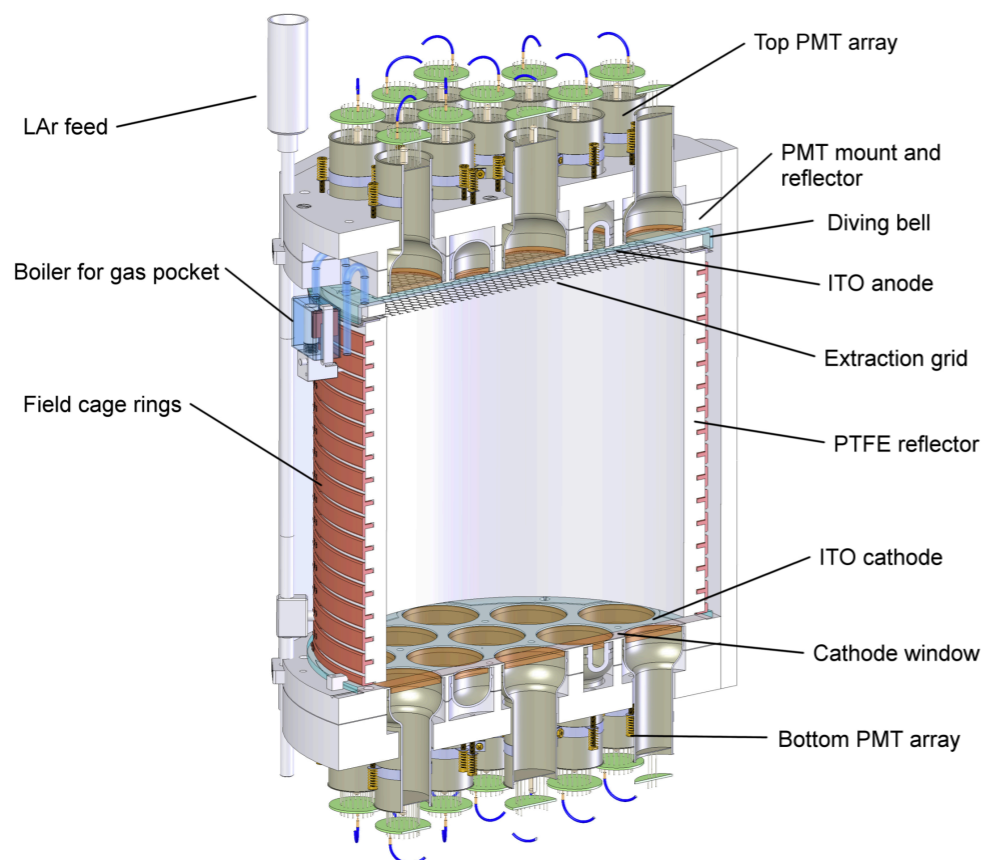
50 kg LAr (dep in ^{39}Ar)
(33 kg fiducial)

38 3-inch PMTs



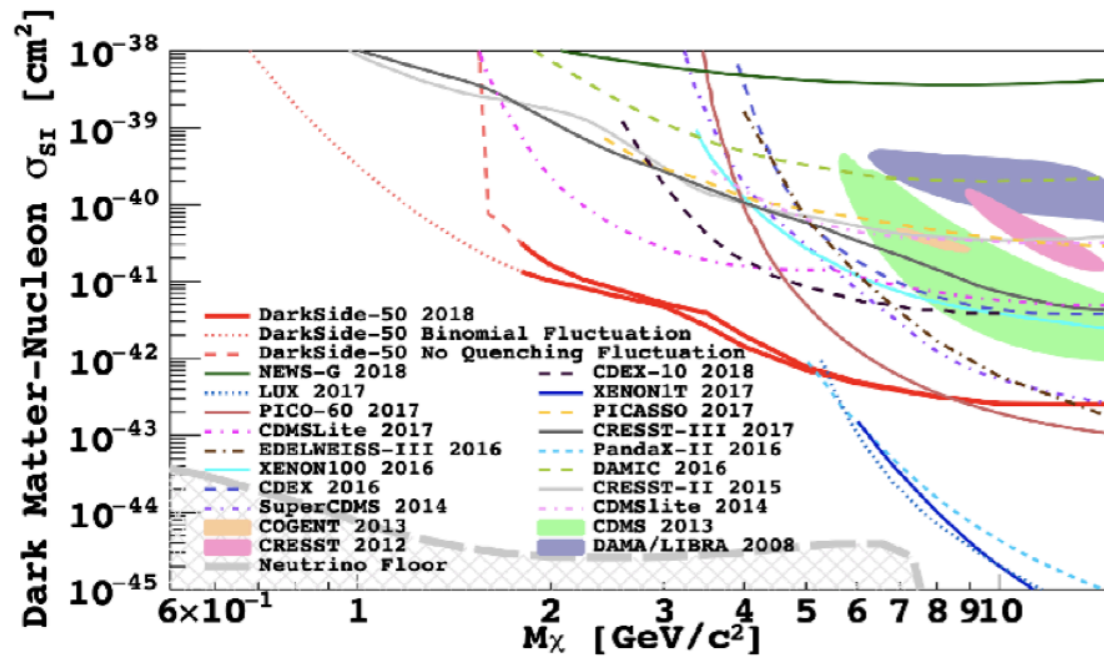
DM search with
underground argon

The DarkSide-50 experiment



- Located underground in Hall C of LNGS; nested detector system:
- LAr TPC contained in stainless steel cryostat, 38 3-inch PMTs in two arrays (QE: 34% at 420 nm)
- TPC: PTFE walls, 200 V/cm drift field
- liquid scintillator veto for radiogenic and cosmogenic neutrons: 4 m diameter stainless steel sphere with borated liquid scintillator, 100 8-inch PMTs
- neutron capture reaction $^{10}\text{B} (n,\alpha)^7\text{Li}$: makes borated LS very effective neutron veto
- water Cherenkov veto for muons, 11 m diameter, 80 8-inch PMTs

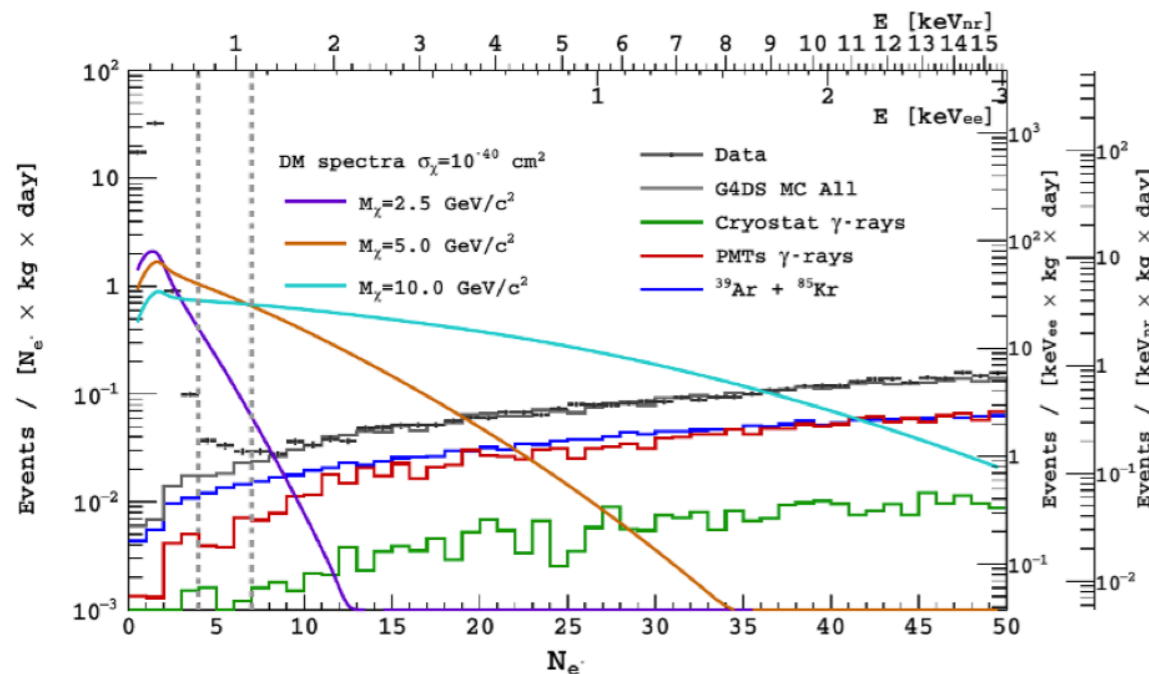
Recent results from DarkSide-50



S2 only events to reach lower energy threshold
Sensitivity to **low mass dark matter** candidates

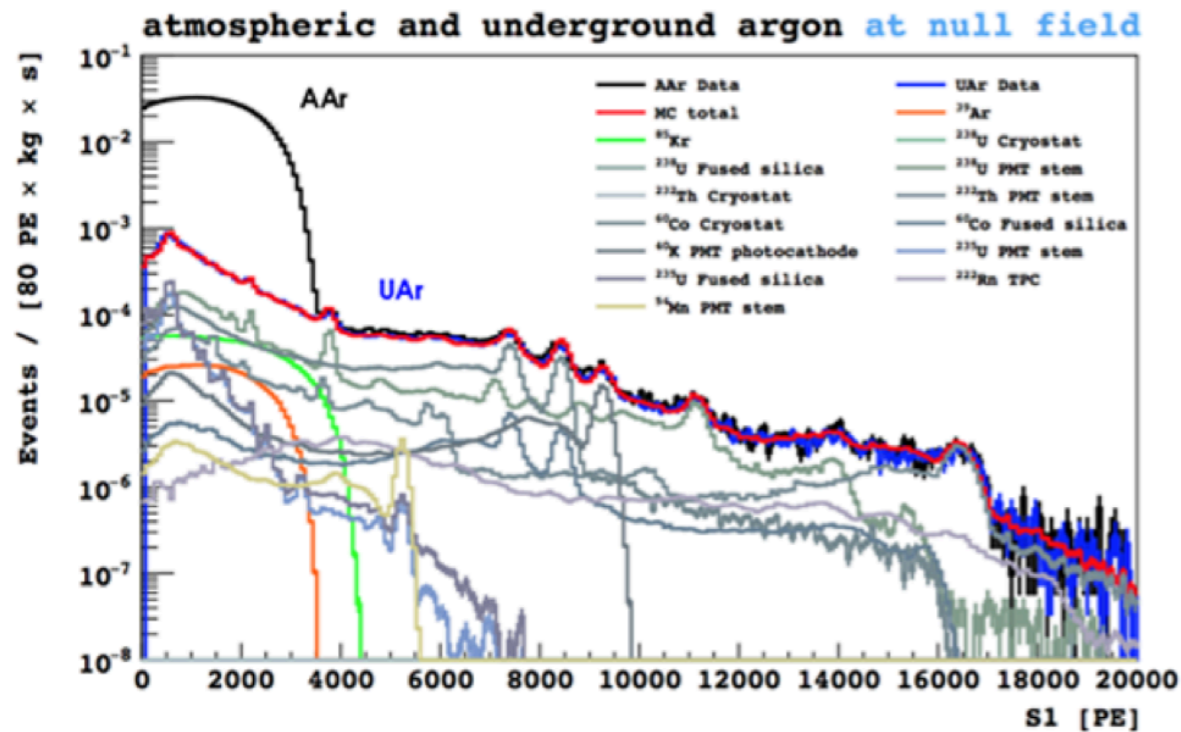
DS-50 best limits above mass 3 GeV/c² - *Phys. Rev. Lett.* 121 (2018) 081307

(work in progress: new limits in many interaction models, including Migdal, scattering on electrons, solar axions, sterile neutrinos ...)



Calibration of low energy nuclear recoils (0.5 keV) with dedicated setup such as **ReD** at LNS Catania
Eur. Phys. J. C 81, 1014 (2021)

Radiopure argon from underground sources



³⁹Ar β decay (Q = 570 keV, half life 269 yr)

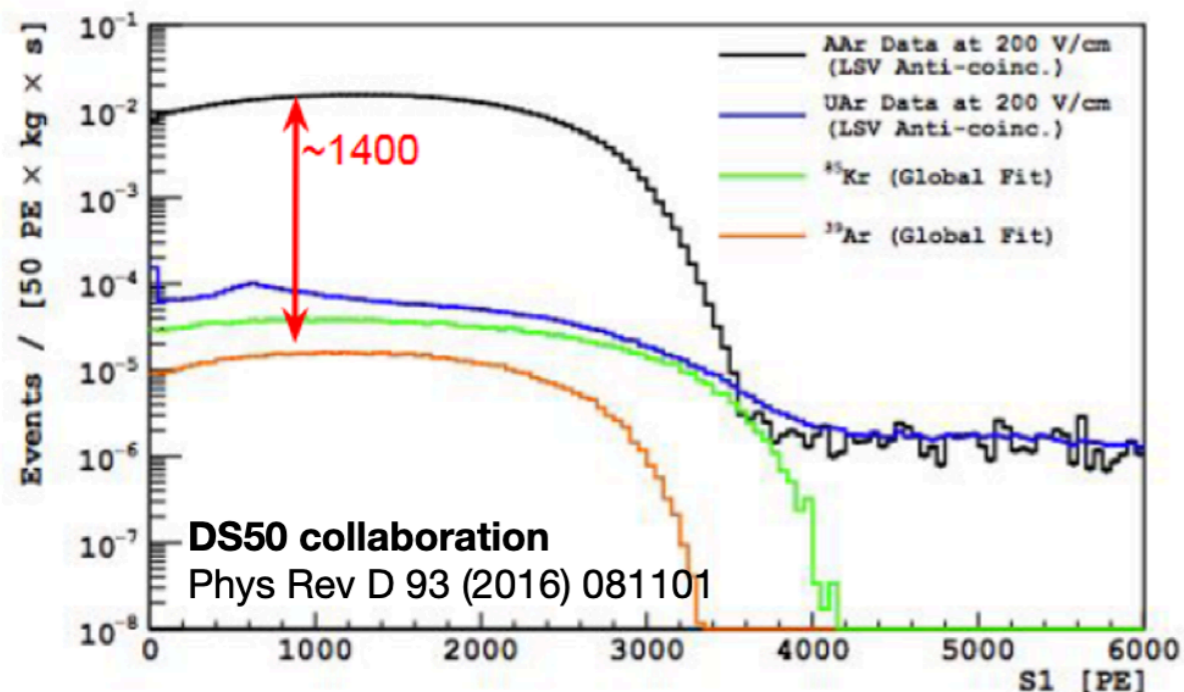
~ 1Bq/kg in **atmosphere** Ar

Origin from ⁴⁰Ar(n, 2n)³⁹Ar in atmosphere

Extraction of Ar from **underground** sources, where such processes are suppressed

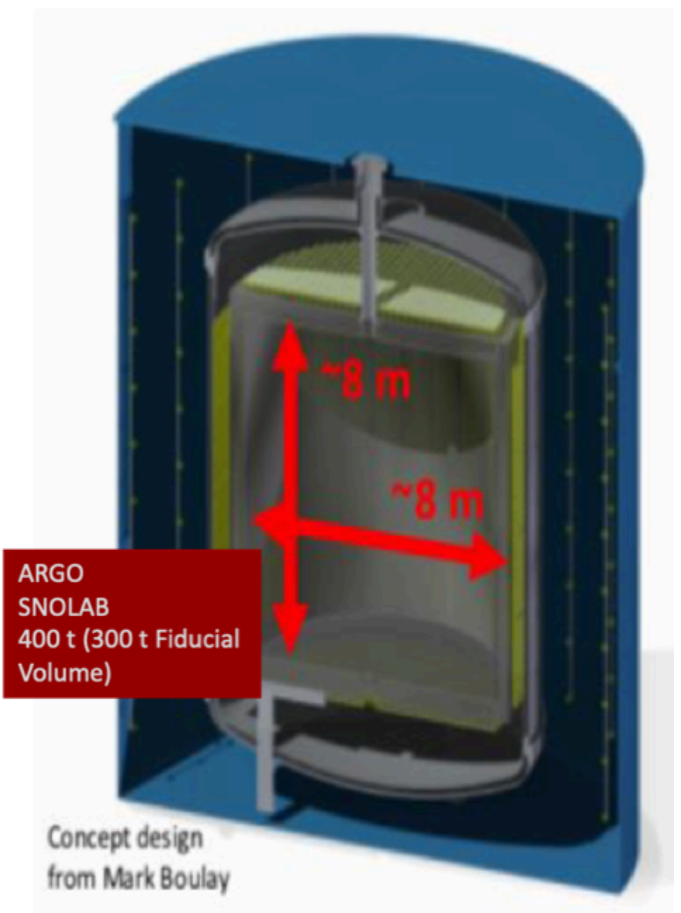
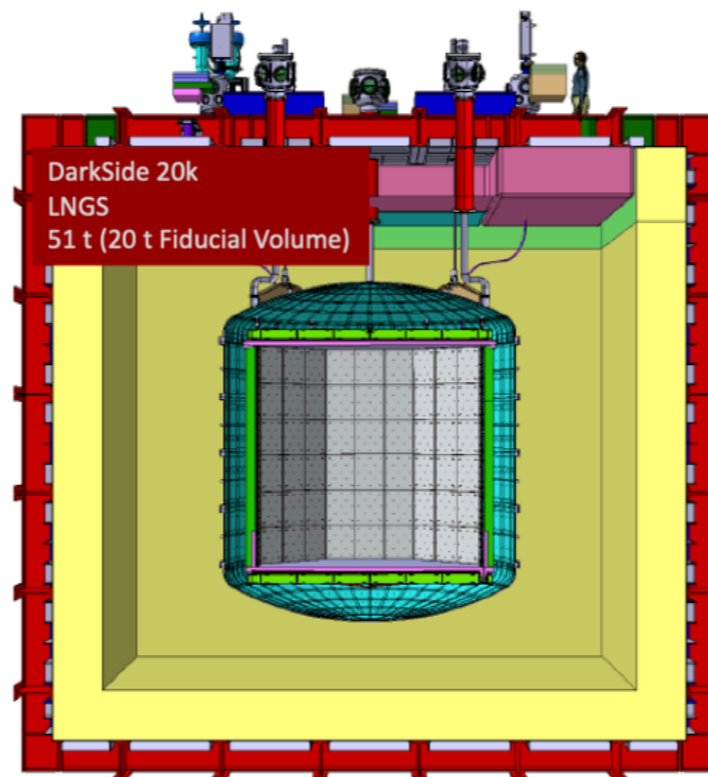
DS50 used 157kg of **UAr**

Depletion factor in ³⁹Ar : 1400 +/- 200



Dark matter direct detection in argon TPCs

- The Global Argon Dark Matter Collaboration



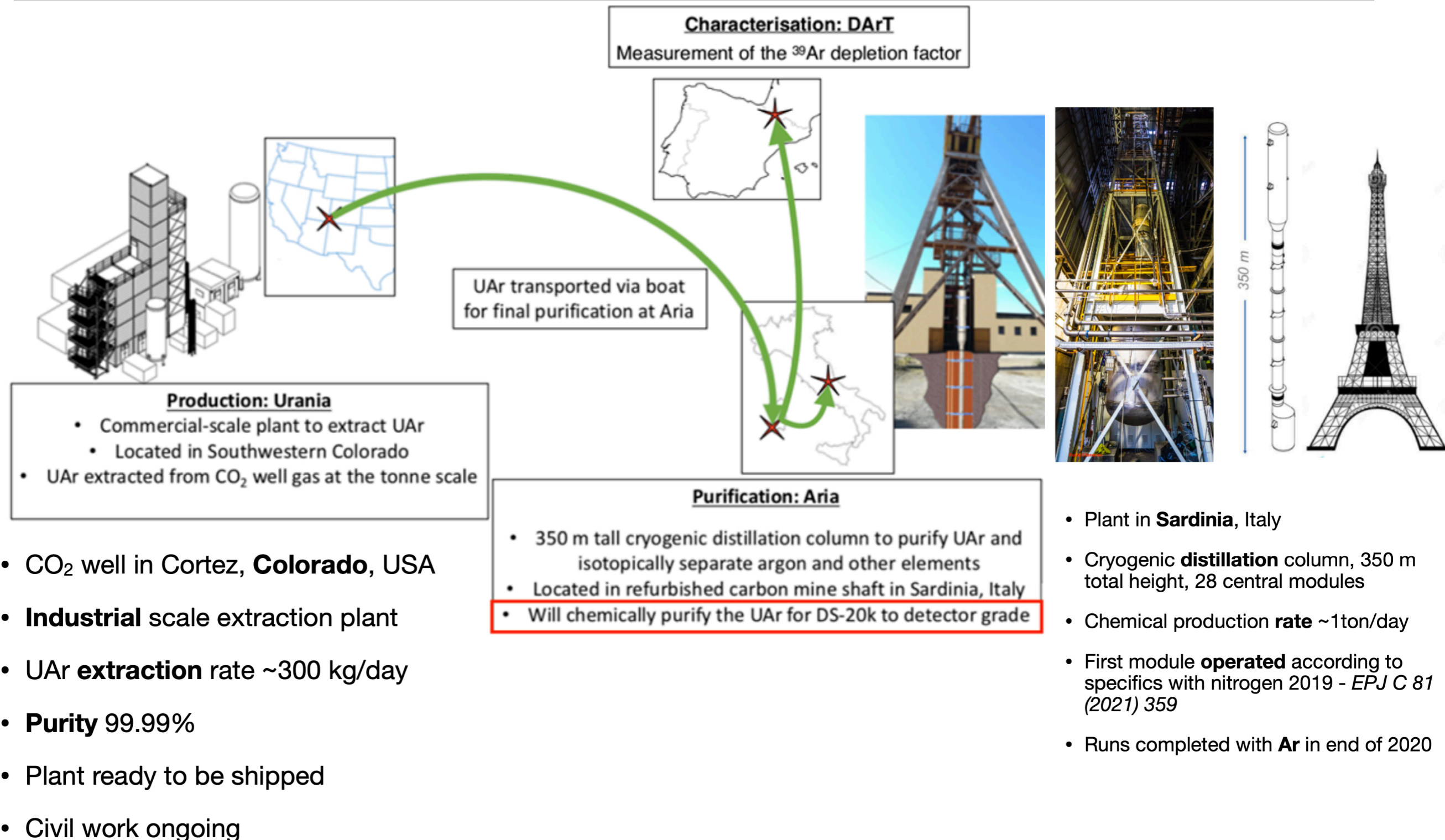
construction starts in 2022
data taking in 2025
nominal run time 10 years

TPCs and single-phase:
past and current

Current: DarkSide-50k

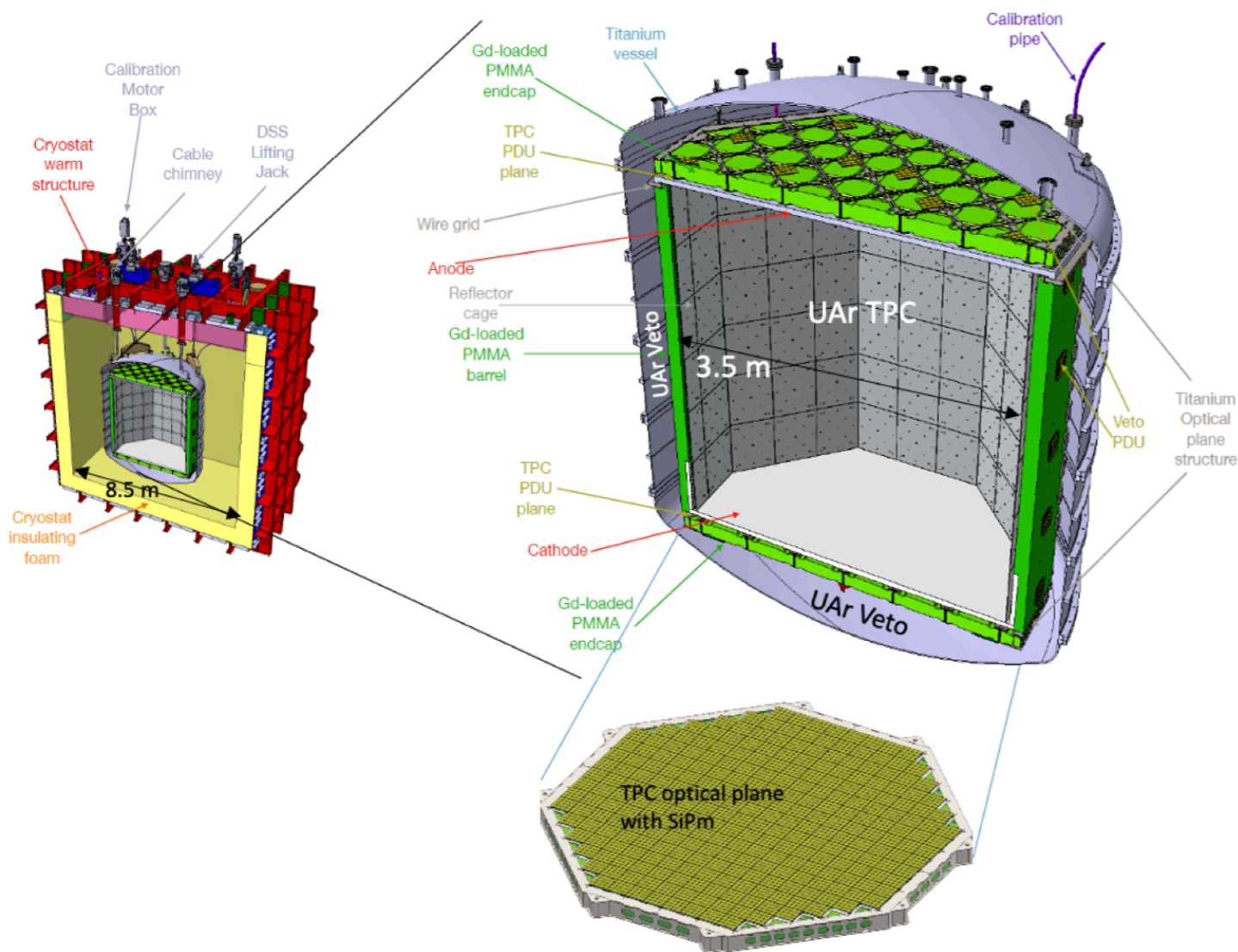
Future: ARGO

Production of underground argon for DarkSide-20k



- CO_2 well in Cortez, **Colorado**, USA
- **Industrial** scale extraction plant
- UAr **extraction** rate ~300 kg/day
- **Purity** 99.99%
- Plant ready to be shipped
- Civil work ongoing

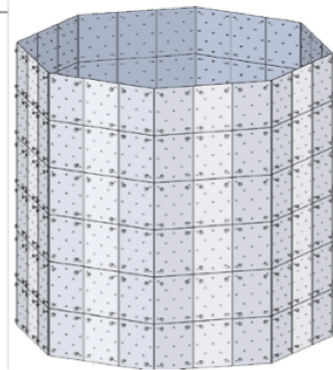
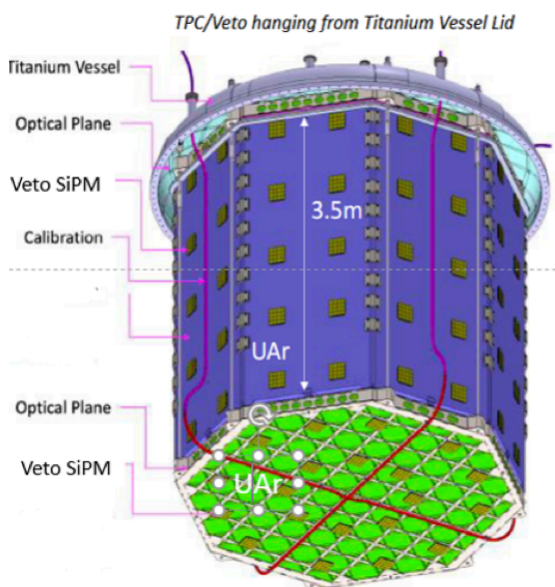
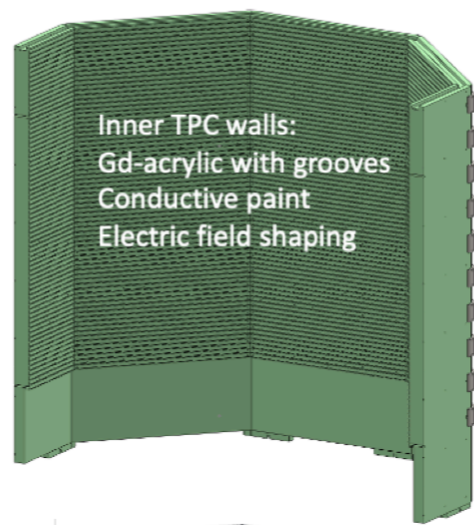
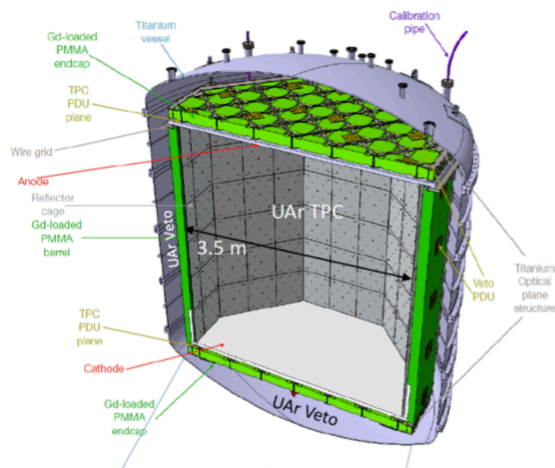
The DarkSide-20k detector



- To be located underground in Hall C of LNGS
- 50 t underground argon (20 t in fiducial volume)
- 21 m² cryogenic silicon photomultipliers (SiPMs)
- inner TPC will be surrounded by a single-phase liquid argon neutron veto detector
- integration of inner TPC + veto into a single object
- vessel with 99 tons of underground argon
- within a 650 ton atmospheric argon membrane cryostat (ProtoDUNE-like) instrumented as a muon veto

The DarkSide-20k detector

The time projection chamber:

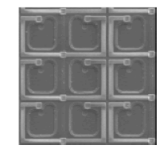


- Maximum drift length of 340 cm
- Electron drift lifetime > 5 ms
- Gas pocket: 5.0 ± 0.7 mm
- Drift field: 200 V/cm
- Electron extraction field: 2.8 kV/cm
- Anode and cathode: transparent pure acrylic covered with Clevios (conduction) and TPB as wavelength shifter
- Reflectors in the inner and outer walls
- Expected yields: S1 ~ 10 PE/keV, S2 > 20 PE/keV

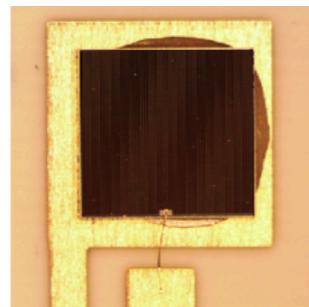
The DarkSide-20k detector

Development of large-area cryogenic, radio-pure SiPMs:

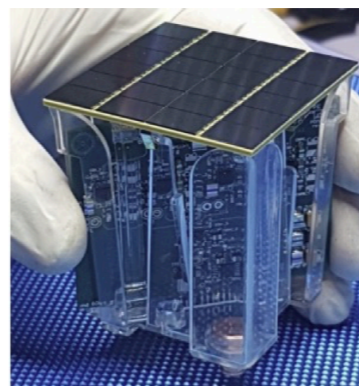
- Two arrays with a total of 8200 channels (photo detector modules, PMDs)
- Each PMD: 24 SiPMs with 12 mm x 8 mm covering an area of 5 x 5 cm², operating as a single channel
- The PMDs are assembled in motherboards of 16-25 units



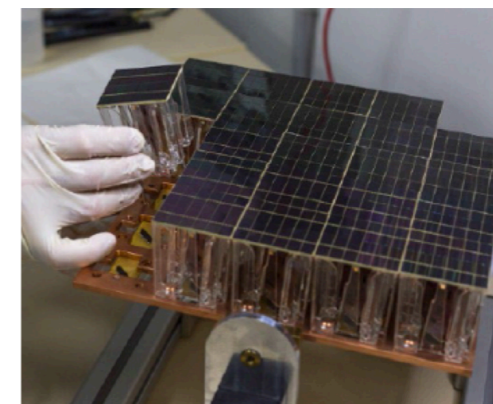
Single SPAD
~25 μm²



Single SiPM ~1 cm²



Photodetector module (PMD)
matrix of 16-24 SiPMs
~5x5 cm²

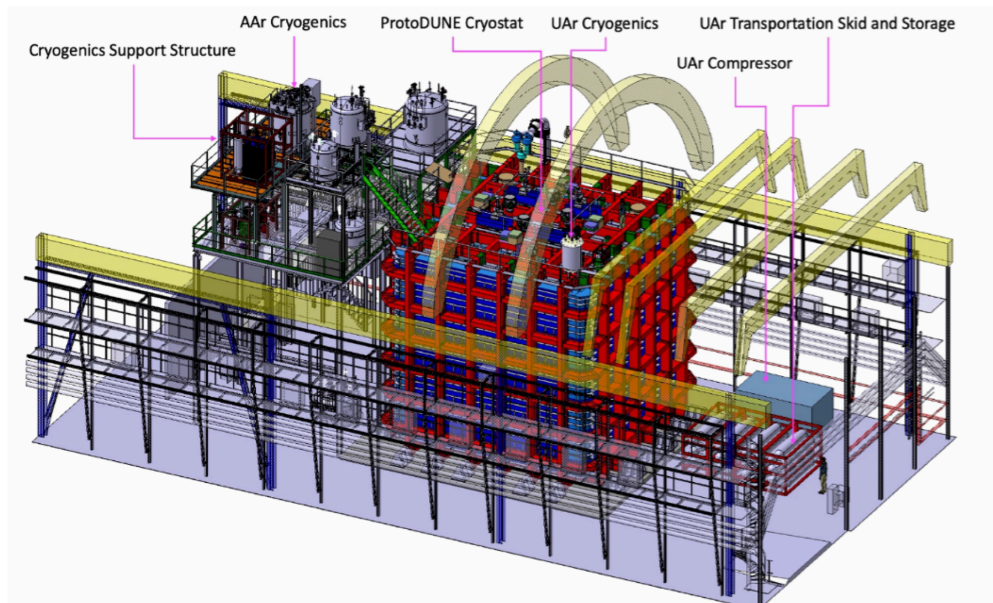


Photodetector Unit
matrix of 16-25 PMDs

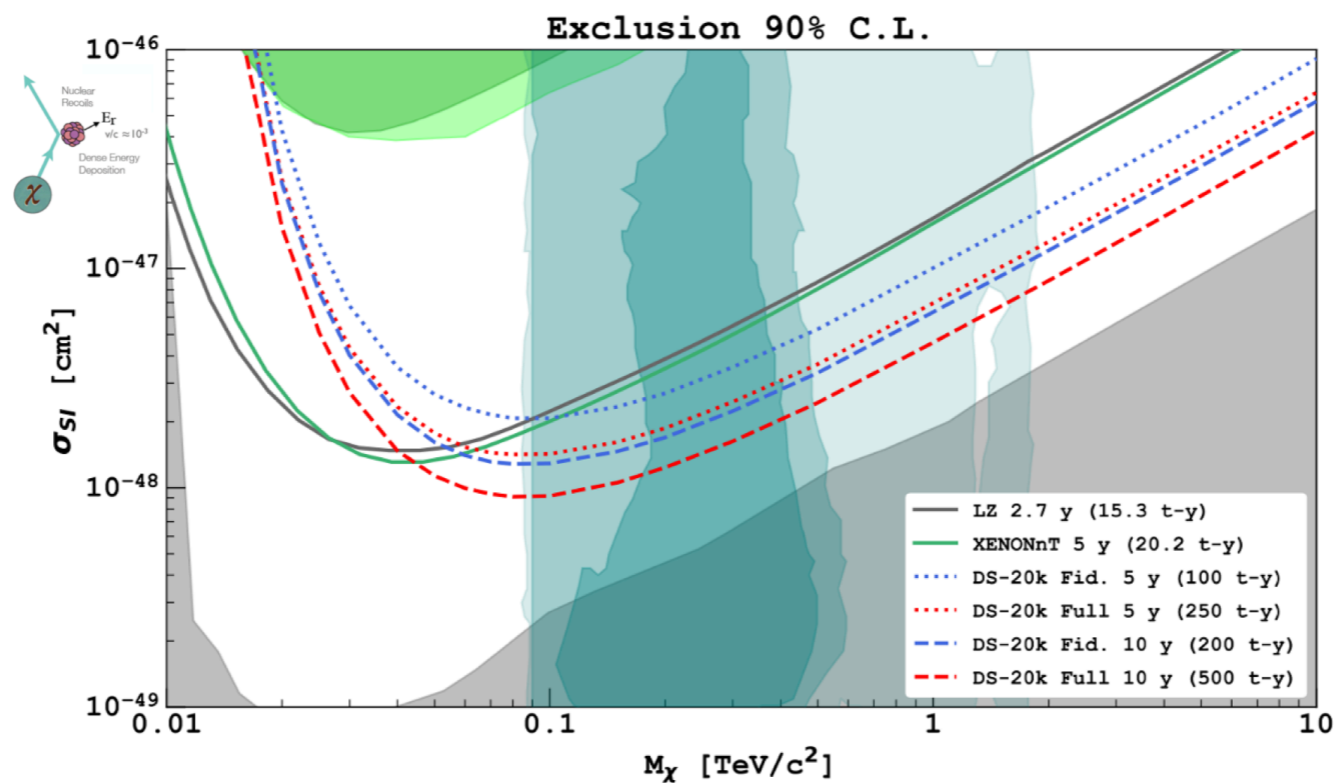
> 8000 PMDs (+2000 in the veto)
21 m² (inner TPC) + 5 m² (veto)
Mass production of the raw **wafers** at **LFoundry** (Italy)
Assembling facility **NOA** at **LNGS**
Other assembling facility for veto in UK
Testing facility in **Napoli**

Radiopure ~2mBq/PMD dominated by substrate and PCB
High **PDE** (~45%) >90% fill factor
Gain ~ 10⁶
Dark Count rate at 87 K < 5 cps/PMD
Time **resolution** (sigma) ~10 ns
Low power consumption < 100 μW/mm²

DarkSide-20k: backgrounds and sensitivity



Background source	Mitigation strategy
^{39}Ar β decay	Use Ar from Underground source (UAr) + Pulse Shape Discrimination (PSD)
γ from rocks and γ , β - from materials	Pulse Shape Discrimination (PSD) Selection of materials & procedures
Neutrons Radiogenic n (α, n) with a from material contaminants	Material screening. Definition of Fiducial Volume in the TPC + active VETO to reject n signal.
Surface contamination due to Rn progeny	Surface cleaning Reduce the number of surfaces Installation in Rn abated air
Neutrino coherent scattering	irriducible



Xenon time projection chambers: past experiments



XENON100 at LNGS

161 kg LXe
(~50 kg fiducial)

242 1-inch PMTs



XENON1T at LNGS

3.3 t LXe
(1000 kg fiducial)

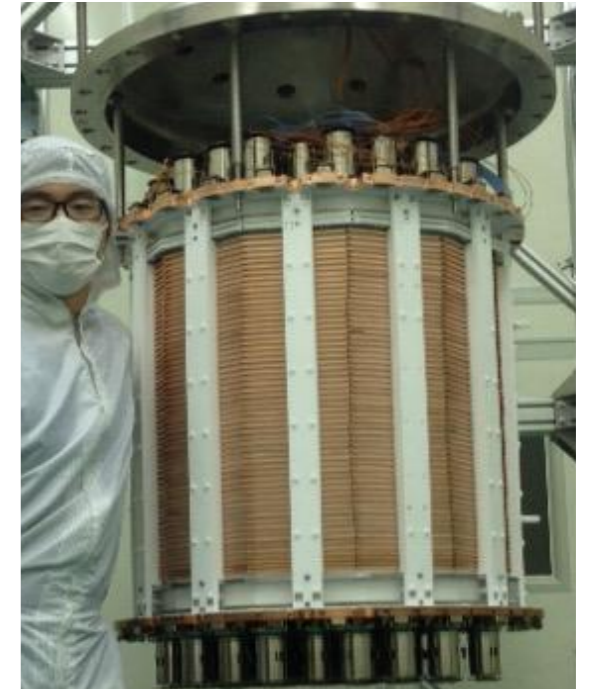
248 3-inch PMTs



LUX at SURF

350 kg LXe
(100 kg fiducial)

122 2-inch PMTs



PandaX-II at Jinping

500 kg LXe
(306 kg fiducial)

110 3-inch PMTs

The XENON1T experiment at LNGS

Water tank &
Cherenkov μ veto

Cryostat &
support
structure for TPC

Time projection
chamber

Cryogenics pipe
(cables, xenon)



Cryogenics &
purification

DAQ,
slow control

Xe storage,
handling &
Kr, Rn removal
via cryogenic
distillation

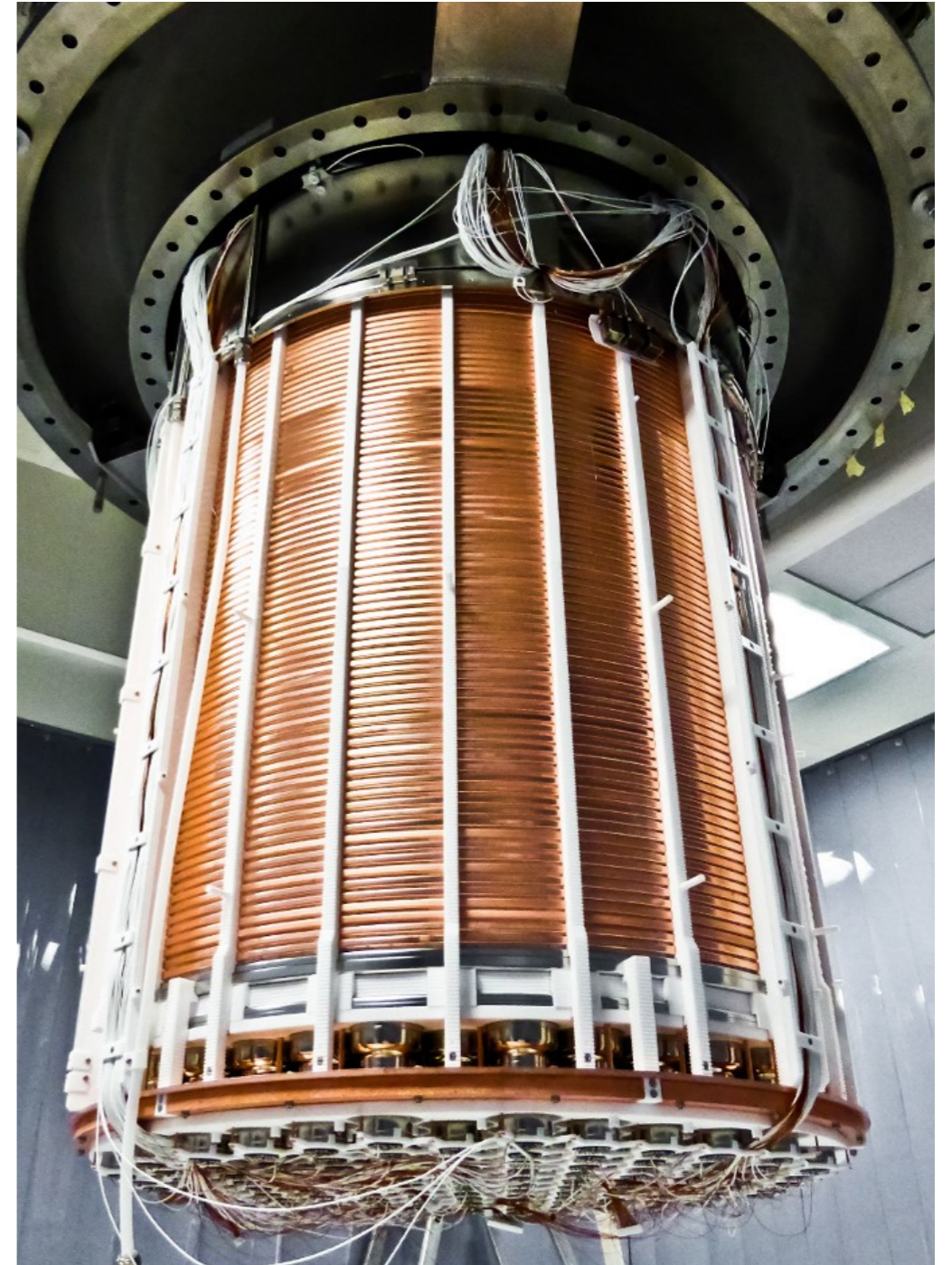
The XENON1T TPC

XENON, EPJ-C 77 (2017) 12

- 3.2 t LXe in total, 2 t in the TPC
- 97 cm drift, 96 cm diameter
- 248 3-inch PMTs
- 74 Cu field shaping rings, 5 electrodes, 4 level meters

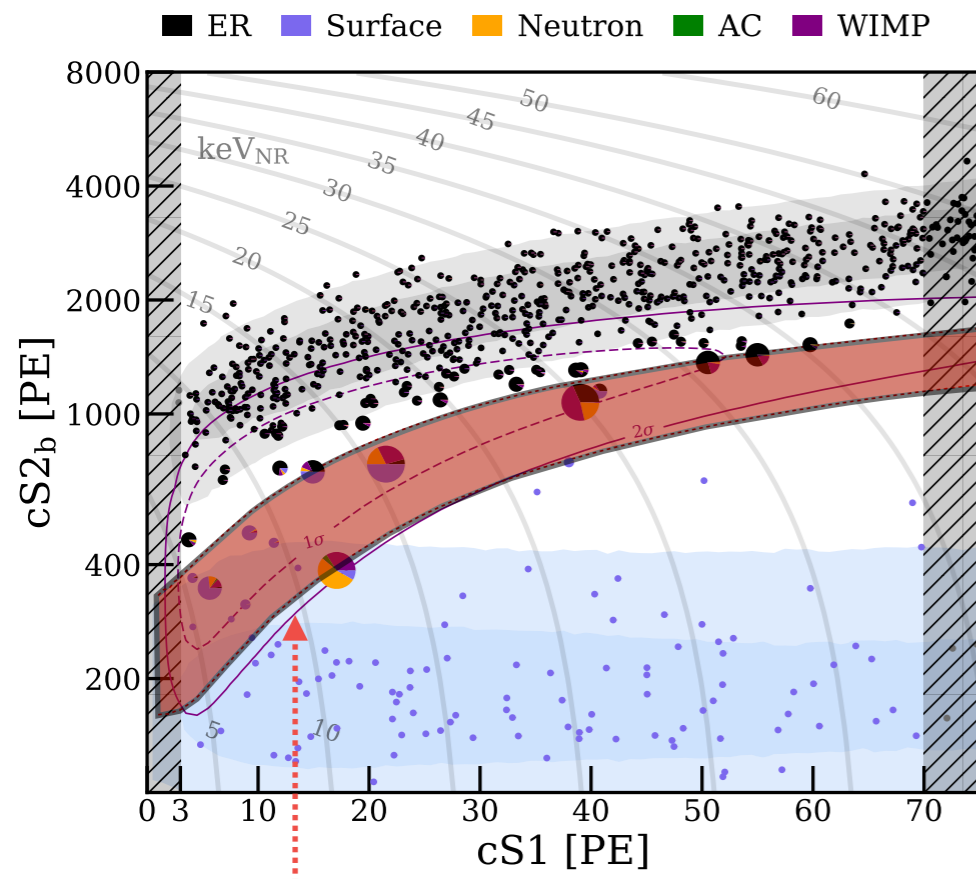
127 PMTs top array

121 PMTs bottom array



XENON1T: nuclear recoil searches

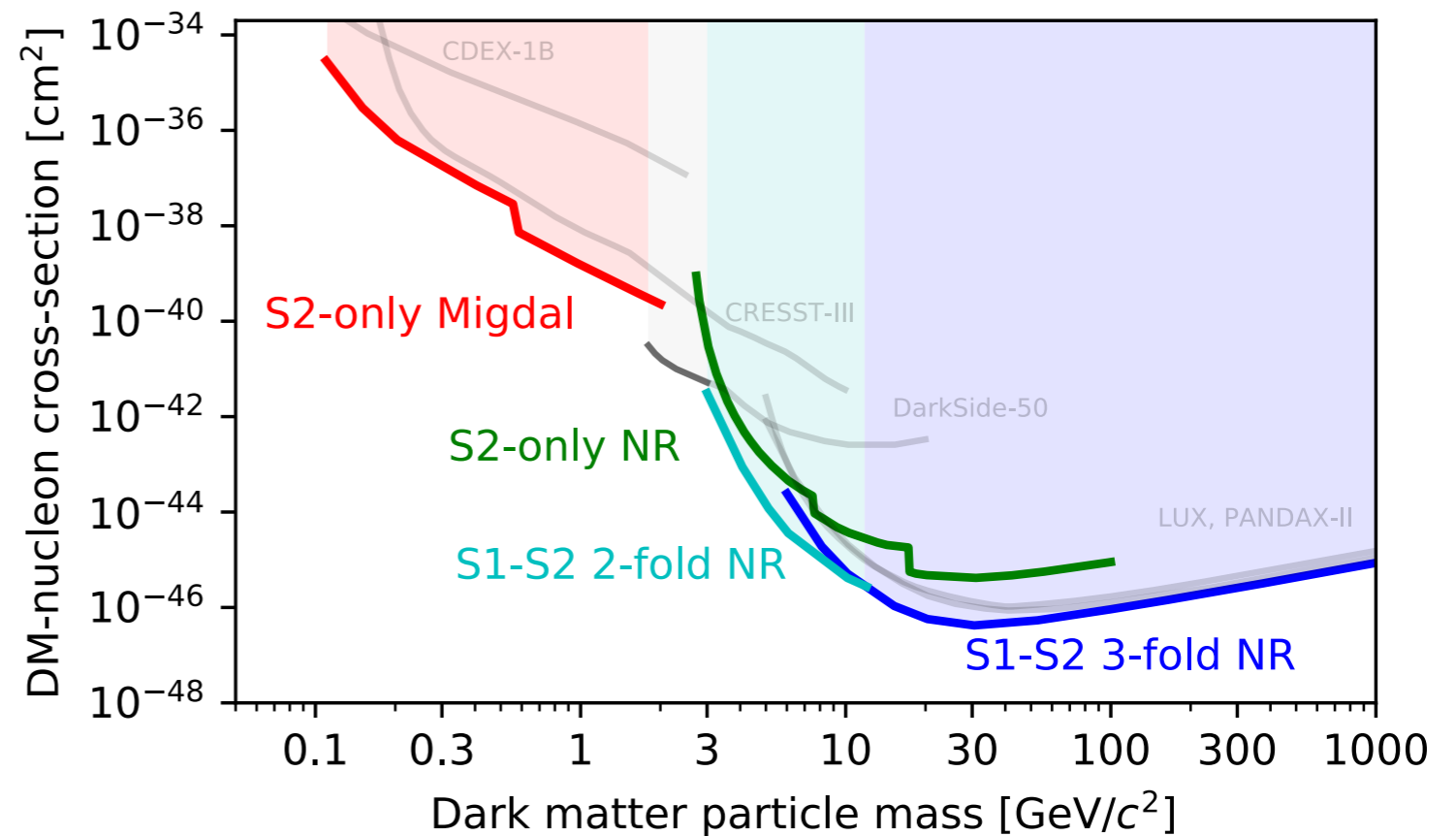
XENON collaboration, PRL 121, 111302 & PRL 123, 251801, PRL 126, 091301



signal region

Energy threshold: 4.9 keV NR
 Exposure: 1 tonne x year (1.3 t fiducial mass, 278.8 live days)

$$\sigma_{SI} < 4.1 \times 10^{-47} \text{ cm}^2 \text{ at } 30 \text{ GeV}/c^2$$

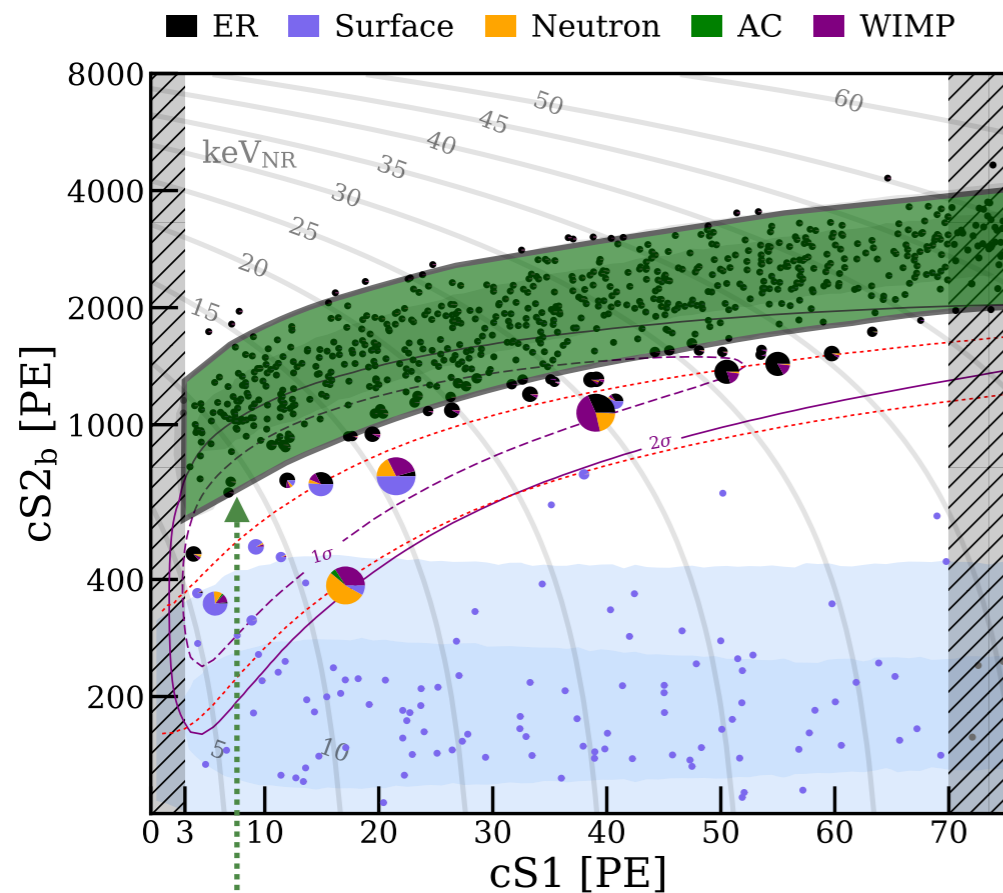


Most stringent constraints on WIMP-nucleon cross section down to ~3 GeV masses

XENON1T: electronic recoil searches

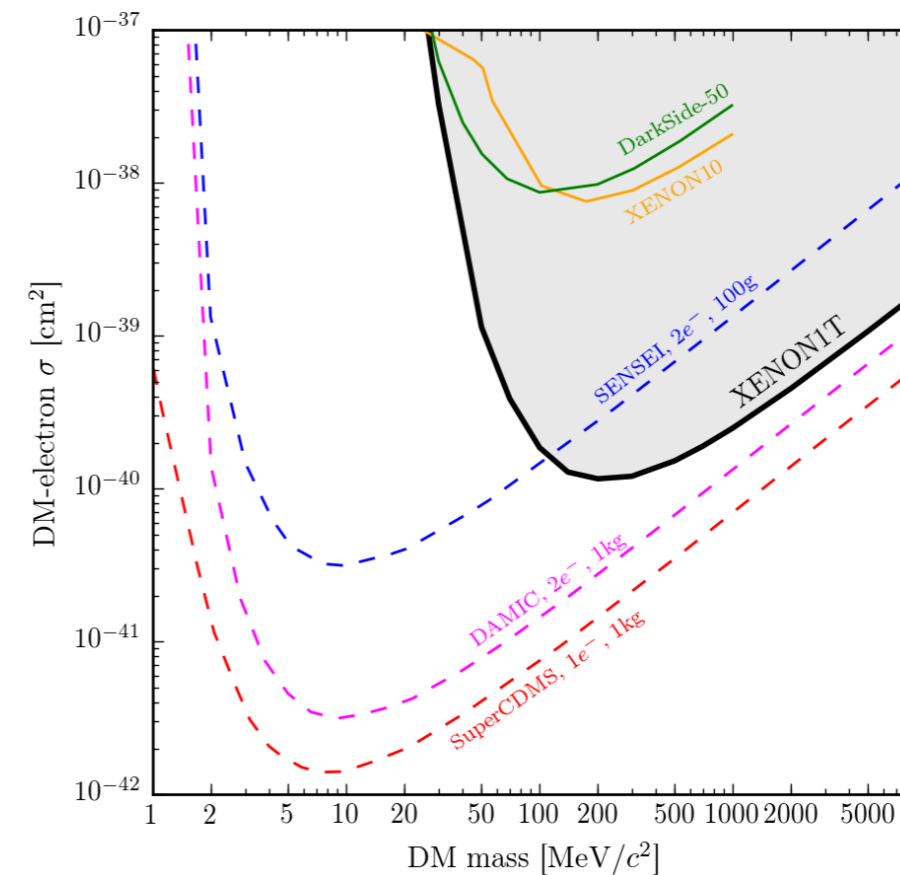
XENON collaboration, PRL 123, 2019

S2-only analysis, DM-e⁻ scattering



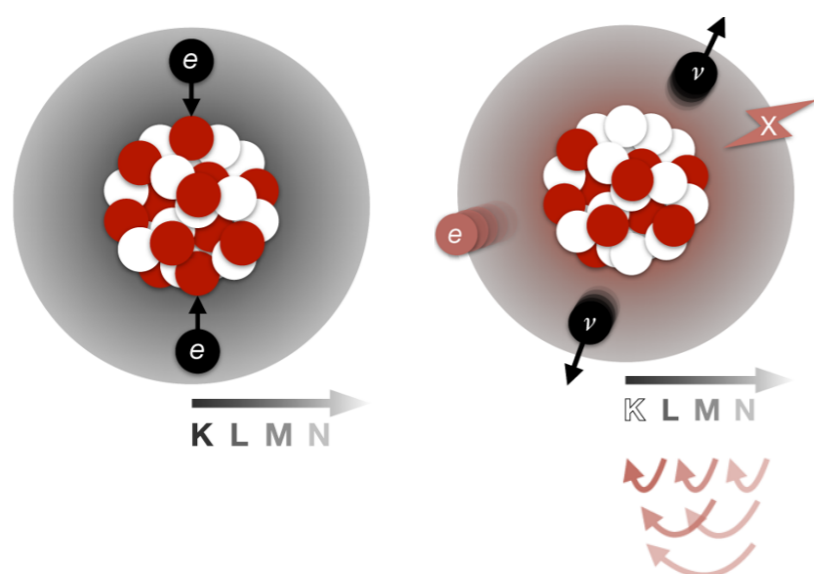
signal region

Energy threshold: 1 keV ER
 Exposure: 1 tonne x year
 Low background: 76 ± 2 events/(t y keV)



Energy threshold: ~ 0.18 keV
 New parameter space excluded for DM masses > 30 MeV

XENON1T: double electron capture



XENON collaboration, Nature 568, April 25, 2019

nature

THE INTERNATIONAL WEEKLY JOURNAL OF SCIENCE



SEX AND SENIOR
TRANSITIONAL INSIGHTS
The world's largest study of transgender people
PAGE 44

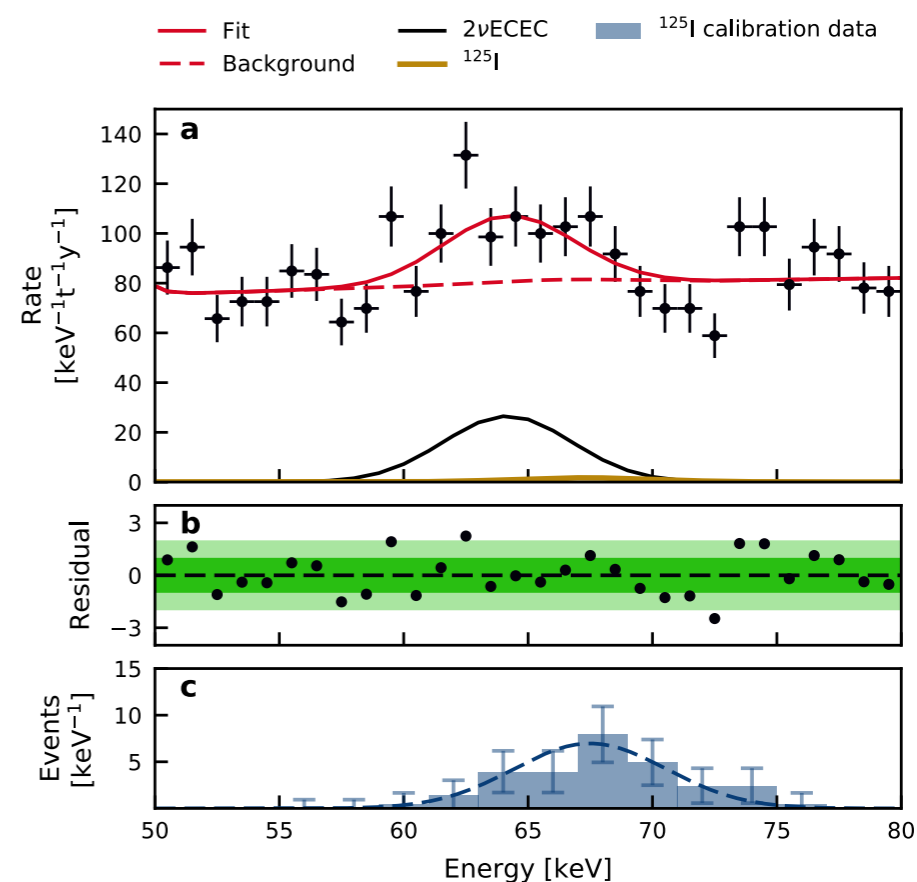
ENVIRONMENT
IN THE DARK
How high-rise living deprives urban centres of natural light
PAGE 41

NEUROSCIENCE
SPEECH SYNTHESIZER
Implant gives voice to brain signals that control movement
PAGE 404

NATURE.COM
25 April 2019
ISSN 0959-462X

$$T_{1/2} = (1.8 \pm 0.5_{\text{stat}} \pm 0.1_{\text{sys}}) \times 10^{22} \text{ y}$$

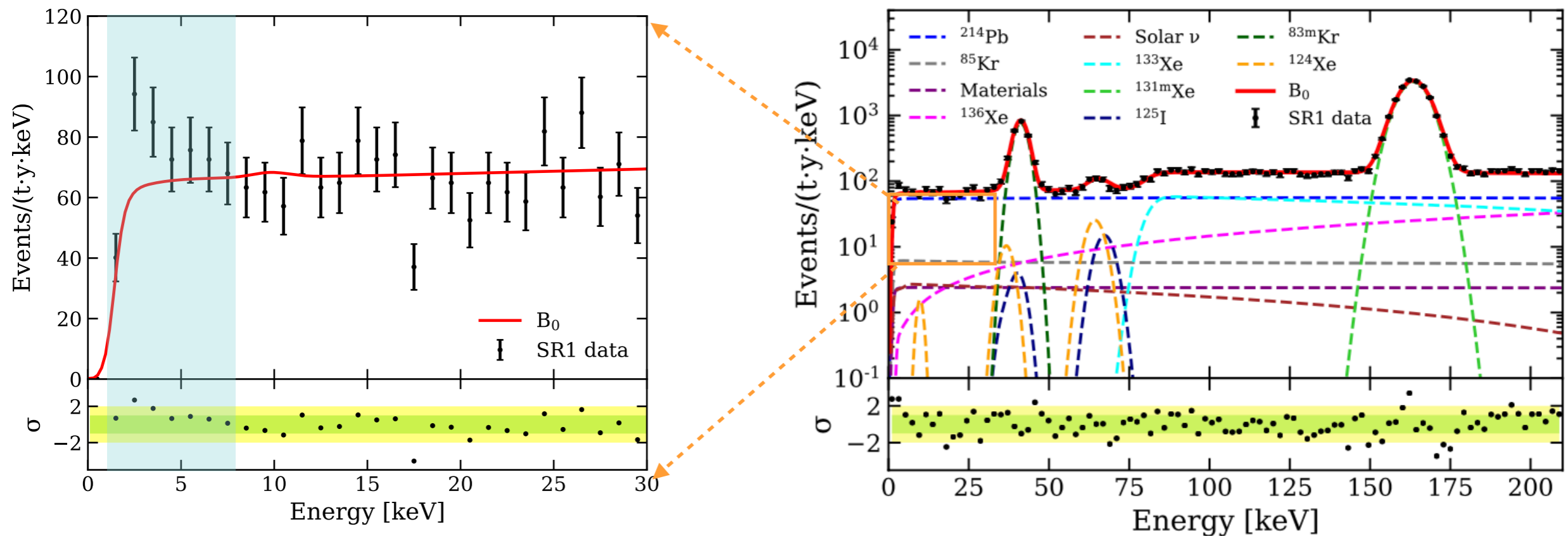
- ^{124}Xe in natXe : 0.095% \Rightarrow 1 t $\text{natXe} \approx$ 1 kg ^{124}Xe
- Total obs energy: 64.33 keV (2 x K-shell binding energy, Q-value: 2.96 MeV)
- Blind analysis: (56-72) keV region masked
- Signal events: (126 ± 29) , expected bg from ^{125}I : (9 ± 7) events (at 67.5 keV)



$$\sigma/E = (4.1 \pm 0.4)\% \text{ at } 64 \text{ keV}$$

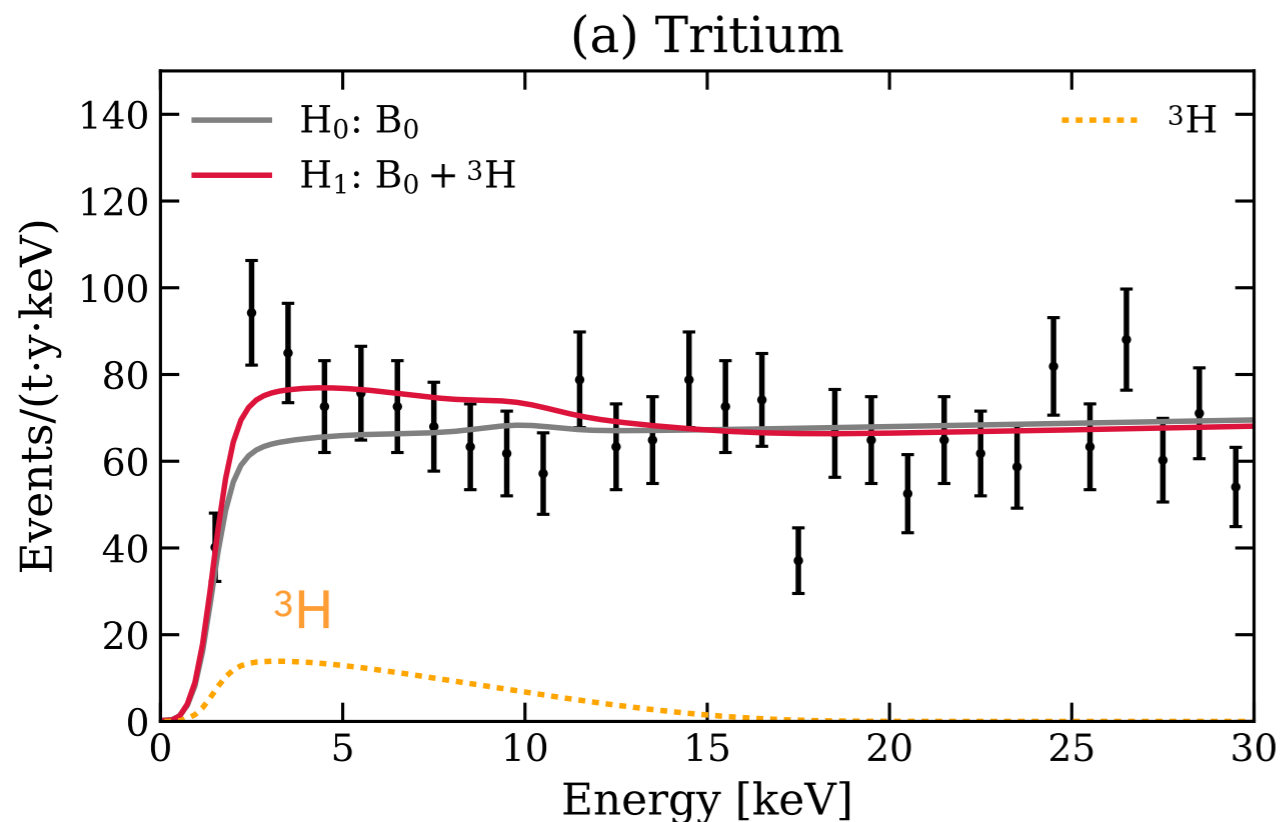
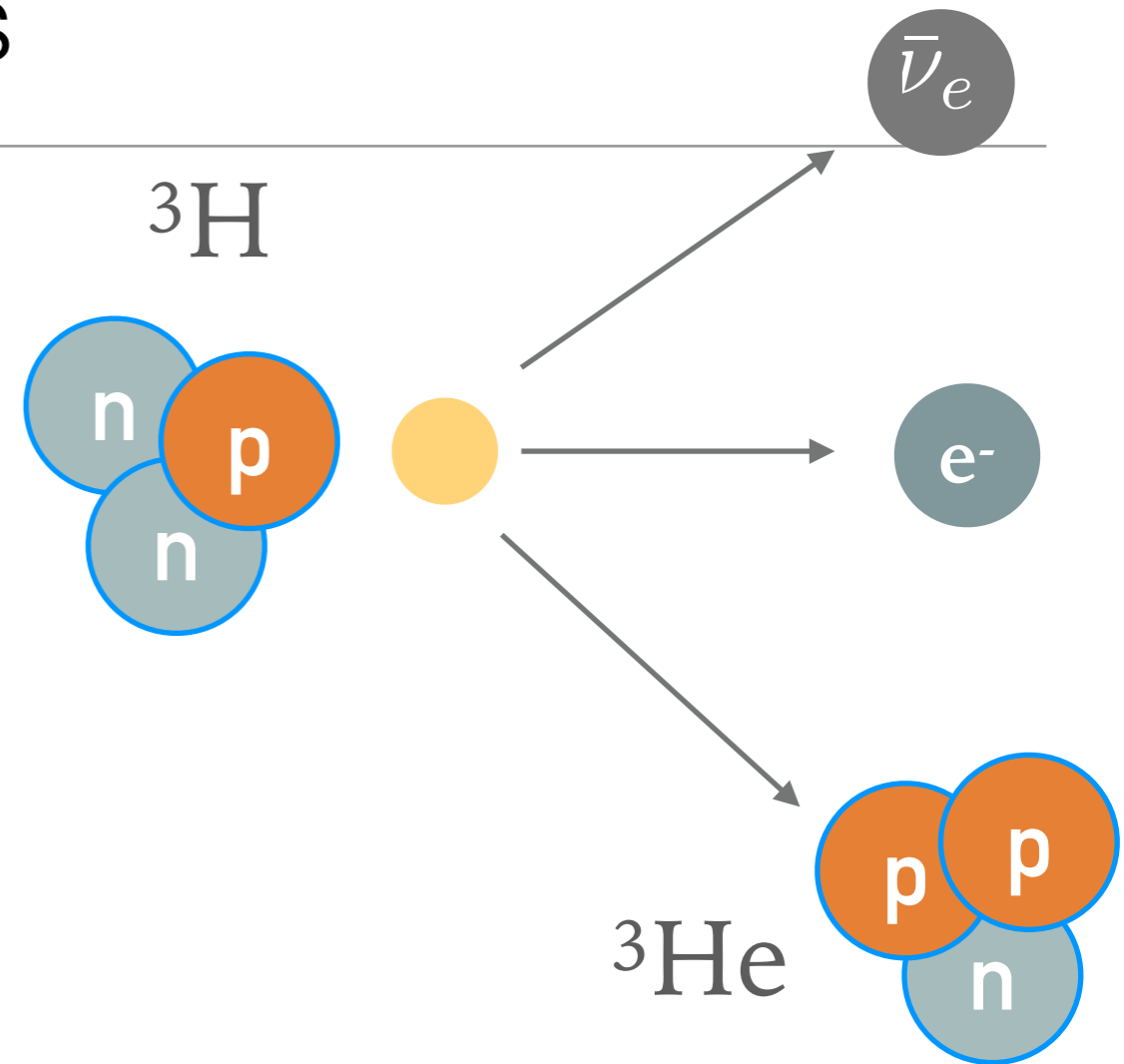
XENON1T: low-energy excess

- Background model: good fit over most of the energy region
- Excess between (1,7) keV
- 285 events observed, (232 ± 15) expected from background (3.3σ fluctuation by naive estimate)



XENON1T: low-energy excess

- Tritium decays?
- Low energy β -decay with 18.6 keV endpoint, $T_{1/2} = 12.3$ y
- Cosmogenic production in xenon & emanation of HTO and HT from detector materials
- Removed by continuous gas purification



Best fit: (159 ± 51) events/(t y)

${}^3\text{H}:\text{Xe}$ concentr.: $(6.2 \pm 2.0) \times 10^{-25}$ mol/mol

< 3 ${}^3\text{H}$ atoms per kg of xenon

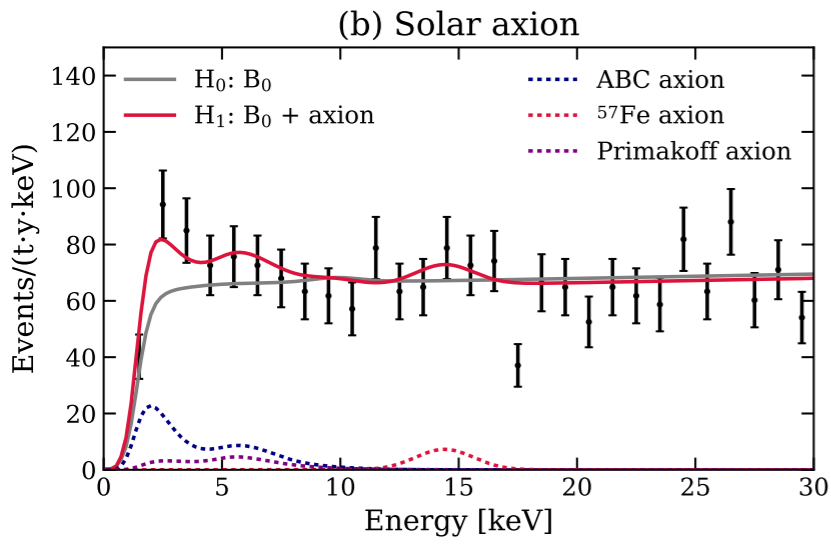
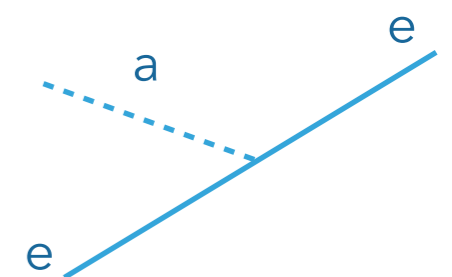
Tritium favoured over background at 3.2σ

XENON1T: low-energy excess

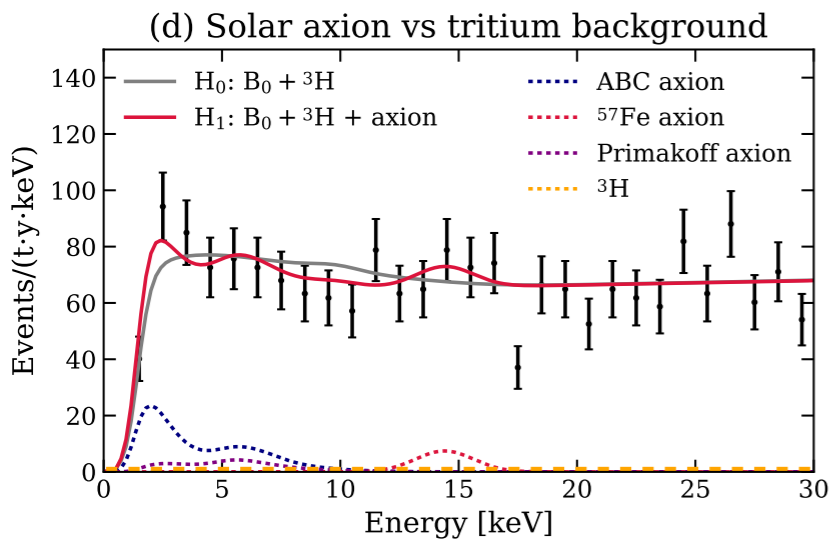
- New physics? Example: solar axions



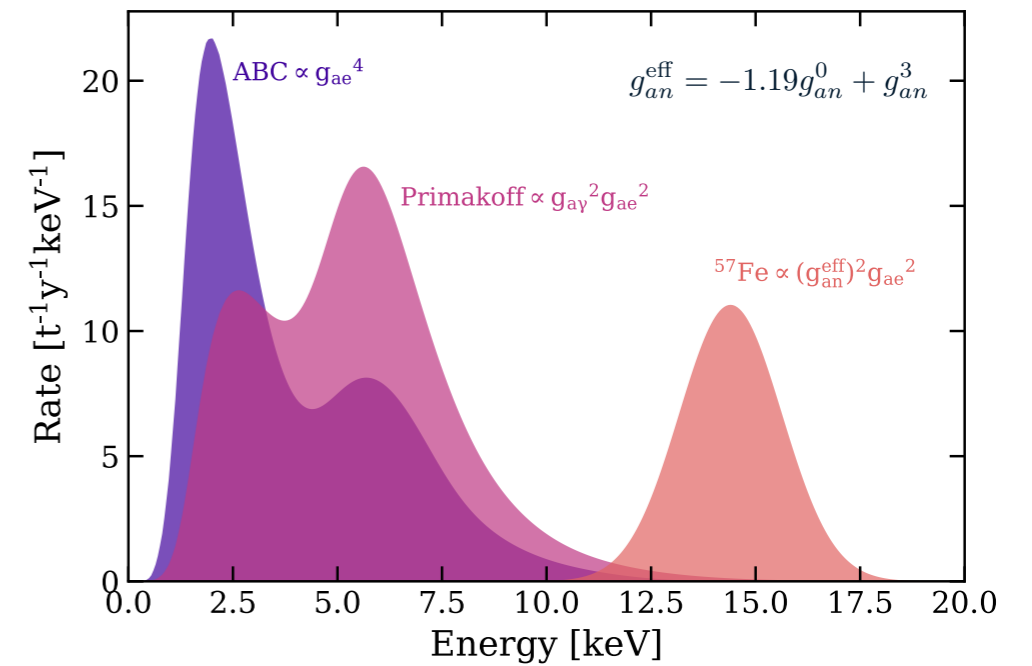
Detection:
Axioelectric effect



Solar axion:
favoured at 3.4 σ
over background
only



Solar axion + ^3H :
favoured at 2.0 σ over
 ^3H hypothesis

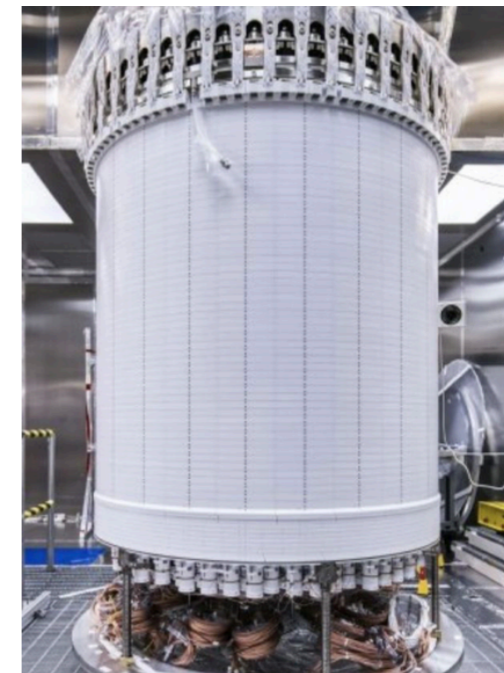


- Null hypothesis: the background model B_0
- Alternative hypothesis: B_0 plus the signal

Xenon time projection chambers: current

- LZ at SURF, PandaX-4T at JinPing, XENONnT at LNGS
- TPC scales: 10 t (LZ), 6 t (PandaX-4T) and 8.6 t LXe (XENONnT) in total
 - TPCs with 2 arrays of 3-inch PMTs
 - Kr and Rn removal techniques
 - Ultra-pure water shields; neutron & muon vetos
 - External and internal calibration sources
- **Status:** PandaX-4T first result from commissioning run at Jinping, LZ science data taking at SURF, XENONnT science data taking at LNGS

LZ



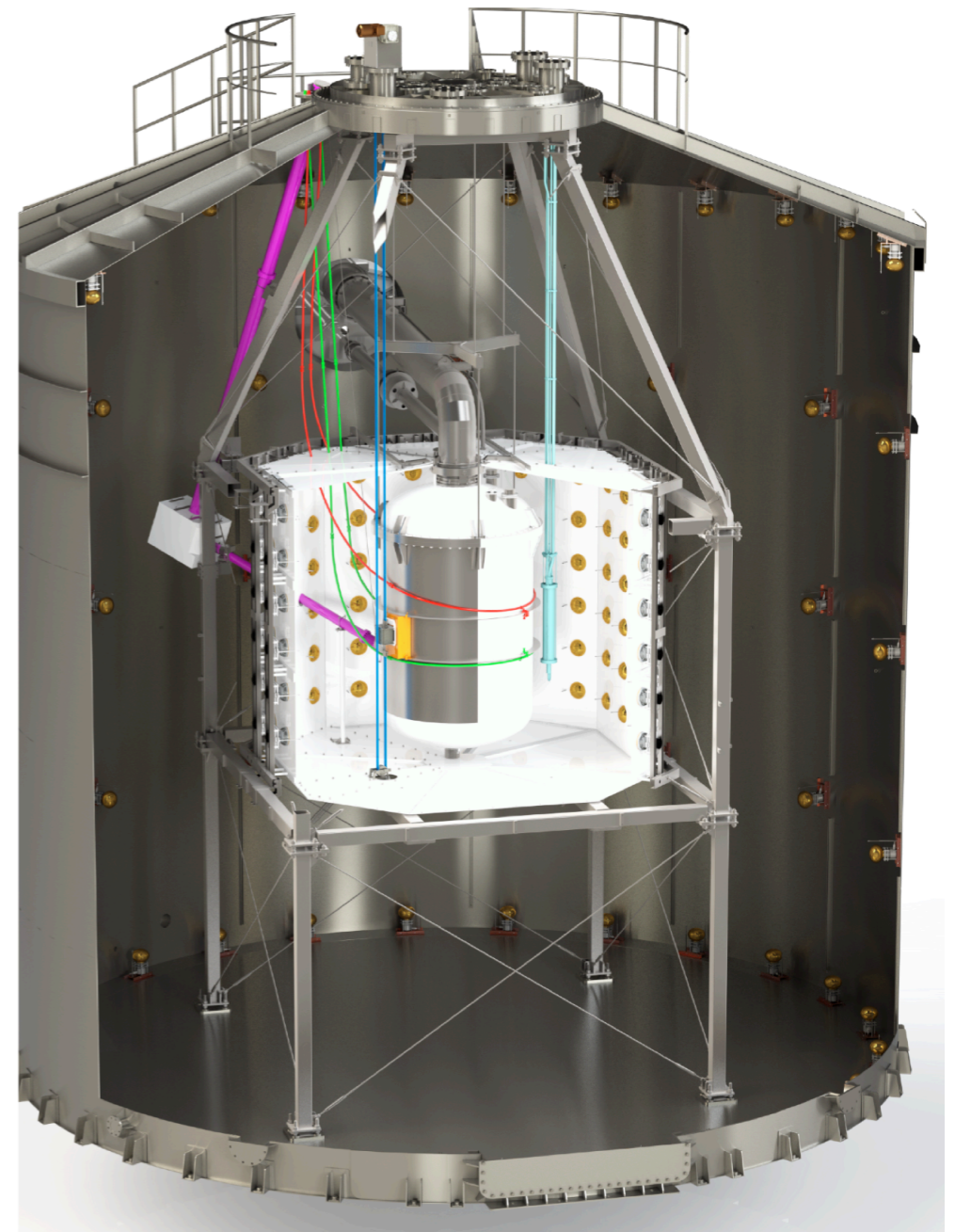
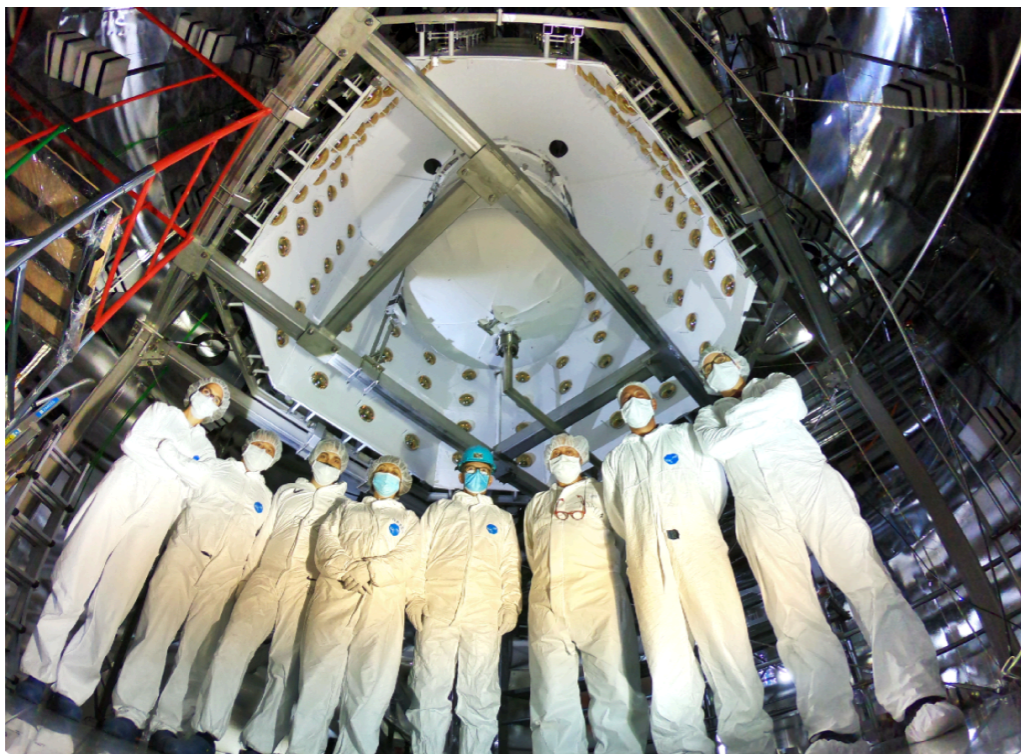
XENONnT



PandaX-4T

XENONnT at LNGS

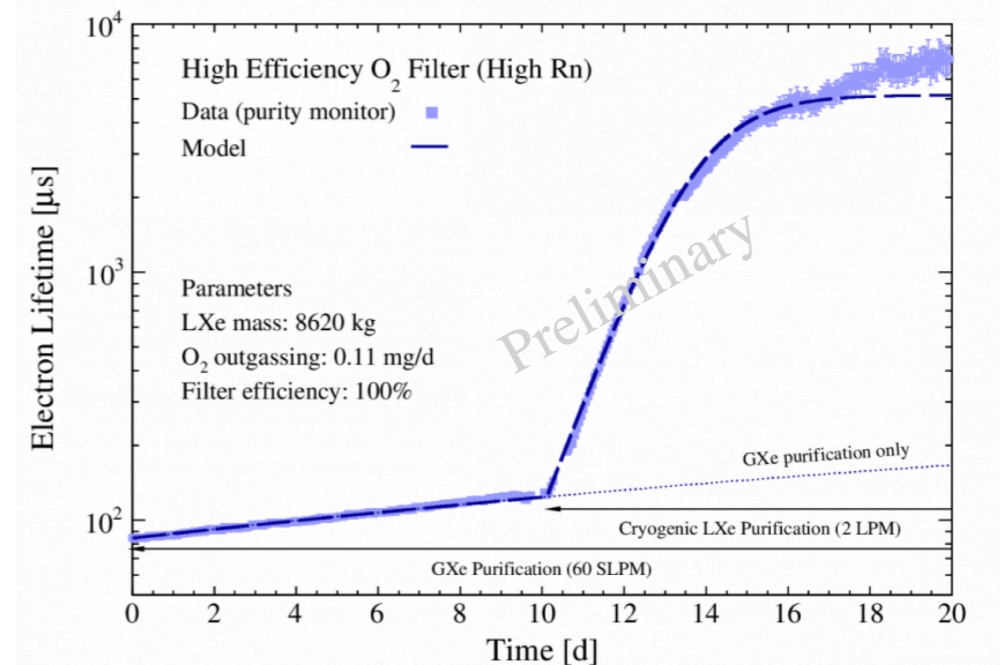
- LXe TPC in double-walled stainless steel cryostat
- Neutron veto: Gd-doped ($0.5\% \text{Gd}_2(\text{SO}_4)_3$) water Cherenkov detector with $\sim 87\%$ neutron tagging efficiency
- Goal is < 1 untagged neutron for 20 t yr exposure
- Muon veto: water Cherenkov detector, 700 t of ultra-pure water



XENONnT at LNGS

- Liquid xenon purification: direct LXe circulation with cryogenic pump; fast flow rate, ultra-low Rn emanation system: > 10 ms
- Radon removal system: cryogenic distillation column, designed to achieve $< 1 \mu\text{Bq/kg}$

LXe purification system (5 L/min LXe, faster cleaning; 2500 slpm)

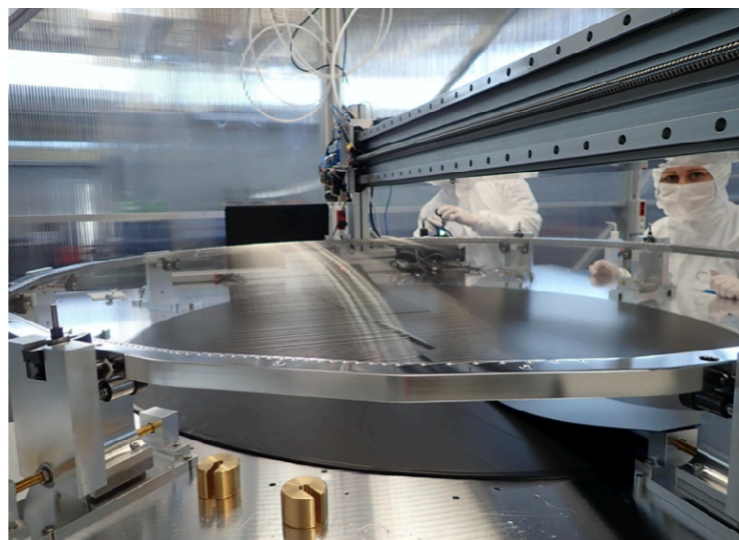


Rn distillation column (reduce ²²²Rn - hence also ²¹⁴Bi - from pipes, cables, cryogenic system)



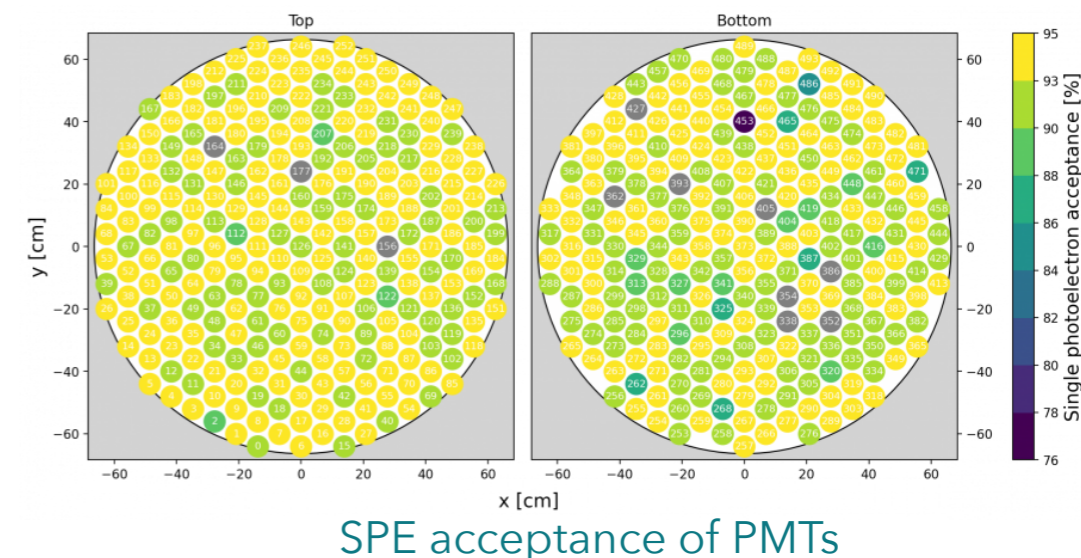
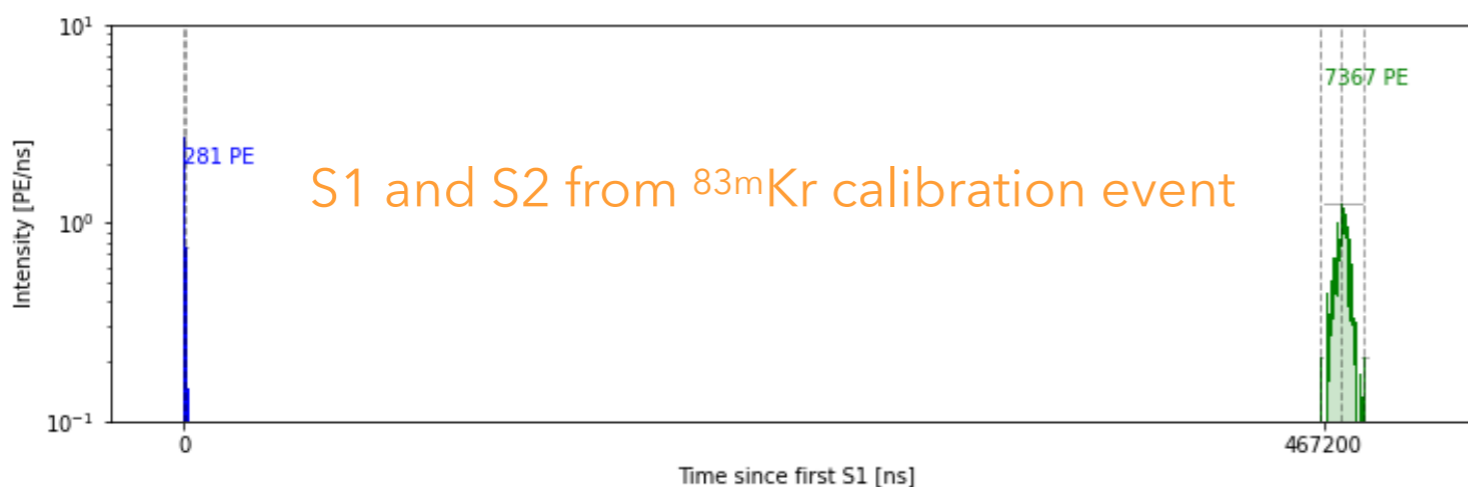
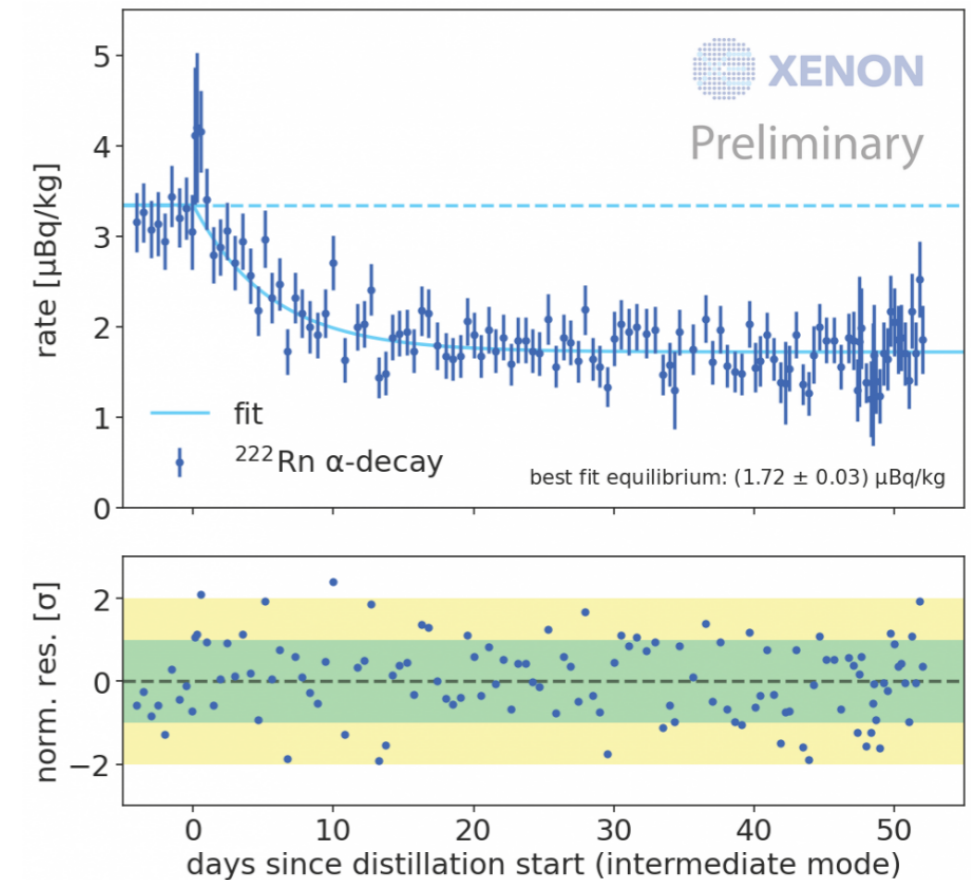
The XENONnT time projection chamber

- 8.6 t LXe in total, 5.9 t in the TPC
- 150 cm drift, 130 cm diameter
- 494 3-inch PMTs
- Cu field shaping rings, 5 electrodes, 4 level meters
- Low-energy background: 1/6 of XENON1T



XENONnT status

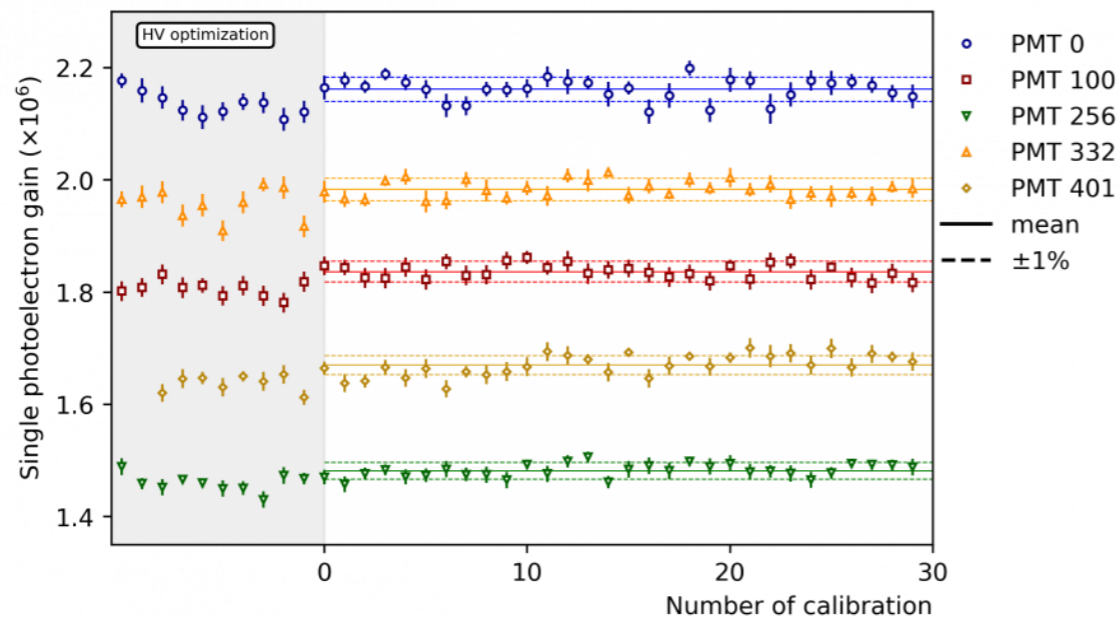
- ▶ All new systems (TPC, liquid purification system, neutron veto, radon distillation column) running smoothly at LNGS
 - Electron lifetime*: > 10 ms (0.6 ms in XENON1T), at 2.2 ms maximum drift time
 - ^{222}Rn level due to initial gas phase only distillation: 1.7 $\mu\text{Bq/kg}$ (aiming for 1 $\mu\text{Bq/kg}$ in current run)
- ▶ First science run started summer 2021, analysis in progress; second science run ongoing



*e-lifetime: a measure of the charge that is lost during e-drift to liquid/gas interface

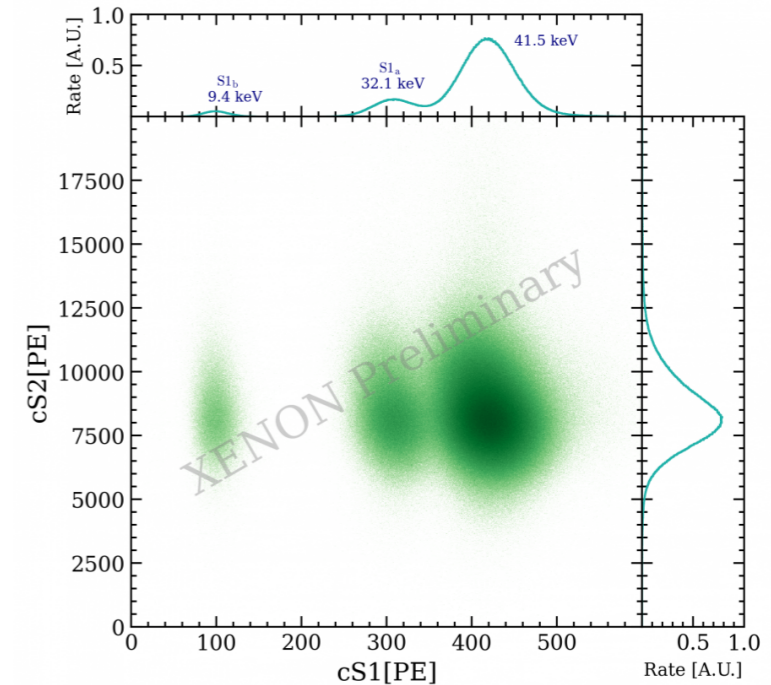
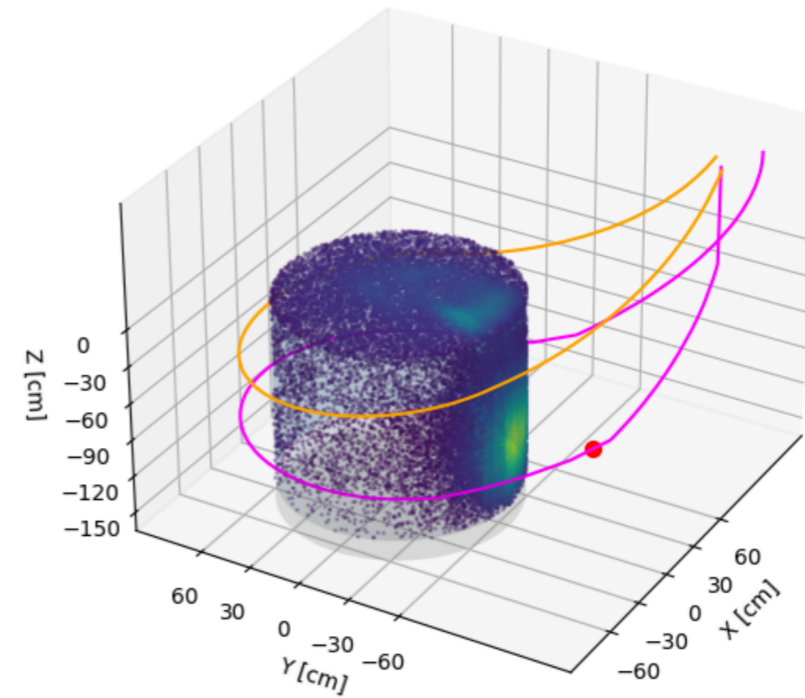
XENONnT calibrations

- ▶ XENONnT's 5.9 t sensitive LXe volume is calibrated from keV to MeV
 - ◉ ^{83m}Kr : uniformity, light & charge yields
 - ◉ ^{220}Rn : low-energy ERs
 - ◉ AmBe: low-energy NRs, high-energy ERs
 - ◉ Regular calibration of PMT gains etc



Single photoelectron gain of 5 random PMTs

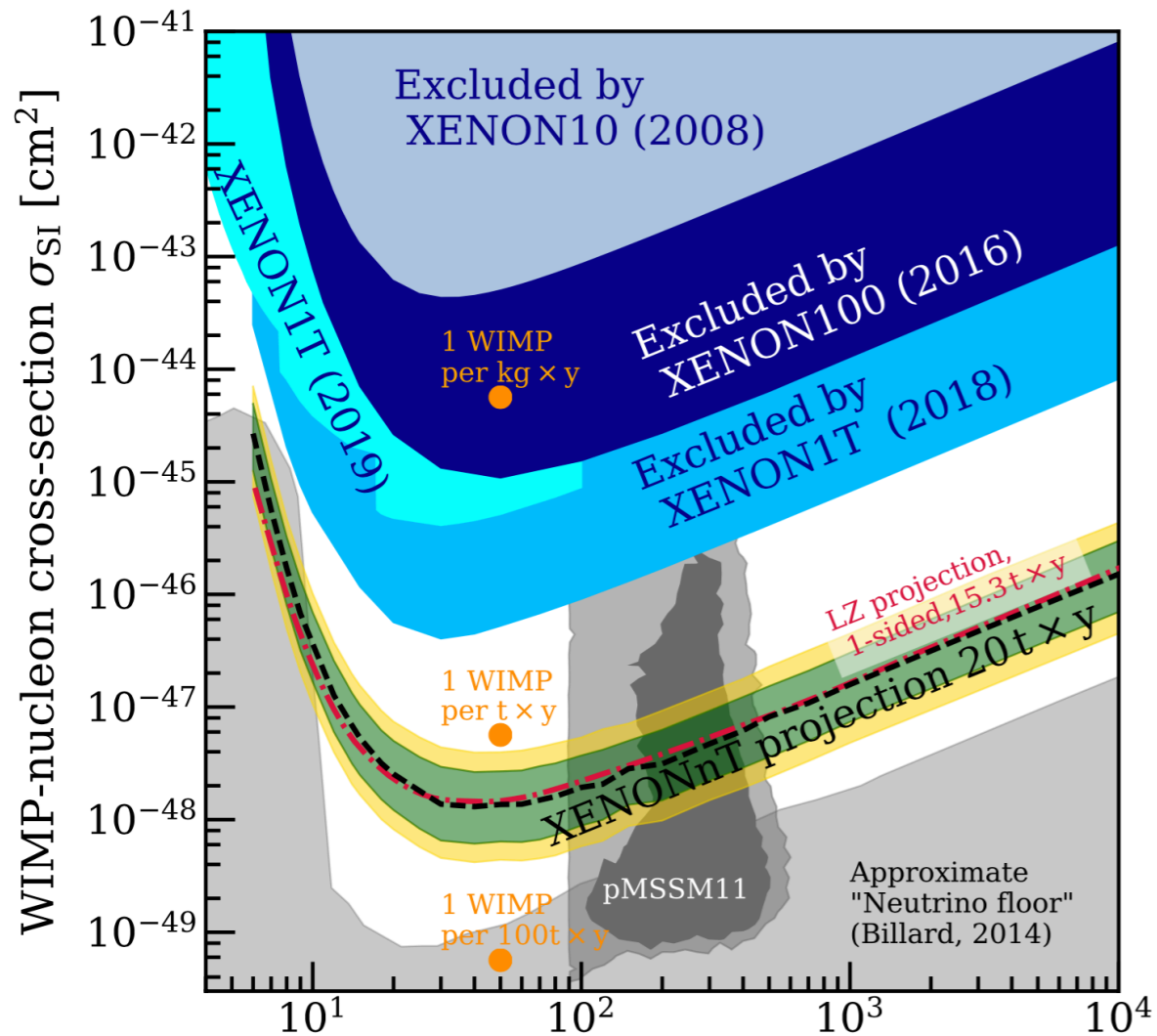
AmBe calibration



S1 and S2 from ^{83m}Kr calibration

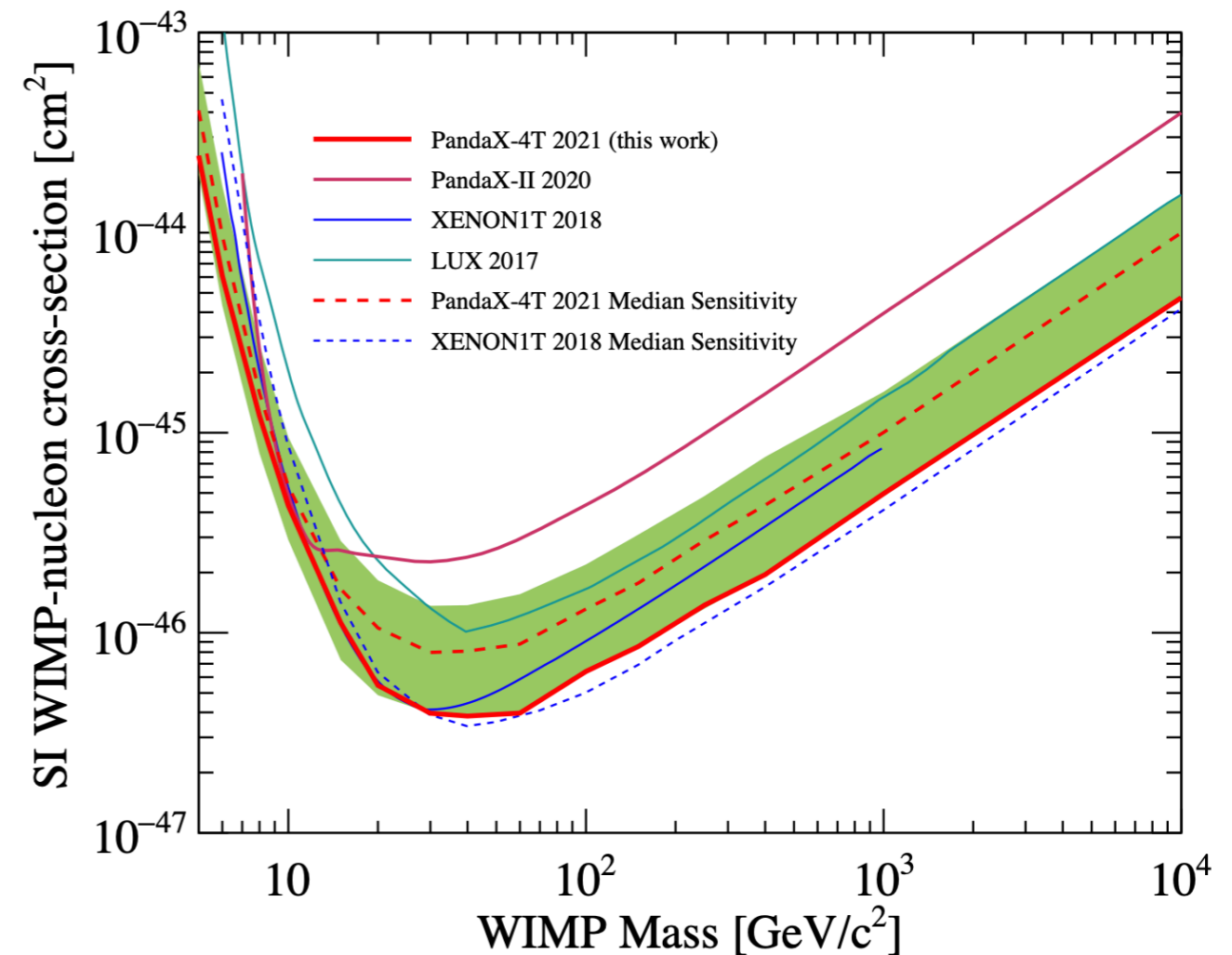
LXe TPCs: dark matter sensitivity

LZ and XENONnT sensitivity projections



PandaX-4T first results from commissioning run, 0.63 t y exposure

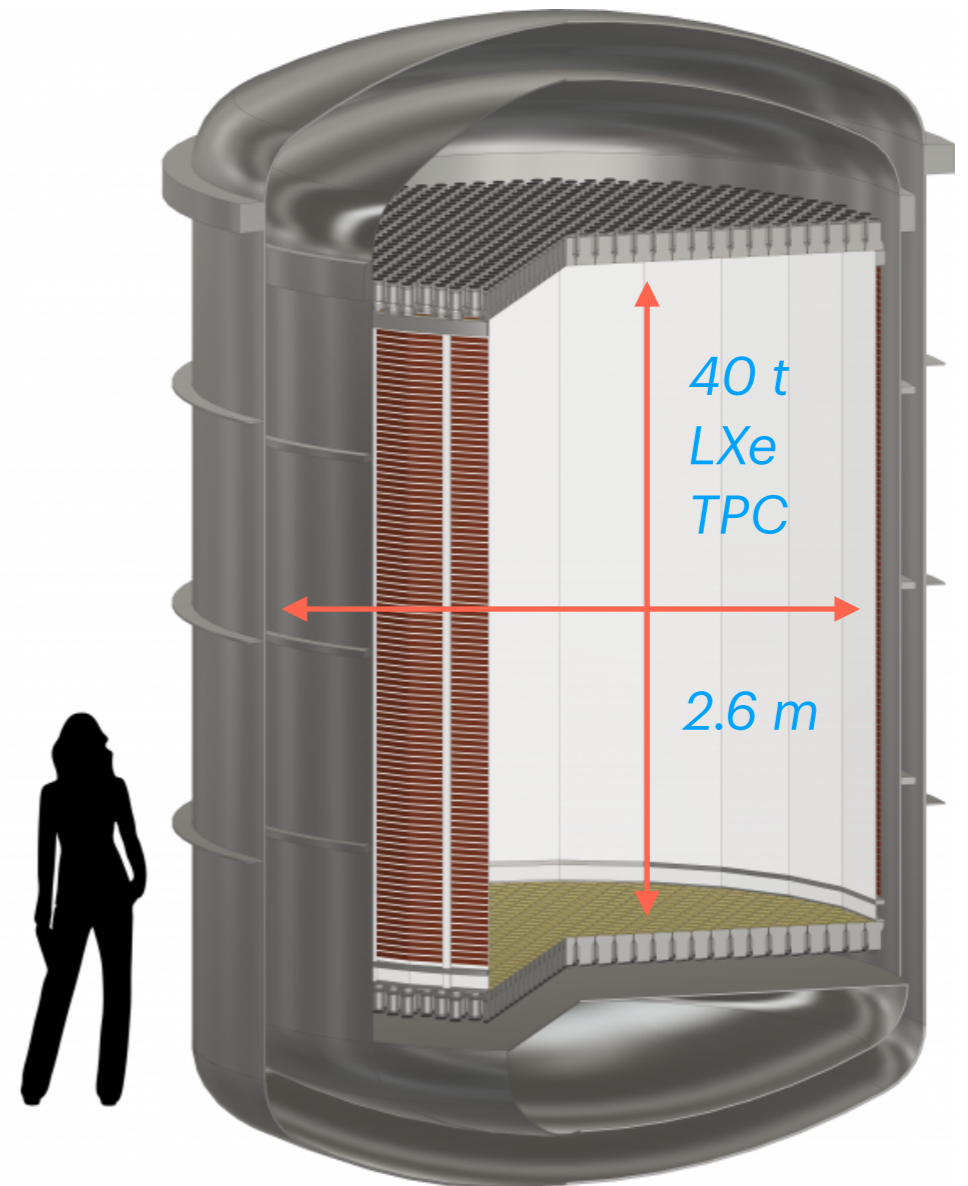
$$\sigma < 3.8 \times 10^{-47} \text{ cm}^2 \text{ at } 40 \text{ GeV}$$



Future xenon TPC: DARWIN

- Two-phase xenon TPC with 2.6 m \varnothing and 2.6 m height in a double-walled cryostat
- 50 t (40 t active) liquid xenon target
- Top & bottom arrays of photosensors (e.g., 1800 3-inch PMTs)
- PTFE reflectors and Cu field shaping rings
- Target drift field: ~ 200 V/cm
- Min 12 m x 12 m water Cherenkov shield (Gd-doped, as n- and μ -vetos)

Alternative TPC designs and photosensors under consideration

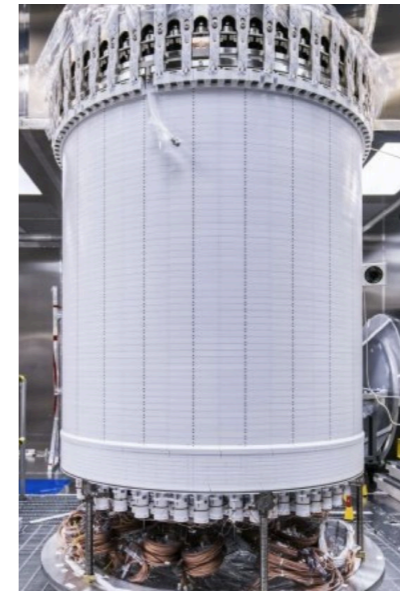


DARWIN collaboration
JCAP 1611 (2016) 017

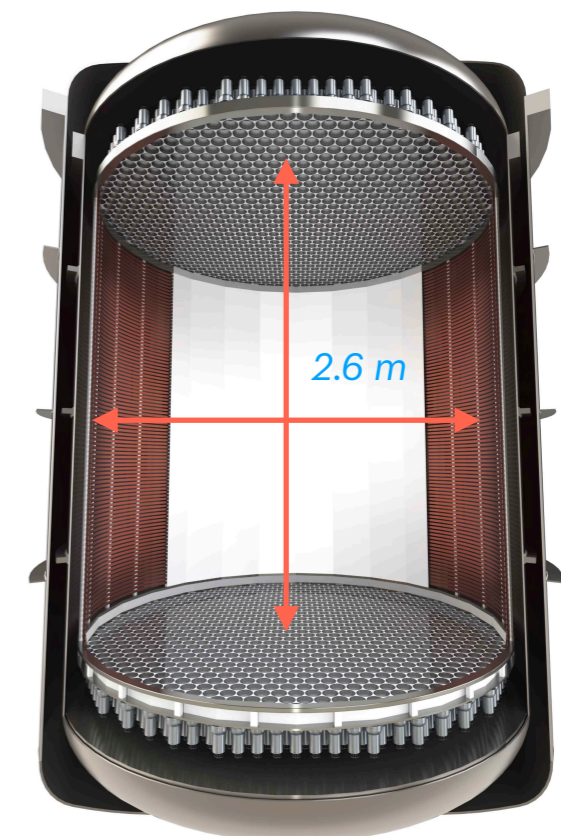
Size matters

- LUX-ZEPLIN and XENONnT: 1.5 m e⁻ drift and ~1.5 m diameter electrodes
- **DARWIN: 2.6 m ⇒ new challenges**
 - Design of electrodes: robustness (minimal sagging/deflection), maximal transparency, reduced e⁻ emission
 - Electric field: ensure spatial and temporal homogeneity, avoid charge-up of PTFE reflectors
 - High-voltage supply to cathode design, avoid high-field region
 - Liquid level control
- Electron survival in LXe: > 10 ms lifetime*
- Diffusion of the e⁻-cloud: size of S2-signals

LUX-ZEPLIN



XENONnT



DARWIN

*G. Plante, E. Aprile, J. Howlett, Y. Zhang, 2205.07336

R&D topics

Detector design and time projection chamber

- demonstrate e^- drift over large distances, electrodes with 2.6 m diameter; high-voltage feedthroughs
- study alternative designs: sealed/hermetic TPC (to prevent radon diffusion into inner volume), single-phase TPC (simplify detector design, mitigate single e^- background)
- cryostat design: stability, reduce amount of material (hence gamma and neutron emitters) close to TPC

Photosensors

- baseline: VUV-sensitive, low-radioactivity PMTs (established technology, low dark count rate of ~ 0.02 Hz/mm²)
- study low-field SiPMs, digital SiPMs & hybrid photosensors; also, low-noise, low heat dissipation, low-radioactivity readouts

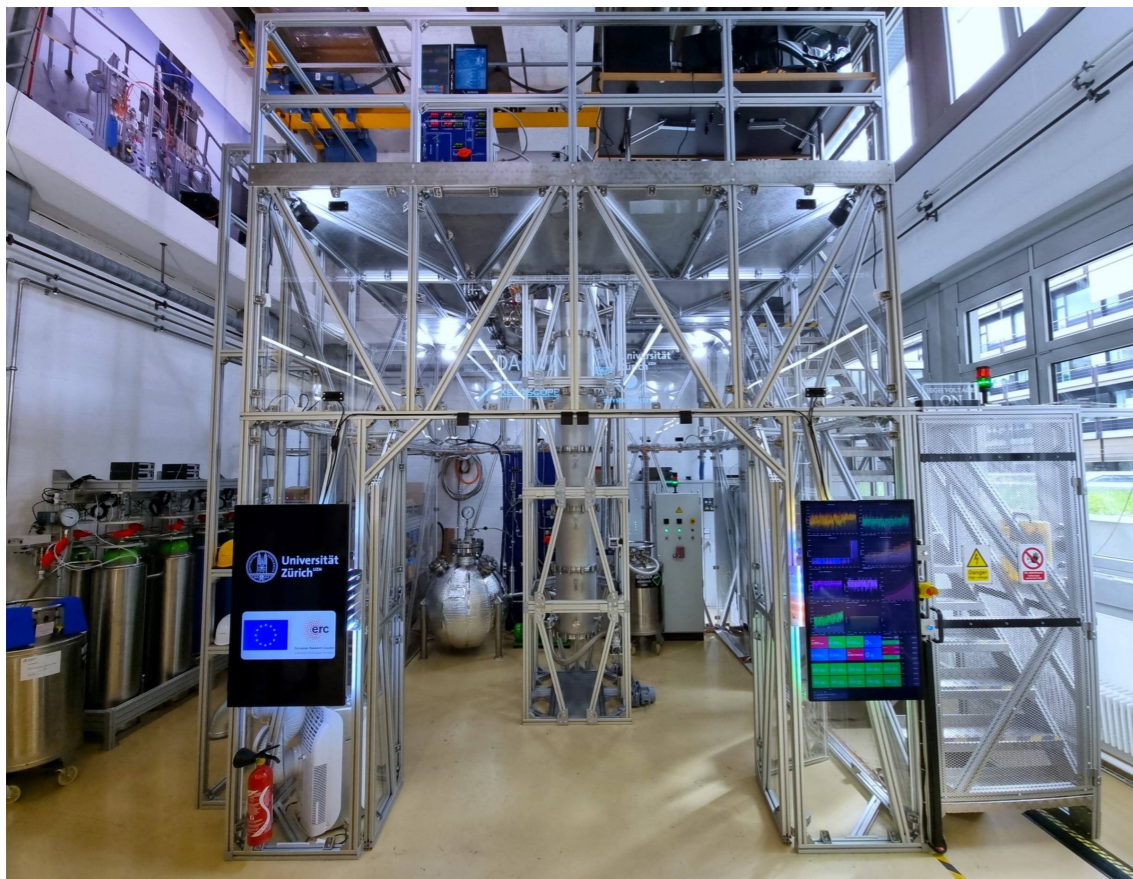
Target and background control

- fast purification for large e^- lifetime, large distillation columns for low ²²²Rn and ⁸⁵Kr levels
- "radon-free" circulation pumps; coating techniques to avoid radon emanation (electrochemical, sputtering, epoxy based); storage and recuperation of large amounts of xenon
- identification of low-radioactivity material components

Detector demonstrators

- Two large-scale demonstrators, in z and in x-y, supported by ERC grants
 - *Xenoscope*, 2.6 m tall TPC and *Pancake*, 2.6 m \varnothing TPC in double-walled cryostats
 - Both facilities available to the collaboration for R&D purposes

Vertical demonstrator: *Xenoscope*



Horizontal demonstrator:



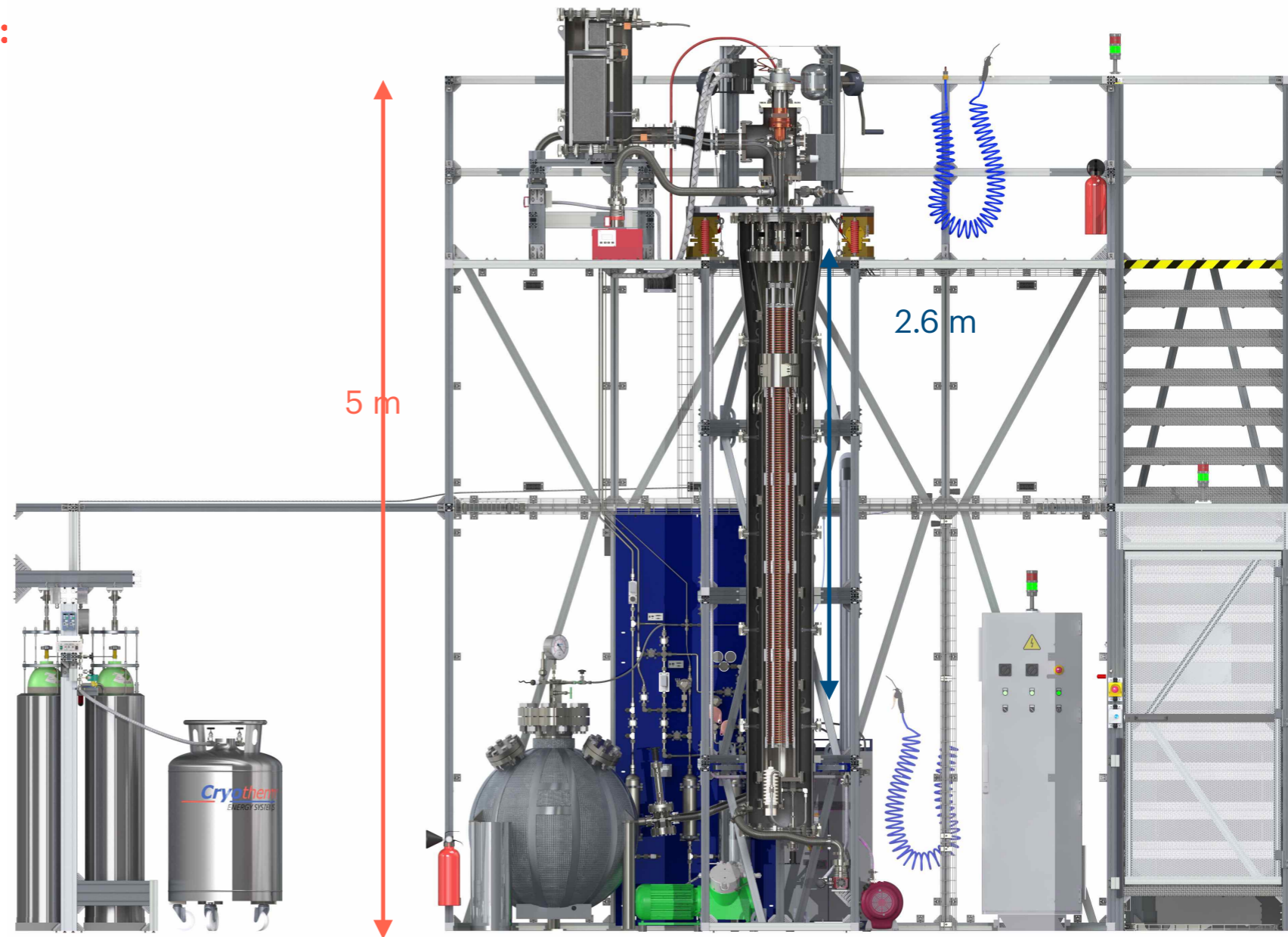
Xenoscope overview

○ Full-height demonstrator goals:

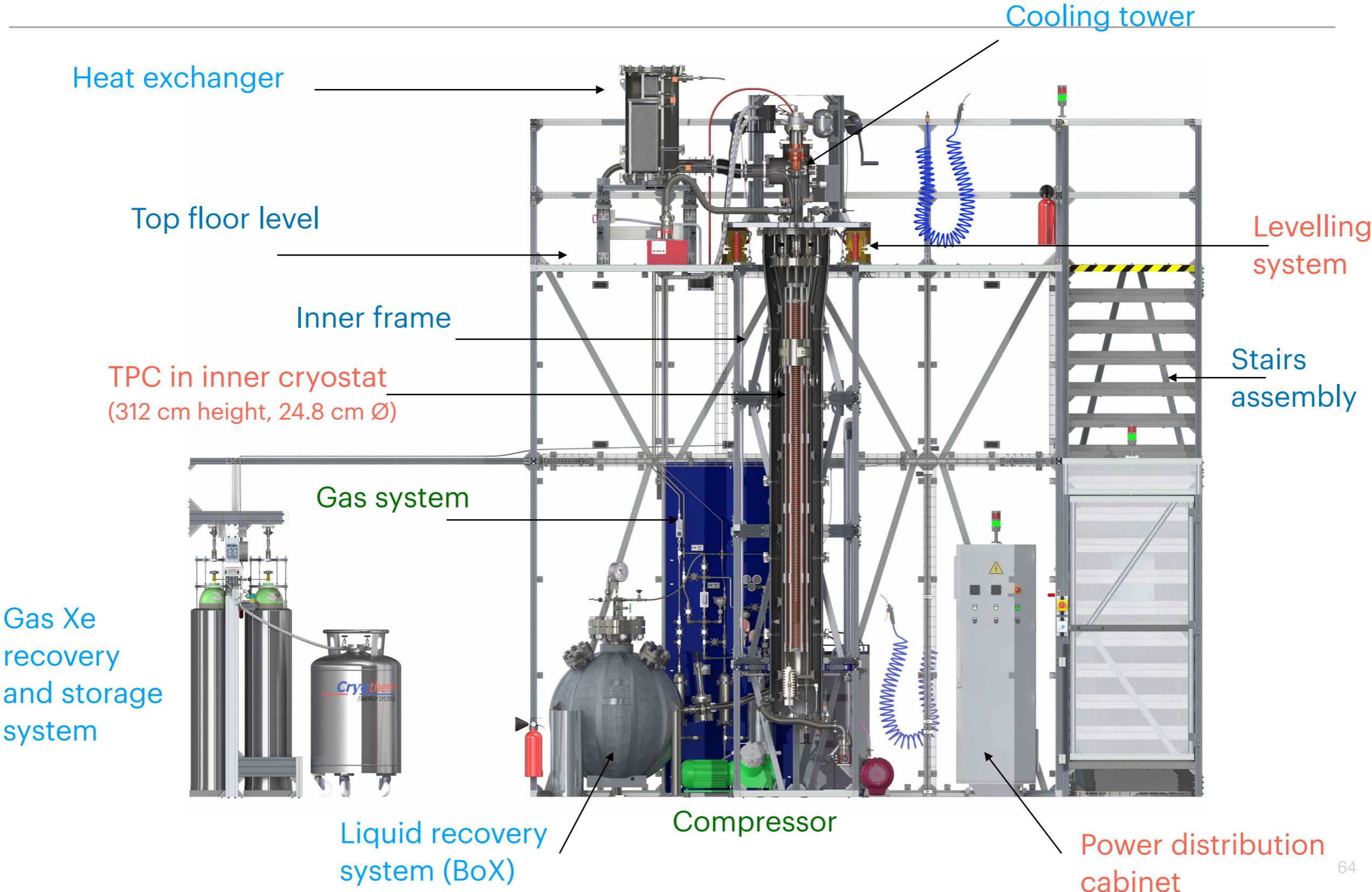
- Electron drift > 2.6 m
- Custom-made HV distribution
- Electron cloud diffusion
- Light attenuation measurements in LXe
- Test of various light sensors (SiPMs, 2-inch PMTs, ...)

○ Total amount of xenon:

- ~ 400 kg



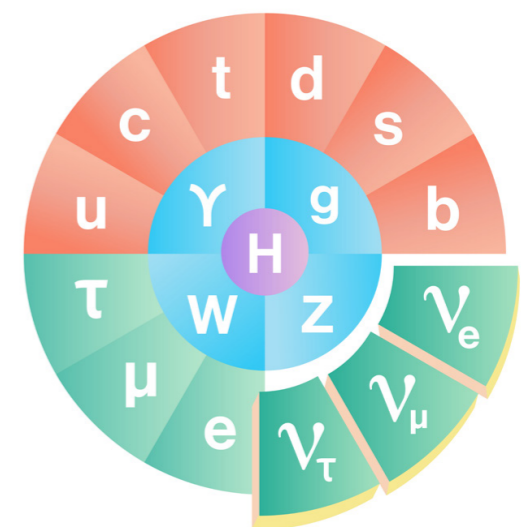
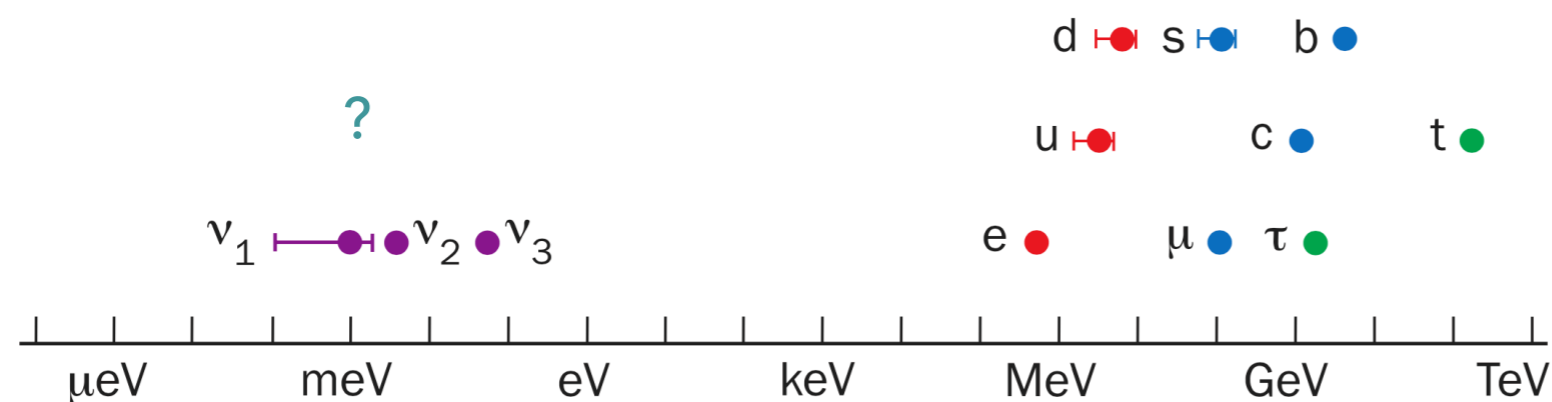
Xenoscope overview



Underground detectors for neutrino physics

Open questions in neutrino physics

- What are the absolute values of neutrino masses, and the mass ordering?
- What is the nature of neutrinos? Are they Dirac or Majorana particles?
- What is the origin of small neutrino masses? $\frac{m_{\nu_j}}{m_{l,q}} \leq 10^{-6}$ for $m_{\nu_j} \leq 0.5 \text{ eV}$
- What are the precise values of the mixing angles, and the origin of the large ν mixing?
- Is the standard three-neutrino picture correct, or do other, sterile neutrinos exist?
- What is the precise value of the CP violating phase δ ?
- ...



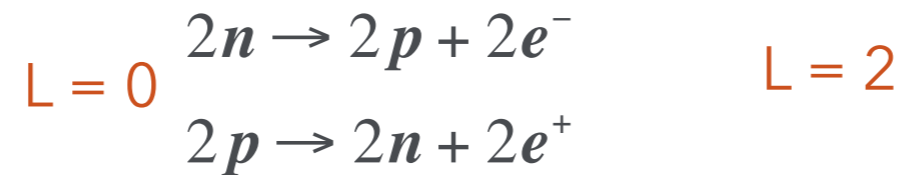
Open questions in neutrino physics

- ⦿ What are the absolute values of neutrino masses, and the mass ordering?
- ⦿ What is the nature of neutrinos? Are they Dirac or Majorana particles?
- ⦿ What is the origin of small neutrino masses? $\frac{m_{\nu_j}}{m_{l,q}} \leq 10^{-6}$ for $m_{\nu_j} \leq 0.5 \text{ eV}$
- ⦿ What are the precise values of the mixing angles, and the origin of the large ν mixing?
- ⦿ Is the standard three-neutrino picture correct, or do other, sterile neutrinos exist?
- ⦿ What is the precise value of the CP violating phase δ ?
- ⦿ ...

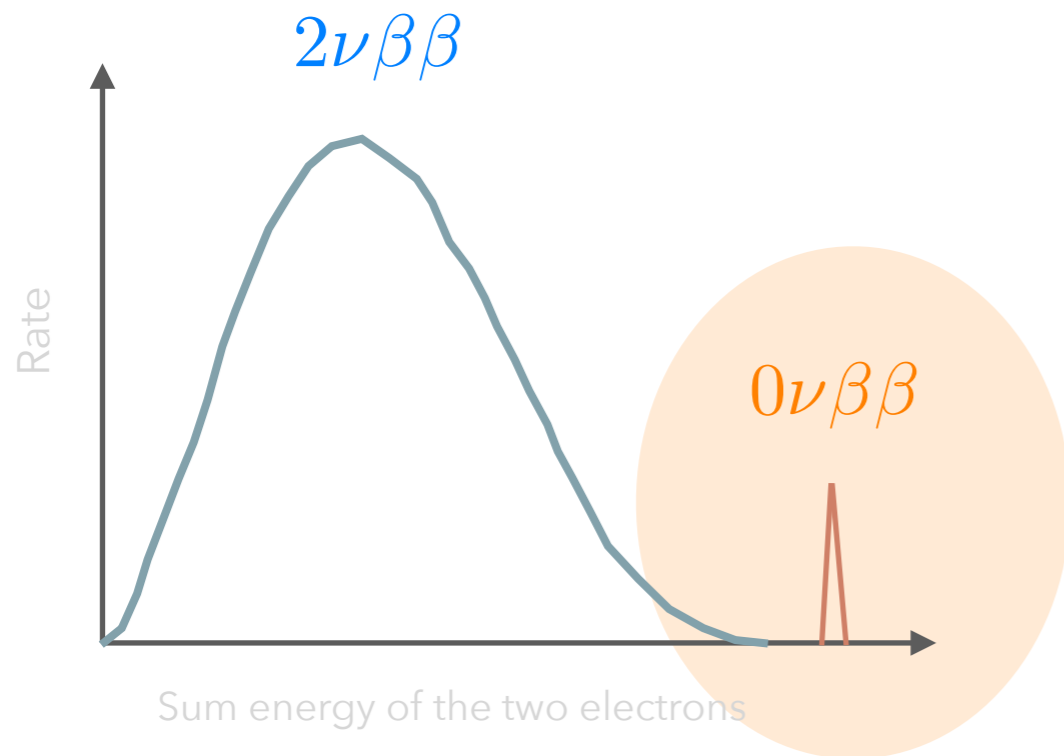
Some of these questions can be answered with noble liquid detectors

The nature of neutrinos

- Can be probed with a rare nuclear decay, the double beta decay mode without emission of neutrinos ($\Delta L = 2$)



- Expected signature: sharp peak at the Q-value of the decay

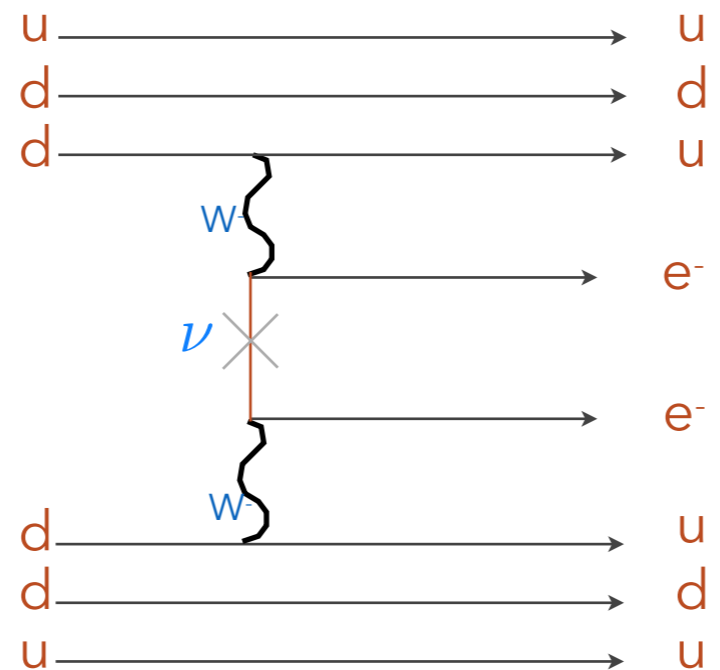


$$Q = E_{e1} + E_{e2} - 2m_e$$

- The double beta decay without neutrinos was first discussed by Wendell H. Furry, 1939 (Majorana had proposed in 1937 that neutrinos could be their own antiparticles)

Neutrinoless double beta decay

- In this decay, a virtual neutrino is exchanged:



Feynman diagram for the neutrinoless double beta decay

Exchange of a virtual neutrino

- the neutron decays under emission of a right handed 'anti-neutrino' ν_L^c
- the ν_L^c has to be absorbed at the second vertex as left handed 'neutrino' ν_L
- for the decay to happen: neutrinos and anti-neutrinos must be identical, thus Majorana particles
- and the helicity must change

Neutrinoless double beta decay

- The expected rate $\Gamma^{0\nu}$ can be calculated as:

$$\Gamma^{0\nu} = \frac{\ln 2}{T_{1/2}^{0\nu}} = G^{0\nu}(Q, Z) |M^{0\nu}|^2 \frac{|m_{\beta\beta}|^2}{m_e^2}$$

from the leptonic part of the matrix element

- with the Q-value of the decay:

$$Q = E_{e1} + E_{e2} - 2m_e$$

the matrix element of the nuclear transition

- and the phase space integral:

$$G^{0\nu} \propto (G_F \cos \theta_C)^4 \cdot \int_{m_e}^{Q+m_e} F(E_{e1}, Z_f) F(E_{e2}, Z_f) p_{e1} p_{e2} E_{e1} E_{e2} dE_{e1}$$

- with Z_f = charge of the daughter nucleus

the phase space is now spanned only by two electrons

$$G^{0\nu} \propto (G_F \cos \theta_C)^4 \cdot \left(\frac{Q^5}{30} - \frac{2Q^2}{3} + Q - \frac{2}{5} \right) \propto (G_F \cos \theta_C)^4 \cdot Q^5$$

Effective Majorana neutrino mass

- $|m_{\beta\beta}|$ is a mixture of m_1, m_2, m_3 , proportional to the U_{ei}^2 , where U_{ei} are the complex entries in the PMNS matrix

$$|m_{\beta\beta}| = |m_1 U_{e1}^2 + m_2 U_{e2}^2 e^{2\phi_1} + m_3 U_{e3}^2 e^{2i(\phi_2 - \delta)}|$$

- with

$$\begin{pmatrix} U_{e1} & U_{e2} & U_{e3} \\ U_{\mu 1} & U_{\mu 2} & U_{\mu 3} \\ U_{\tau 1} & U_{\tau 2} & U_{\tau 3} \end{pmatrix} = \begin{pmatrix} c_{12}c_{13} & s_{12}c_{13} & s_{13}e^{-i\delta} \\ -s_{12}c_{23} - c_{12}s_{23}s_{13}e^{i\delta} & c_{12}c_{23} - s_{12}s_{23}s_{13}e^{i\delta} & s_{23}c_{13} \\ s_{12}s_{23} - c_{12}c_{23}s_{13}e^{i\delta} & -c_{12}s_{23} - s_{12}c_{23}s_{13}e^{i\delta} & c_{23}c_{13} \end{pmatrix} \times \begin{pmatrix} e^{i\phi_1} & 0 & 0 \\ 0 & e^{i\phi_2} & 0 \\ 0 & 0 & 1 \end{pmatrix}$$

- and
 - $c_{ij} = \cos\theta_{ij}$, $s_{ij} = \sin\theta_{ij}$, $\phi_1, \phi_2 =$ Majorana phases and $|U_{e1}|^2$ is for instance the probability that ν_e has the mass m_1

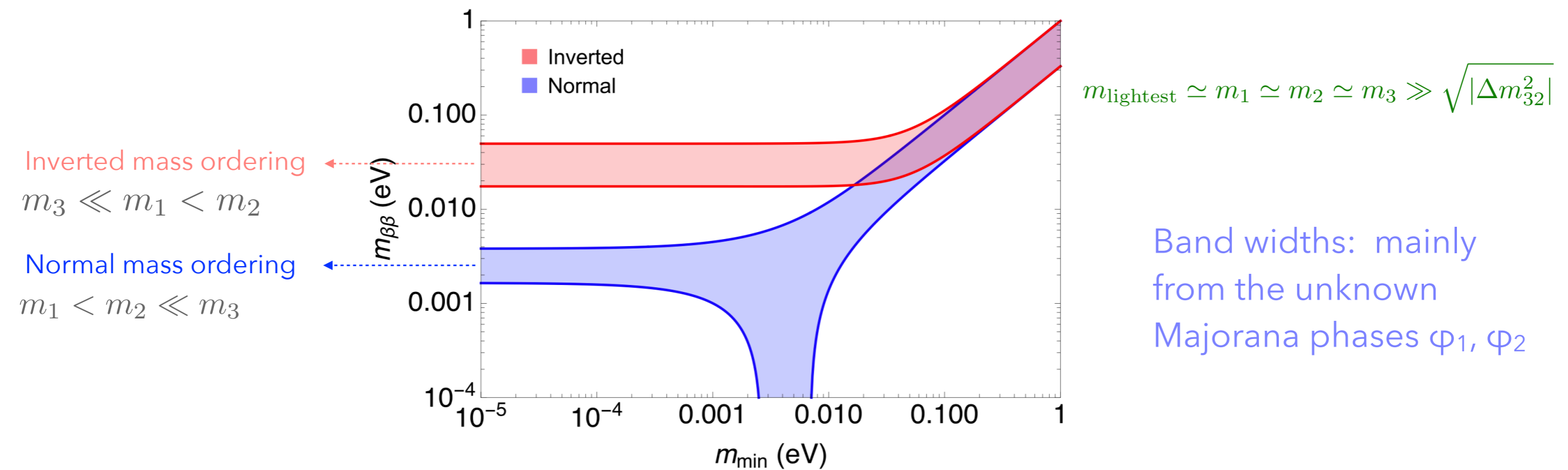
Remember that in general a $n \times n$ unitary matrix U can be parametrised by $n(n-1)/2$ Euler angles and $n(n+1)/2$ phases

For neutrinos as Dirac particles: $(n-1)(n-2)/2$ phases are physical ($n = 3 \Rightarrow 1$ phase)

For neutrinos as Majorana fermions: $n(n-1)/2$ phases $\Rightarrow (n-1)$ more phases, as the massive Majorana fields can not "absorb" phases ($n = 3 \Rightarrow 2$ more phases)

Predictions for the effective Majorana neutrino mass

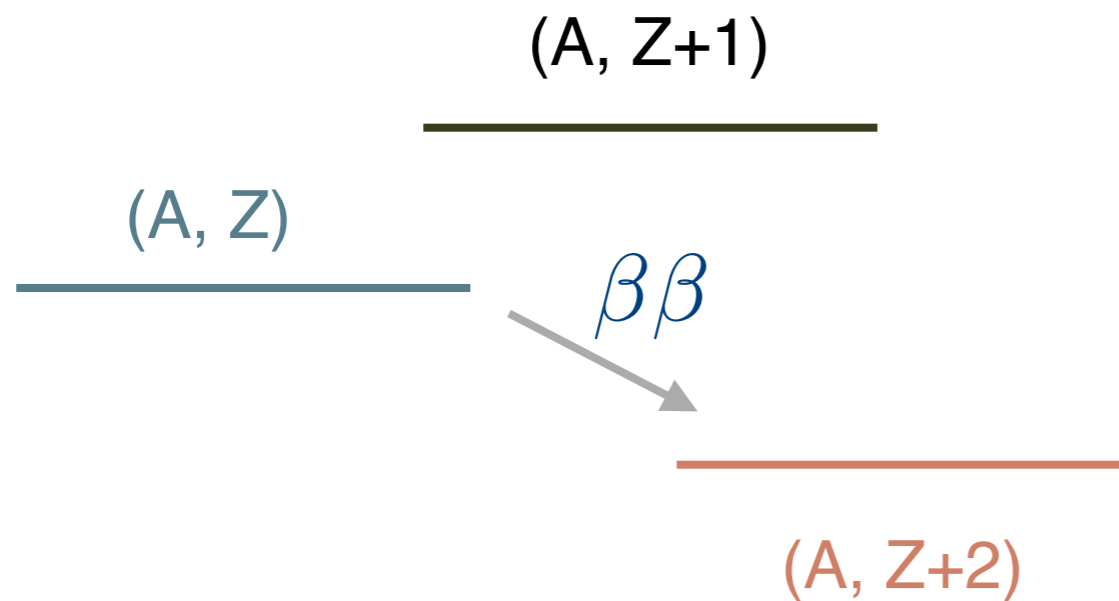
- The predicted values depend critically on the neutrino mass spectrum and on the values of the two Majorana phases in the PMNS matrix



Data from PDG Review: PTEP 8, August 2020

Which nuclei can decay via $0\nu\beta\beta$?

- Even-even nuclei
- Natural abundance is low (except ^{130}Te)
- Must use enriched material



Candidate*	Q [MeV]	Abund [%]
$^{48}\text{Ca} \rightarrow ^{48}\text{Ti}$	4.271	0.187
$^{76}\text{Ge} \rightarrow ^{76}\text{Se}$	2.039	7.8
$^{82}\text{Se} \rightarrow ^{82}\text{Kr}$	2.995	9.2
$^{96}\text{Zr} \rightarrow ^{96}\text{Mo}$	3.350	2.8
$^{100}\text{Mo} \rightarrow ^{100}\text{Ru}$	3.034	9.6
$^{110}\text{Pd} \rightarrow ^{110}\text{Cd}$	2.013	11.8
$^{116}\text{Cd} \rightarrow ^{116}\text{Sn}$	2.802	7.5
$^{124}\text{Sn} \rightarrow ^{124}\text{Te}$	2.228	5.64
$^{130}\text{Te} \rightarrow ^{130}\text{Xe}$	2.530	34.5
$^{136}\text{Xe} \rightarrow ^{136}\text{Ba}$	2.479	8.9
$^{150}\text{Nd} \rightarrow ^{150}\text{Sm}$	3.367	5.6

* Q-value > 2 MeV ⁷³

Experimental requirements

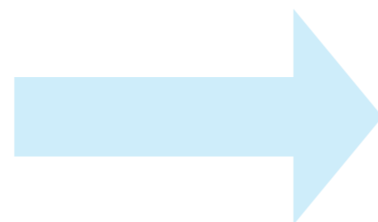
- Experiments measure the half life of the decay, $T_{1/2}$ with a sensitivity (for non-zero background)

$$T_{1/2}^{0\nu} \propto a \cdot \epsilon \cdot \sqrt{\frac{M \cdot t}{B \cdot \Delta E}}$$



Minimal requirements:

large detector masses
high isotopic abundance
ultra-low background noise
good energy resolution



$$\langle m_{\beta\beta} \rangle \propto \frac{1}{\sqrt{T_{1/2}^{0\nu}}}$$

Additional tools to distinguish signal from background:

event topology
pulse shape discrimination
particle identification

Experimental techniques

TPCs:
LXe: EXO-200, nEXO
DARWIN
NEXT, PandaX-III (high-pressure gas, tracking)

Ionisation

Tracking:
SuperNEMO

Crystals:
GERDA
Majorana
LEGEND
COBRA

Scintillation

Isotope in LS:
KamLAND-Zen
SNO+

Crystals:
CANDLES

Scintillating
bolometers:

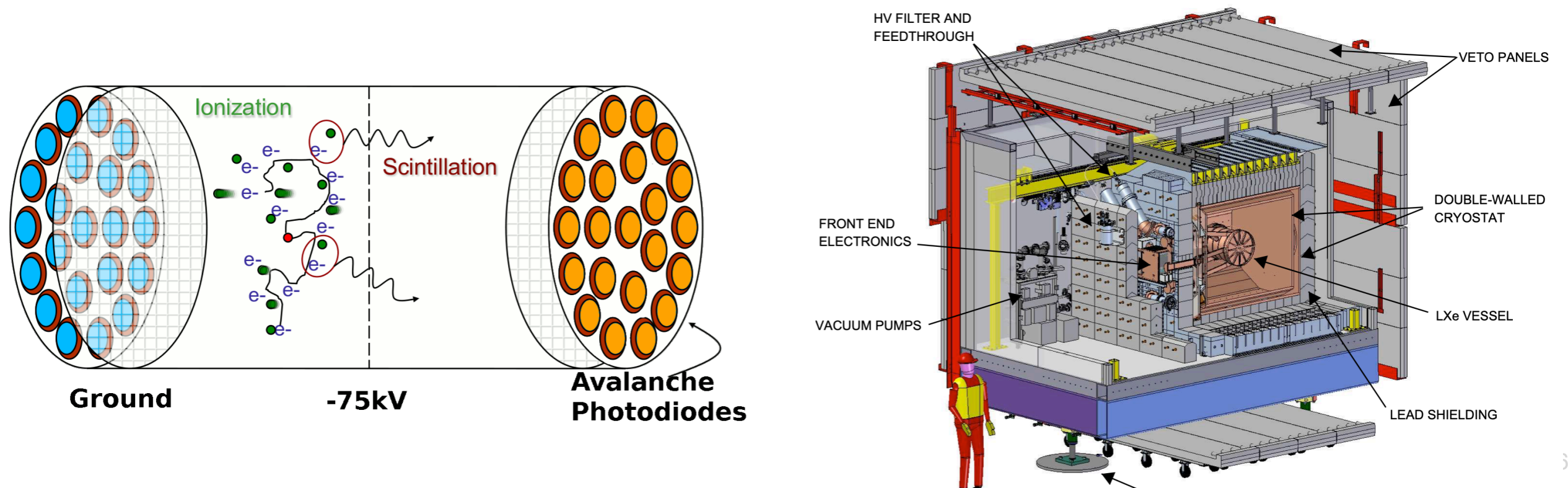
AMoRE
Lucifer
Lumineu } CUPID

Phonons

Bolometer:
CUORE

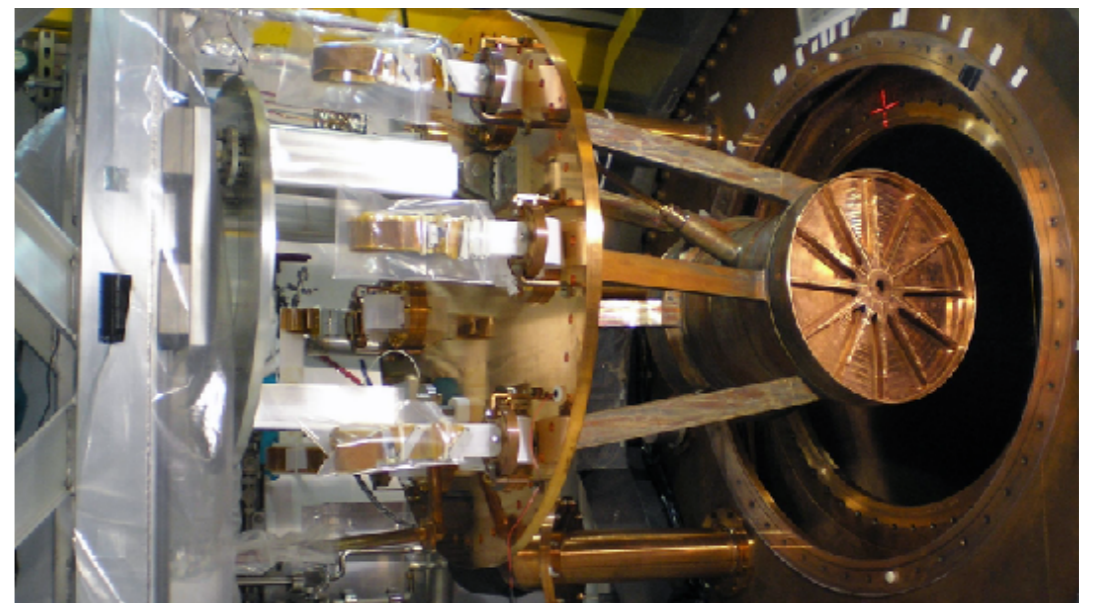
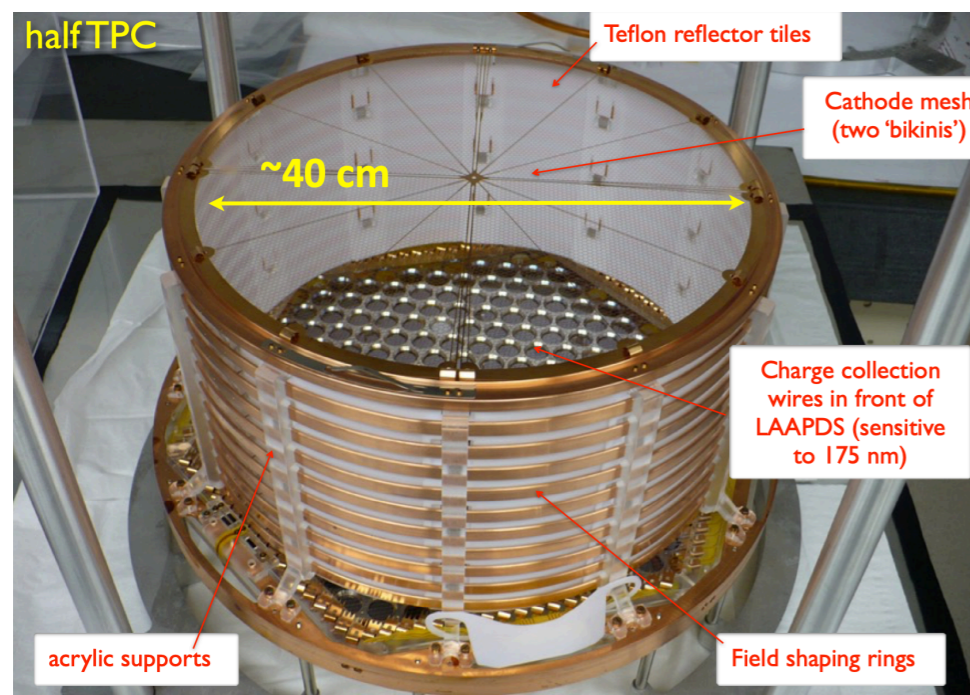
Liquid xenon TPC: EXO-200

- At Waste Isolation Pilot Plant (WIPP, ~1600 m w.e.), took data from, Sept 2011 - Dec 2018, in two phases
- 175 kg LXe in total, 80.6% enriched in ^{136}Xe
- TPC with two drift regions, each with a radius of 18 cm and drift length of 20 cm; drift field: 380 V/cm (phase I) and 567 V/cm (phase II)
- Charge drifted to crossed-wire planes at each anode; light collected by large area avalanche photodiodes
- TPC enclosed by a radio-pure, thin-walled Cu vessel in cryofluid, surrounded by passive shielding and an active muon veto system



Liquid xenon TPC: EXO-200

- At Waste Isolation Pilot Plant (WIPP, ~1600 m w.e.), took data from, Sept 2011 - Dec 2018, in two phases
- 175 kg LXe in total, 80.6% enriched in ^{136}Xe
- TPC with two drift regions, each with a radius of 18 cm and drift length of 20 cm; drift field: 380 V/cm (phase I) and 567 V/cm (phase II)
- Charge drifted to crossed-wire planes at each anode; light collected by large area avalanche photodiodes
- TPC enclosed by a radio-pure, thin-walled Cu vessel in cryofluid, surrounded by passive shielding and an active muon veto system



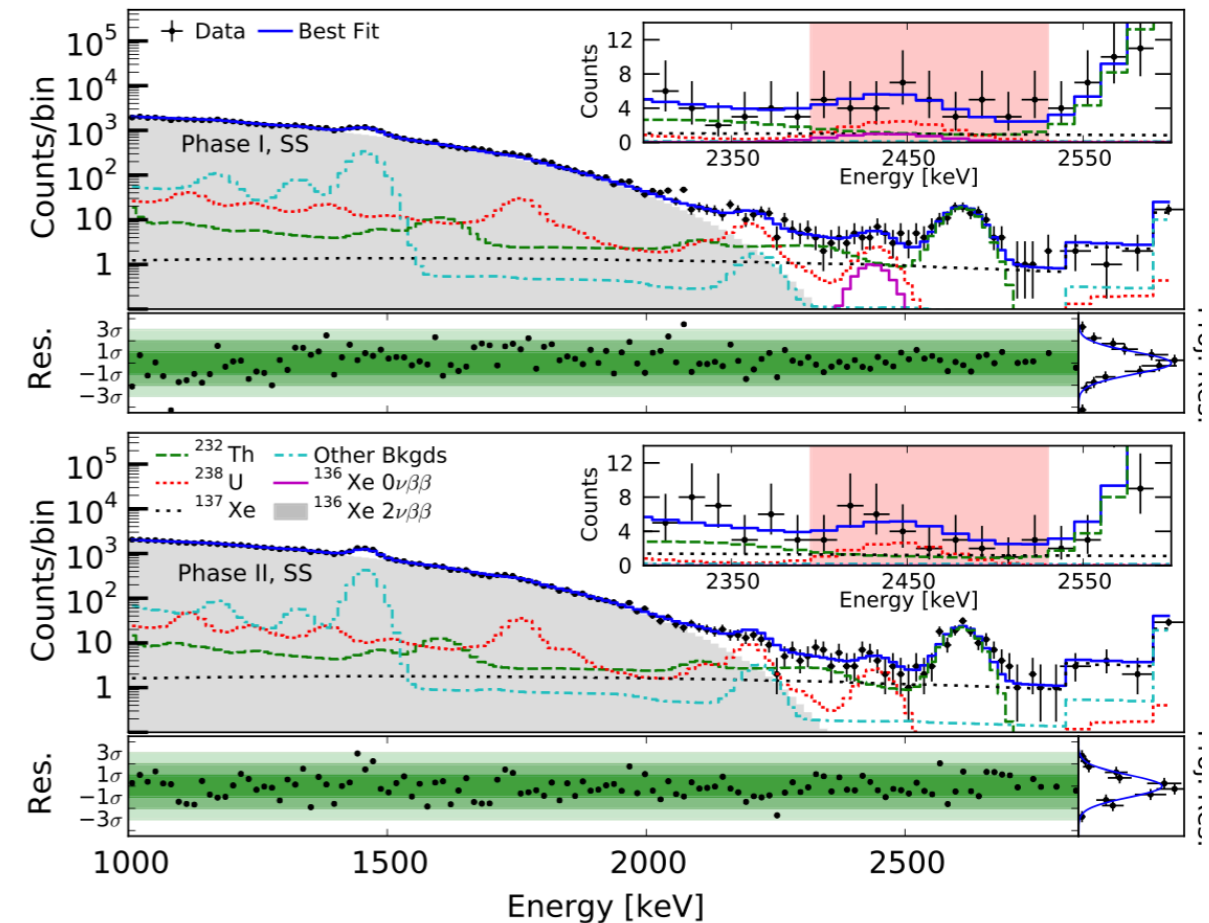
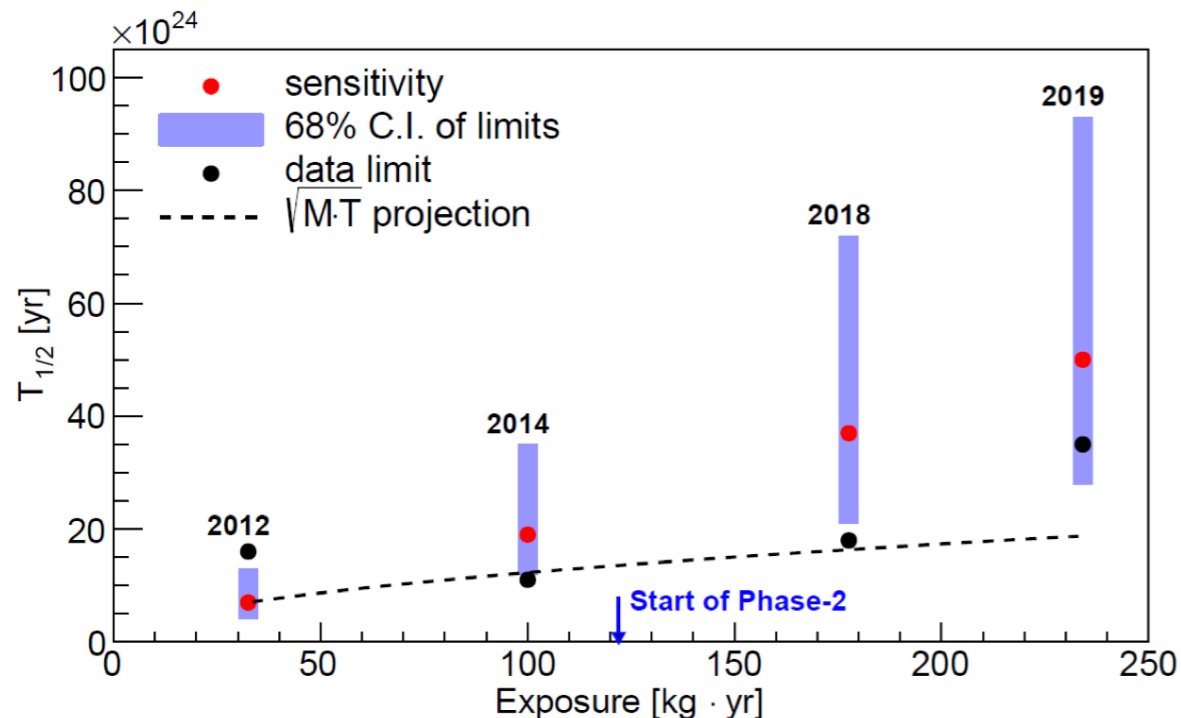
Liquid xenon TPC: EXO-200

- Fiducial volume: 74.7 kg of ^{136}Xe (3.31×10^{26} atoms)
- Total exposure: 231.4 kg years
- No statistically significant signal observed

TABLE II. Best-fit background contributions to $Q_{\beta\beta} \pm 2\sigma$ versus observed number of events in data.

(counts)	^{238}U	^{232}Th	^{137}Xe	Total	Data
Phase I	12.6	10.0	8.7	32.3 ± 2.3	39
Phase II	12.0	8.2	9.3	30.9 ± 2.4	26

EXO-200 collaboration, PRL 123, 2019



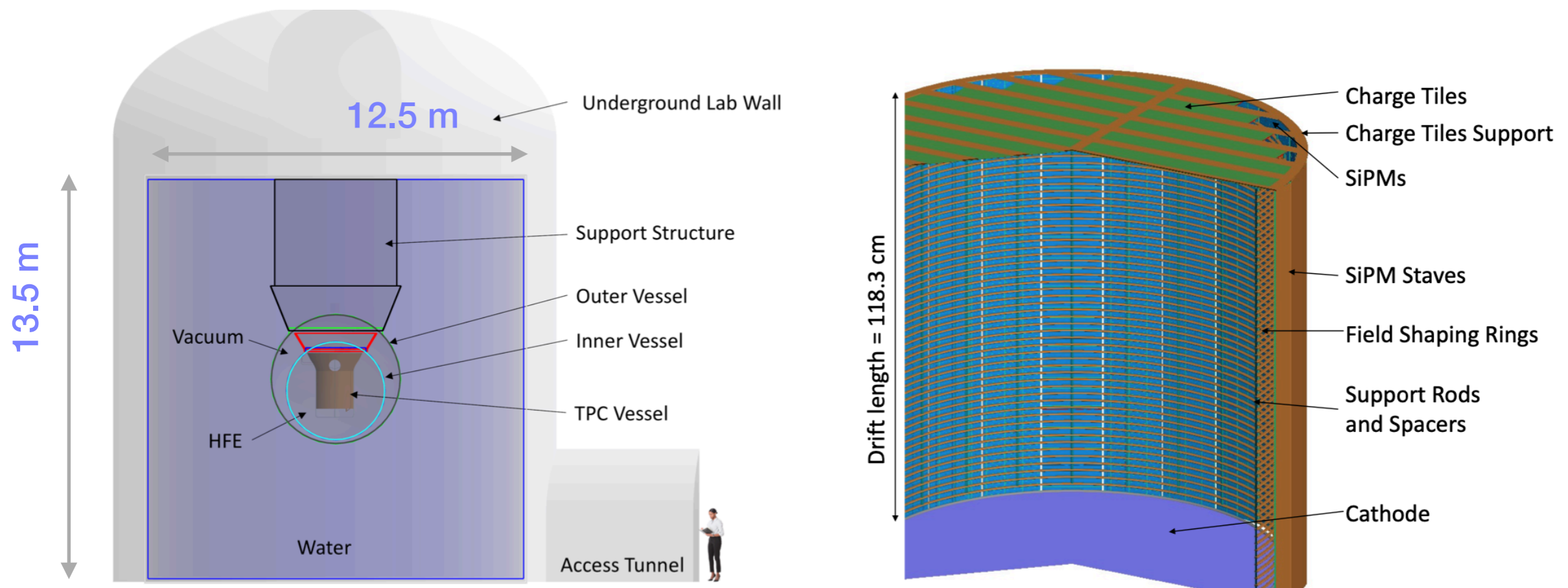
Q-value of the decay: 2457.83 ± 0.37 keV
 Energy resolution at Q-value: $\sigma/E \sim 1.15\%$

$$T_{1/2} > 3.5 \times 10^{25} \text{ yr}$$

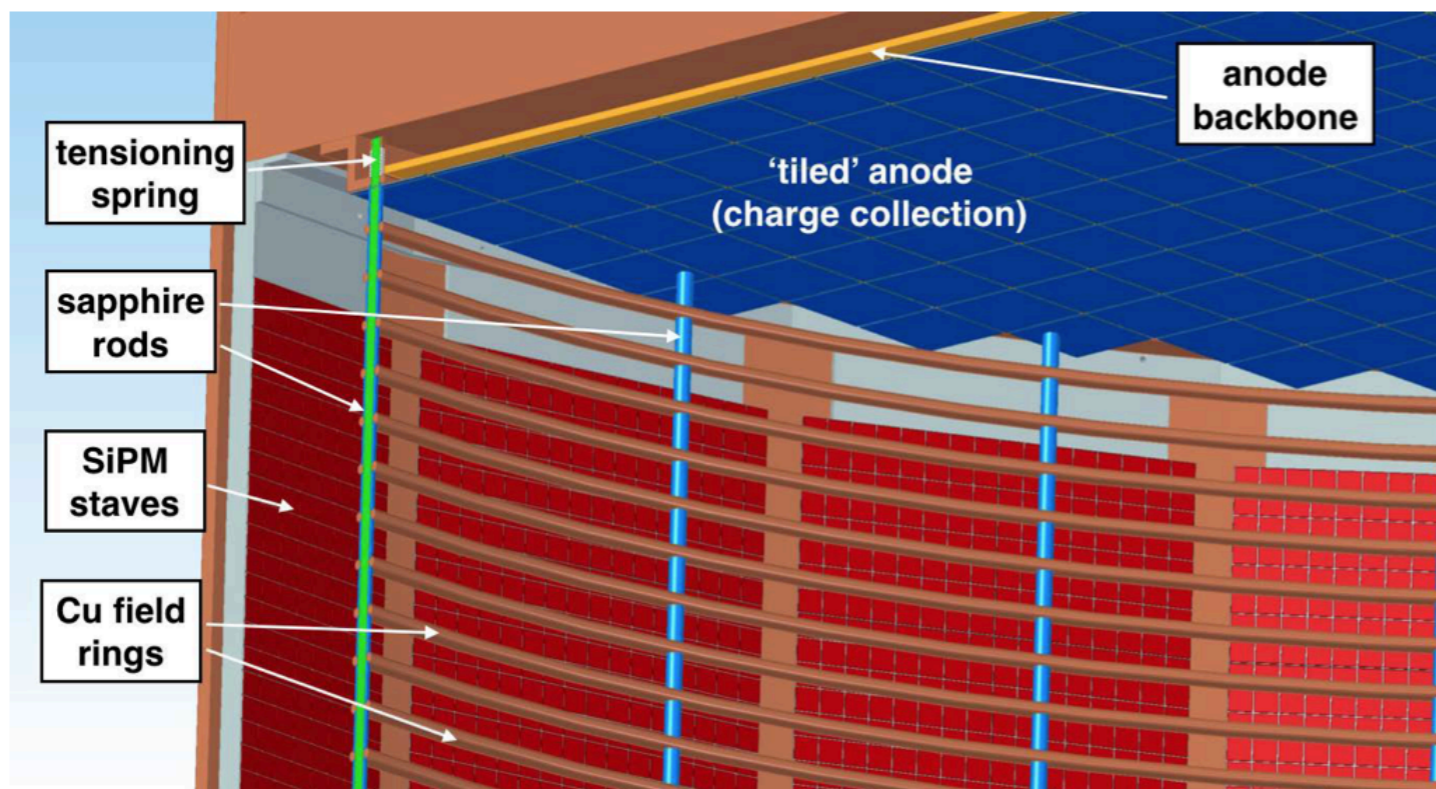
$$\langle m_{\beta\beta} \rangle < (93 - 286) \text{ meV}$$

Liquid xenon TPC: the nEXO experiment

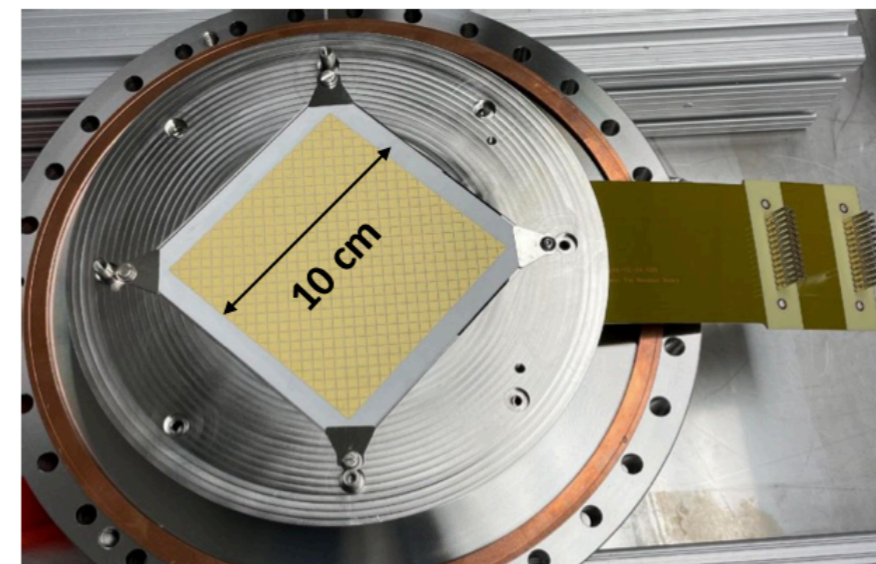
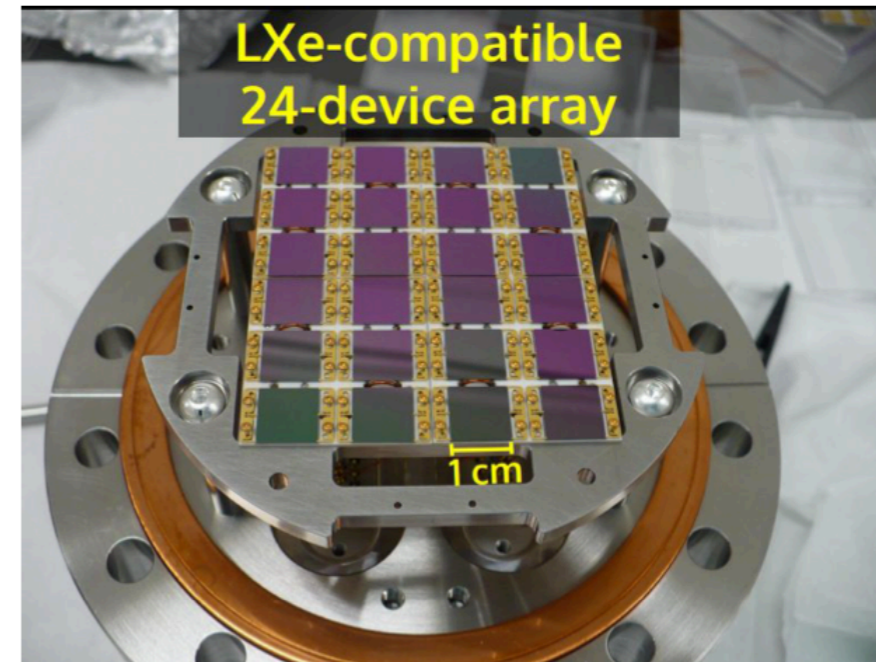
- TPC filled with enriched xenon, surrounded by 33 t of hydro-fluoro ether (HFE) as thermal bath and radiation shield; thin-walled, electro-formed Cu cryostat, water Cherenkov muon veto
- TPC vessel: Cu cylinder with 127.7 cm height & ϕ with 4.8 t (3.65 t) contained (active) Xe
- Charge: collected at the anode by 0.6 cm pitch and 9.6 m long electrode strips
- Scintillation light: collected by SiPM arrays arranged in a barrel configuration



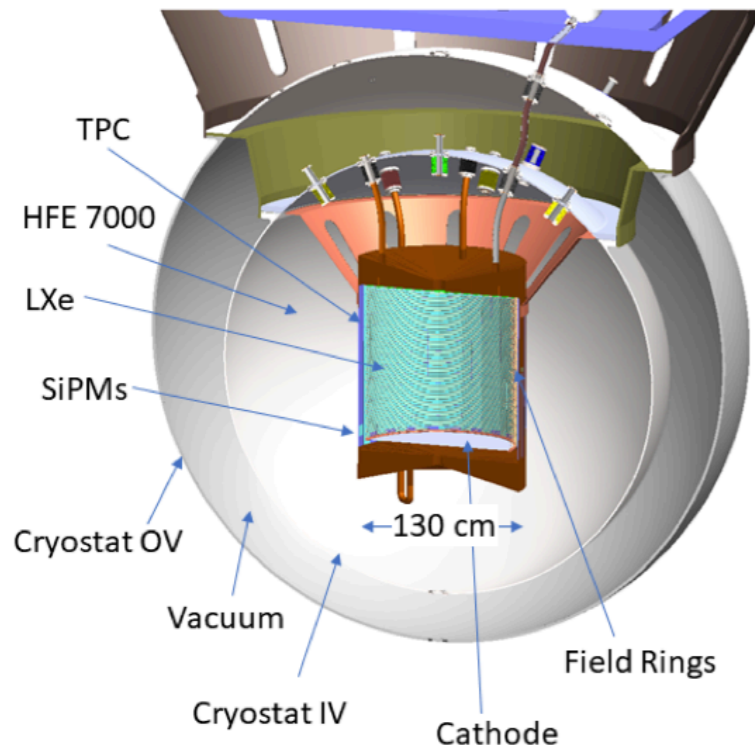
The nEXO experiment: charge and light readout



- SiPMs instead of PMTs
- no reflector panels
- Field rings and cathode coated with reflective aluminum deposition (capped by fluoride)



The nEXO experiment: evolution from EXO-200

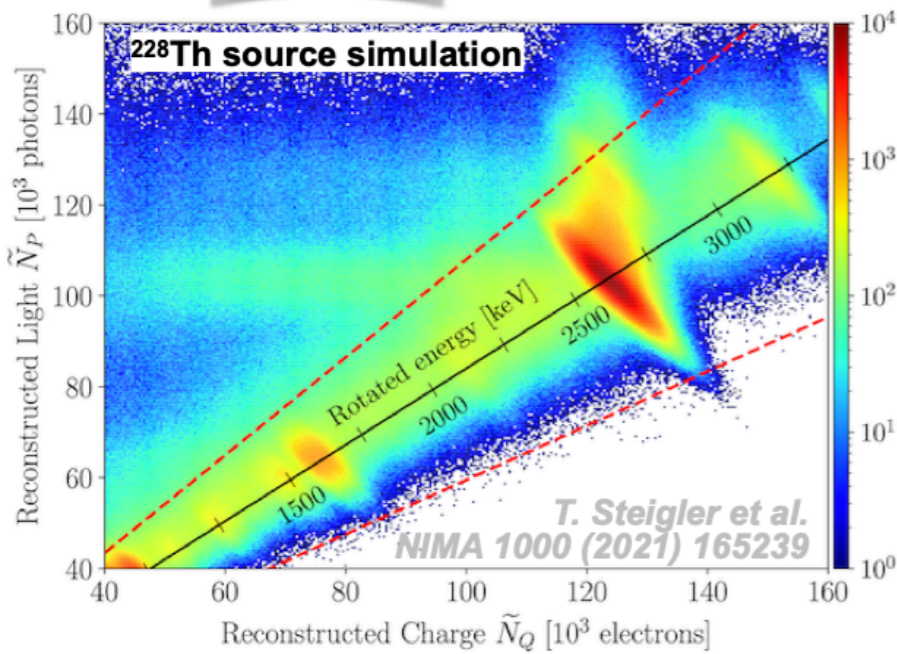


- 5000 kg of 90%-enriched LXe
- Single 120 cm drift volume; 130 cm diameter
- Drift E-field ~ 400 V/cm
- Ionization electrons collected on charge tile detectors at the anode (no gain), $\sim 6,000$ channels
- VUV (178 nm) scintillation light is detected by a large array of SiPMs ($\sim 45,000$ devices, ~ 4.5 m²)

	EXO-200:	nEXO:	Improvements:
Vessel and cryostat	Thin-walled commercial Cu w/HFE	Thin-walled electroformed Cu w/HFE	Lower background
High voltage	Max voltage: 25 kV (end-of-run)	Operating voltage: 50 kV	Full scale parts tested in LXe prior to installation to minimize risk
Cables	Cu clad polyimide (analog)	Cu clad polyimide (digital)	Same cable/feedthrough technology, R&D identified 10x lower bkg substrate and demonstrated digital signal transmission
e⁻ lifetime	3-5 ms	5 ms (req.), 10 ms (goal)	Minimal plastics (no PTFE reflector), lower surface to volume ratio, detailed materials screening program
Charge collection	Crossed wires	Gridless modular tiles	R&D performed to demonstrate charge collection with tiles in LXe, detailed simulation developed
Light collection	APDs + PTFE reflector	SiPMs around TPC barrel	SiPMs avoid readout noise, R&D demonstrated prototypes from two vendors
Energy resolution	1.2%	1.2% (req.) 0.8% (goal)	Improved resolution due to SiPMs (negligible readout noise in light channels)
Electronics	Conventional room temp.	In LXe ASIC-based design	Minimize readout noise for light and charge channels, nEXO prototypes demonstrated in R&D and follow from LAr TPC lineage
Background control	Measurement of all materials	Measurement of all materials	RBC program follows successful strategy demonstrated in EXO-200
Larger size	>2 atten. length at center	>7 atten. length at center	Exponential attenuation of external gammas and more fully contained Comptons

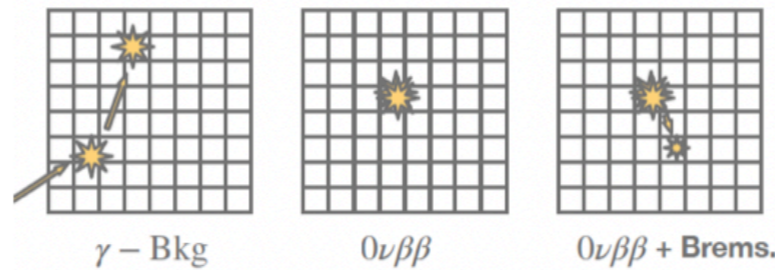
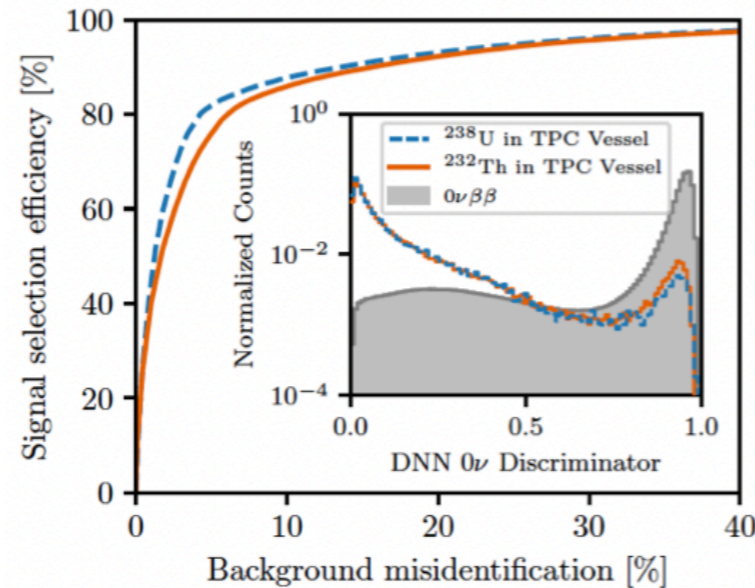
The nEXO experiment: expected performance

Energy



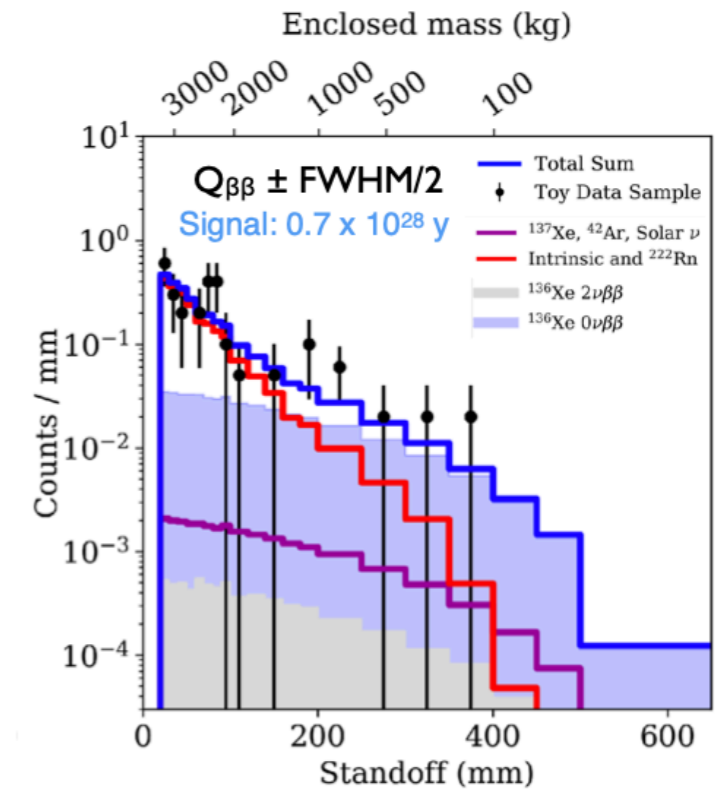
- ▶ Event-by-event anti-correlation between ionization and scintillation (known since the early EXO R&D)
- ▶ Improved energy resolution
 - ▶ expect $\sigma/Q_{\beta\beta} = 0.8\%$ (1.2% with EXO-200)
- ▶ Optically open TPC field cage

Event topology



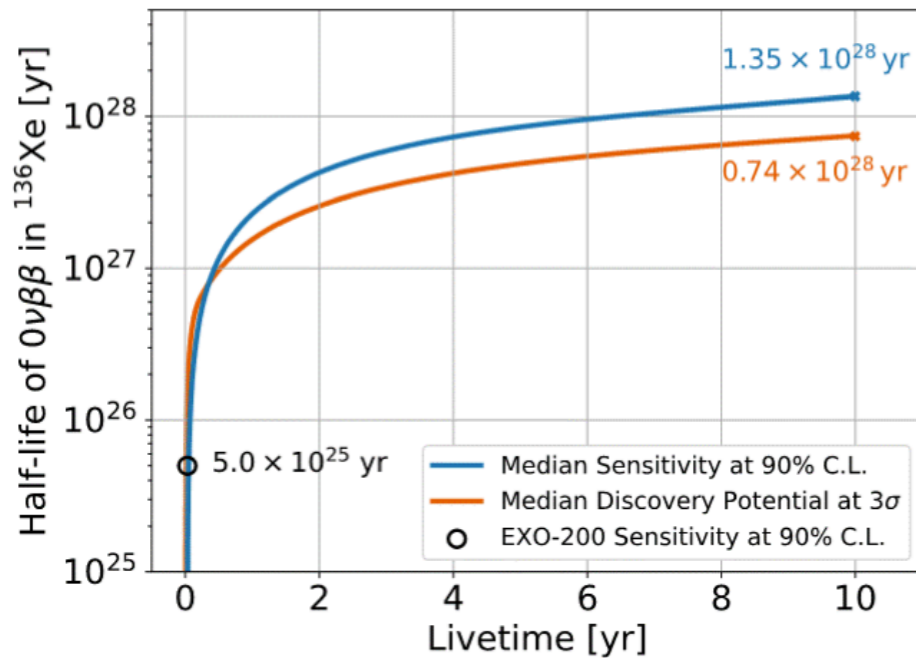
- ▶ Single- vs. multi- site energy depositions

Standoff distance

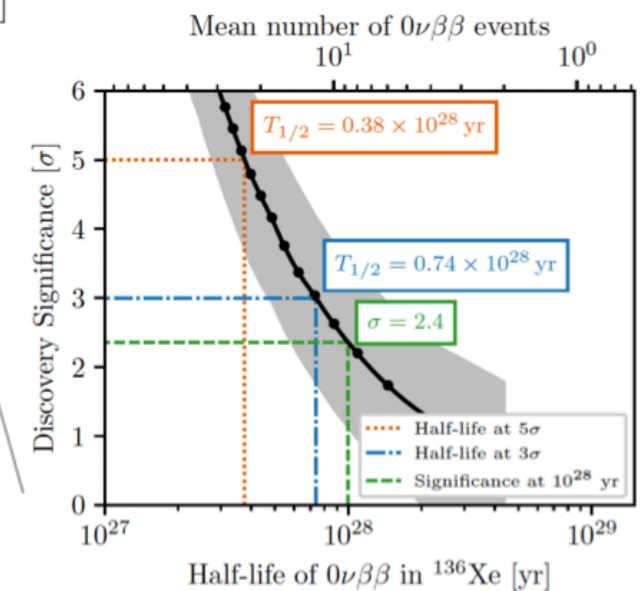
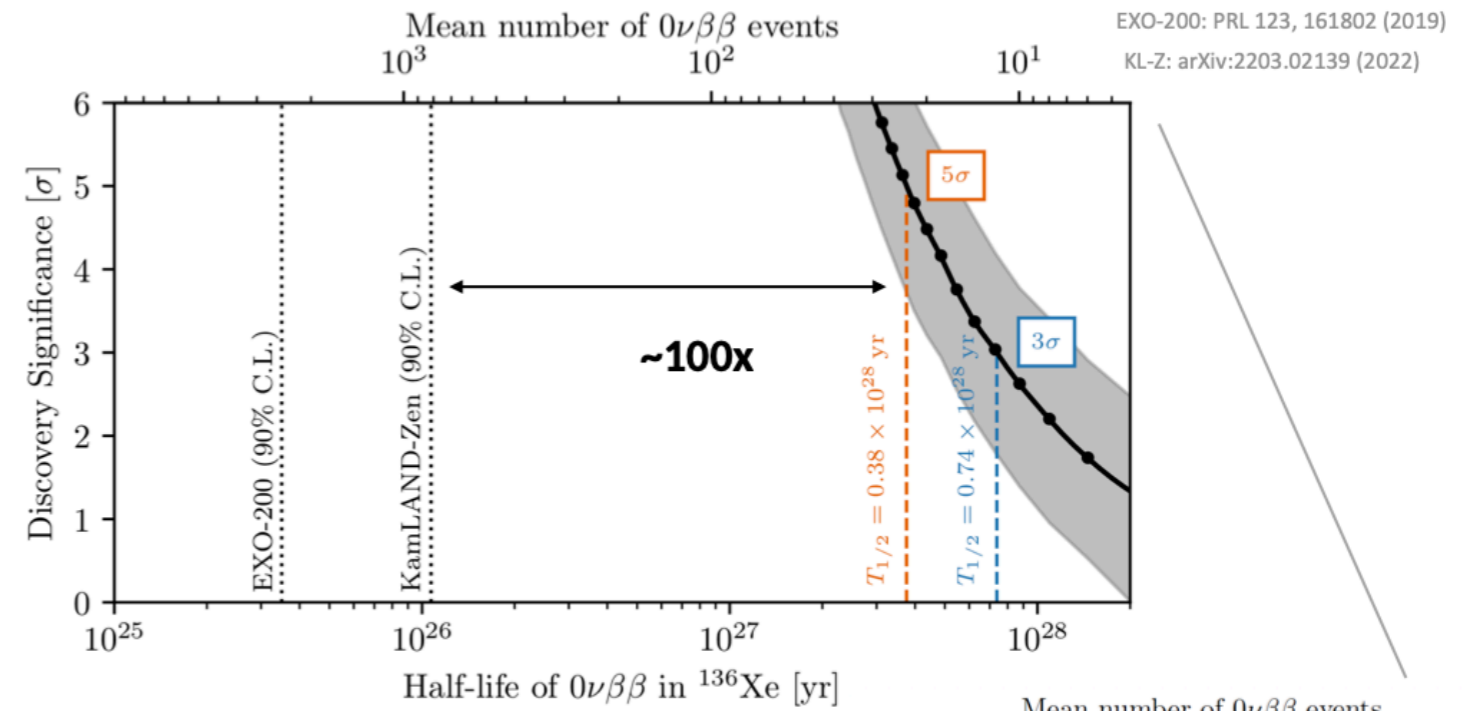


- ▶ $\beta\beta$ events are uniformly distributed in the LXe volume
- ▶ Most backgrounds originate from outside of the TPC

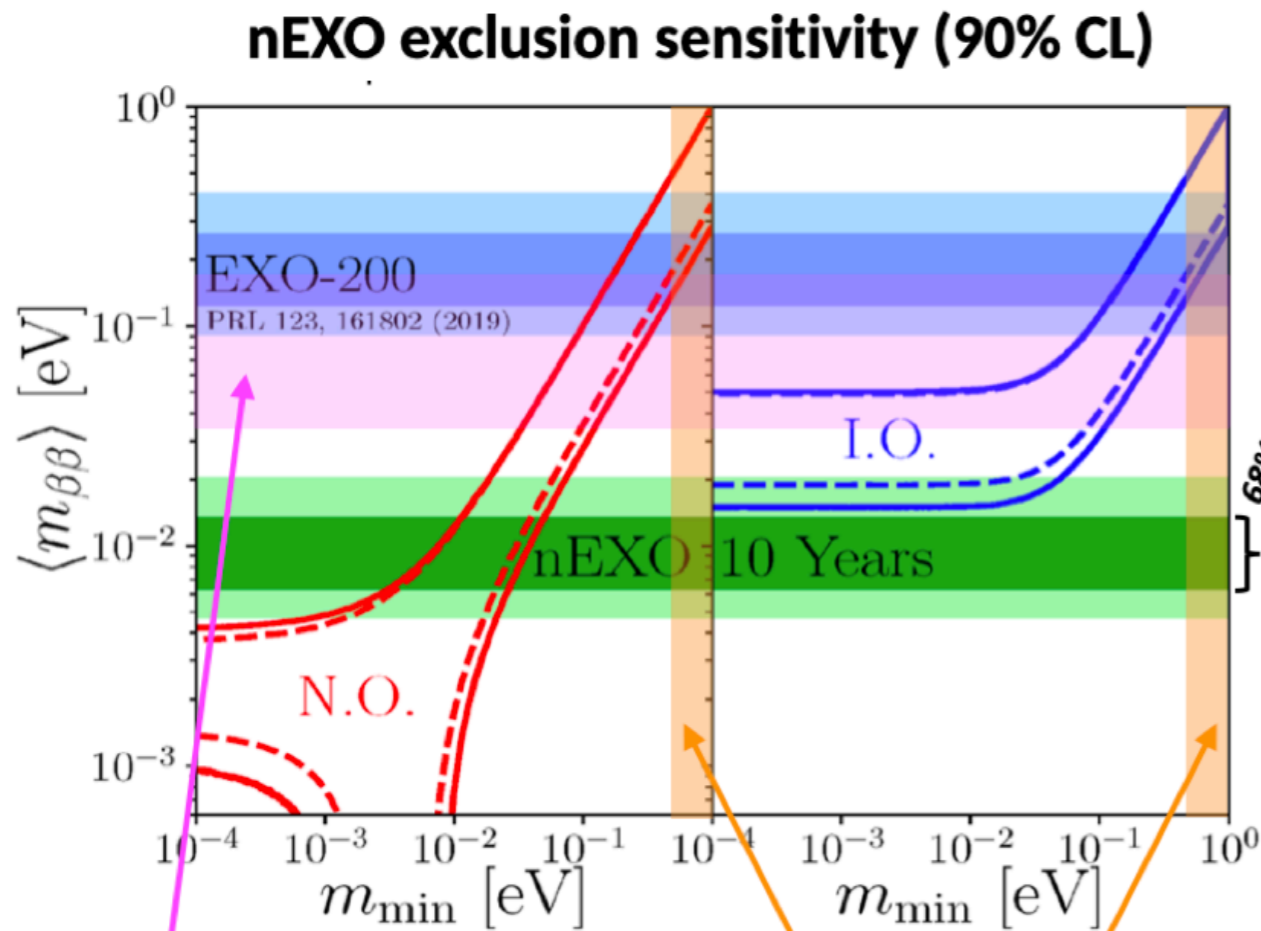
The nEXO experiment: sensitivity to $T_{1/2}$



- $>10^{28}$ year sensitivity reach in 10 years
- Can provide compelling evidence of $0\nu\beta\beta$ decay discovery
- Probes $m_{\beta\beta} \sim 15$ meV (model and NME dependent)



The nEXO experiment: sensitivity to the ν mass



KamLAND-Zen
36-156 meV
(2203.02139)

Katrin
<math><0.8</math> eV
(2105.08533)

Phase-space factor

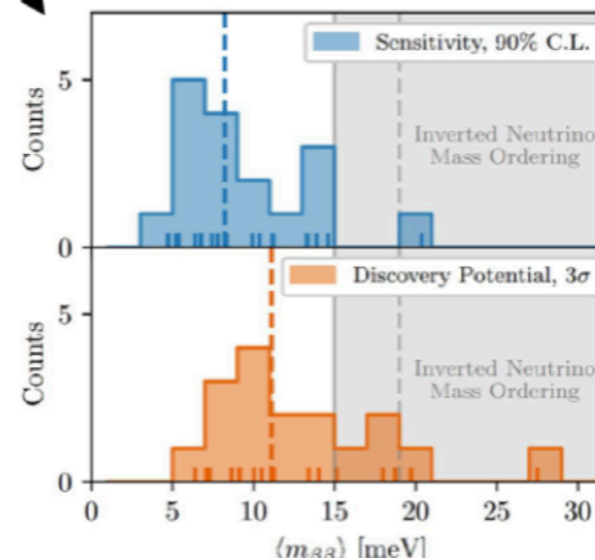
*J. Kotila and F. Iachello,
Phys Rev C 85, 034316 (2012)*

Axial coupling

$g_A = 1.27$

$$\frac{1}{T_{1/2}^0} = \frac{\langle m_{\beta\beta} \rangle^2}{m_e^2} G^{0\nu} g_A^4 |\mathcal{M}^{0\nu}|^2$$

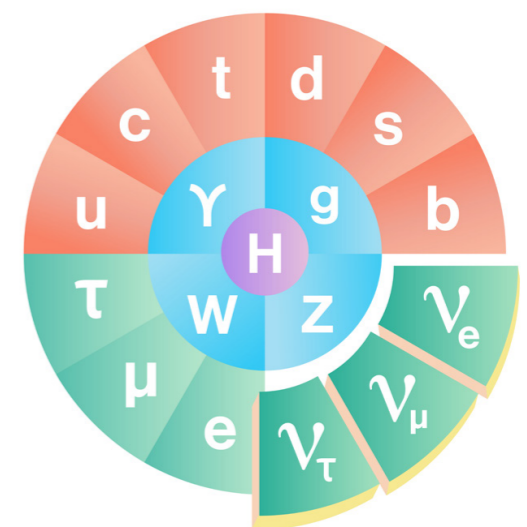
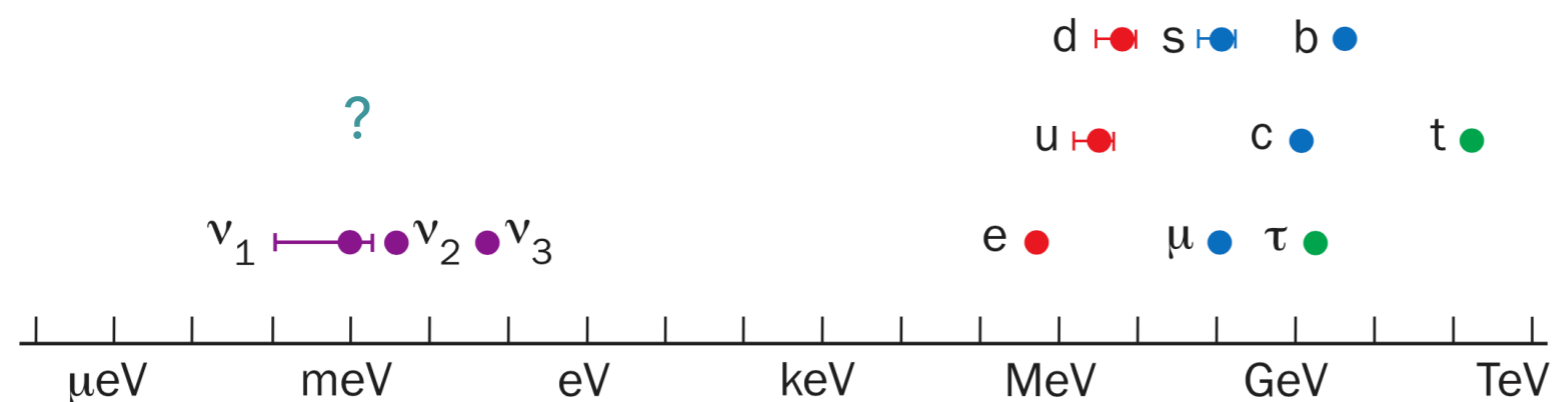
Nuclear Matrix Element



- Agnostic approach: show all published NMEs
- nEXO 3σ discovery sensitivity for the median NME is 11.1 meV, below/beyond I.O.

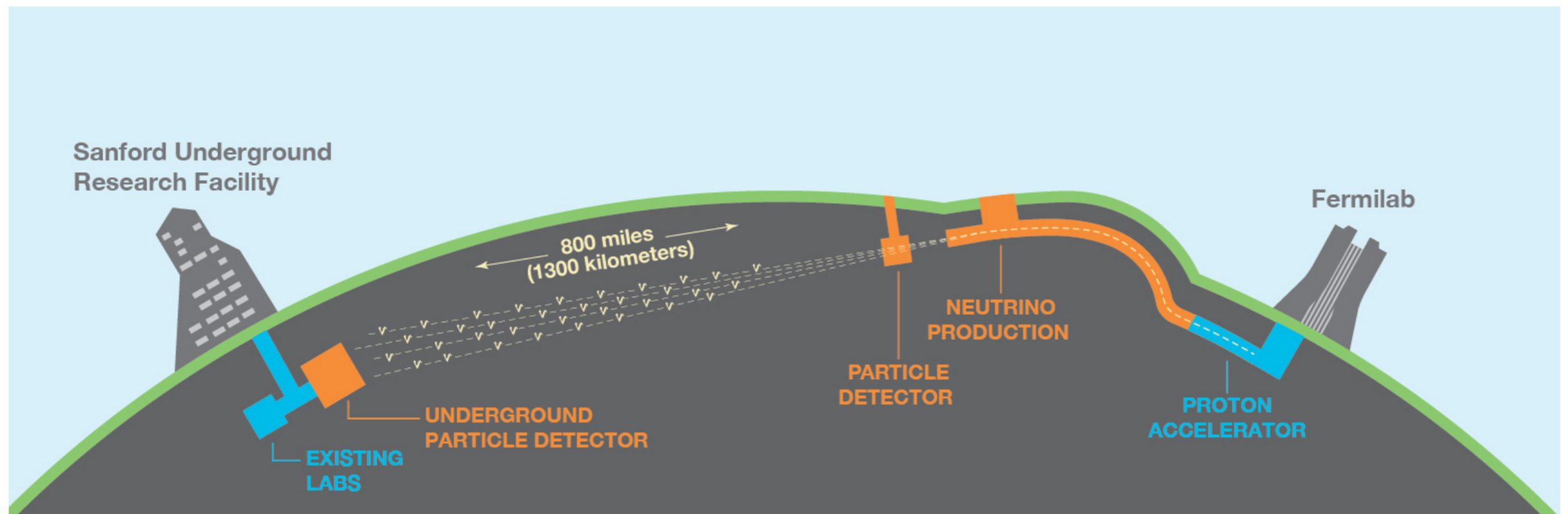
Open questions in neutrino physics

- What are the absolute values of neutrino masses, and the mass ordering?
- What is the nature of neutrinos? Are they Dirac or Majorana particles?
- What is the origin of small neutrino masses? $\frac{m_{\nu_j}}{m_{l,q}} \leq 10^{-6}$ for $m_{\nu_j} \leq 0.5 \text{ eV}$
- What are the precise values of the mixing angles, and the origin of the large ν mixing?
- Is the standard three-neutrino picture correct, or do other, sterile neutrinos exist?
- What is the precise value of the CP violating phase δ ?
- ...

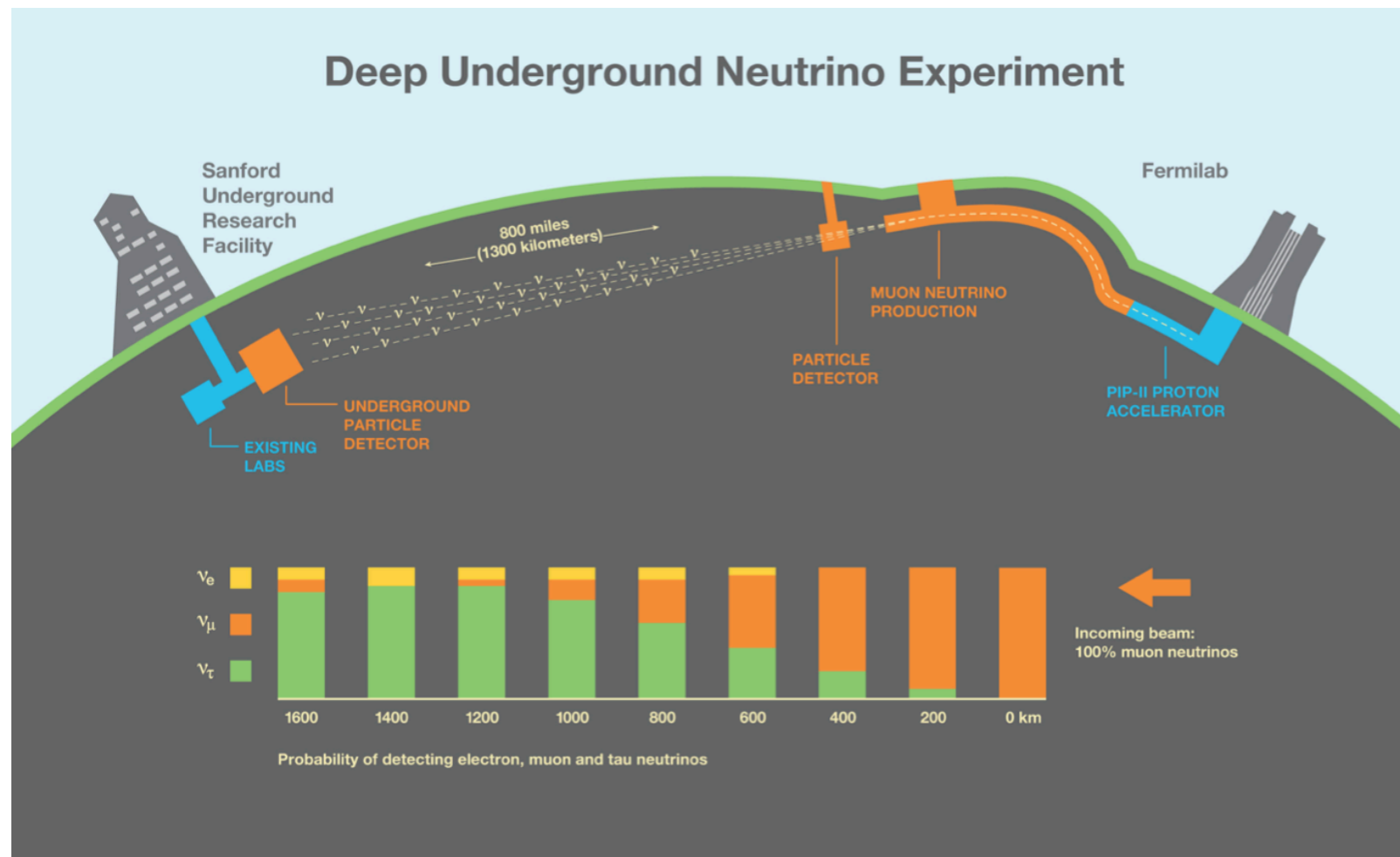


Long-baseline experiments

- **T2HyperK:** Beam from J-PARC to the Hyper-Kamiokande Detector; $L = 250$ km, Detector made of $2 \times 260'000$ tons of water
- **DUNE/LBNF:** ν -beam from Fermilab to Sanford Lab; $L = 1300$ km; DUNE far detector using 4×17.5 kilotons of LAr; two prototypes at CERN



The deep underground neutrino experiment

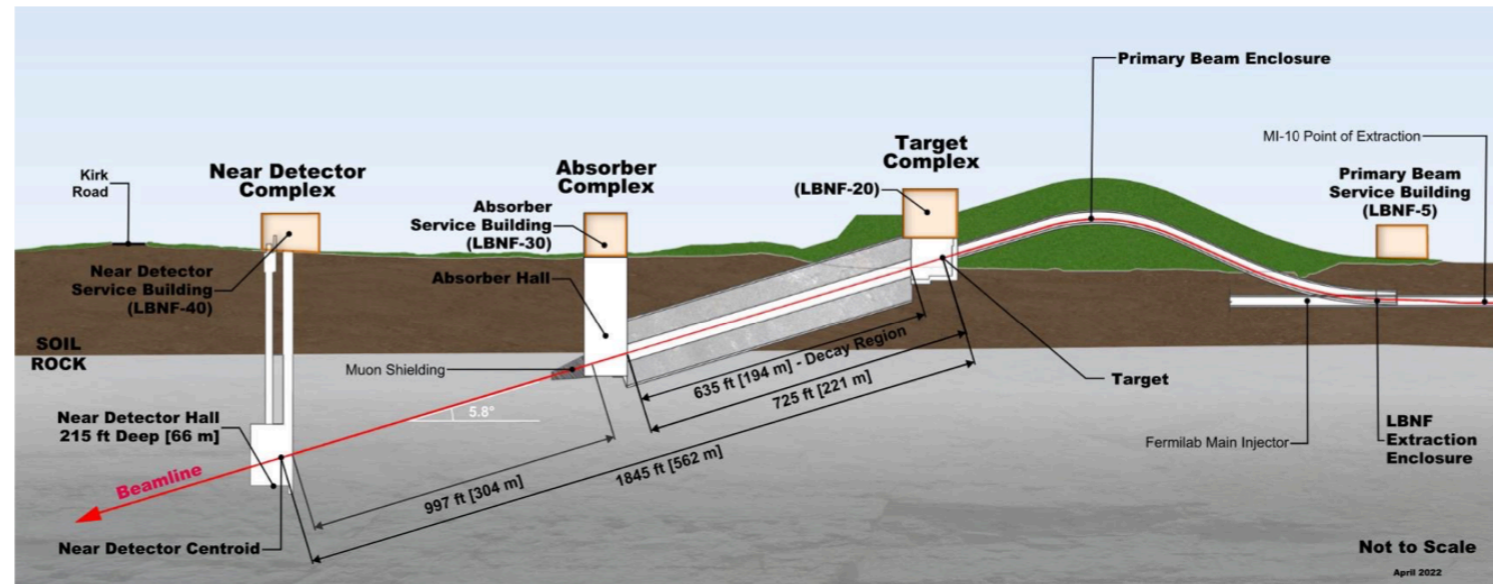


- Long-baseline: 1300 km
- LBNF beamline: beam power 1.2 - 2.4 MW
- Near detector: multi technology, including a 67 t LAr TPC
- Far detector: 4 modules, each with 17.5 kton LAr TPCs

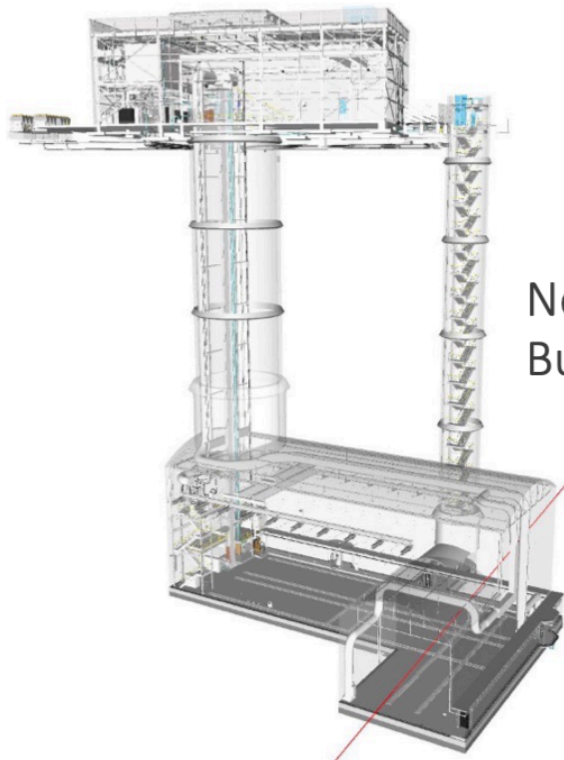
The deep underground neutrino experiment

Facilities

- LBNF Beamline
- Near Detector Complex
- Far Detector Complex

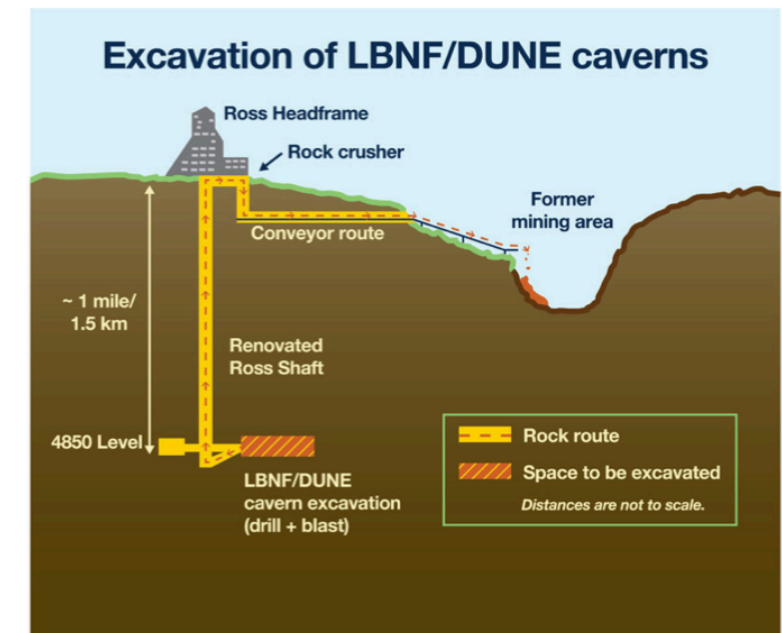


LBNF beam line construction is started



Near Detector Complex: @574 m from target
Building design and construction on the way

Far Detector Complex:
Excavation at 1.5 km
underground is advancing

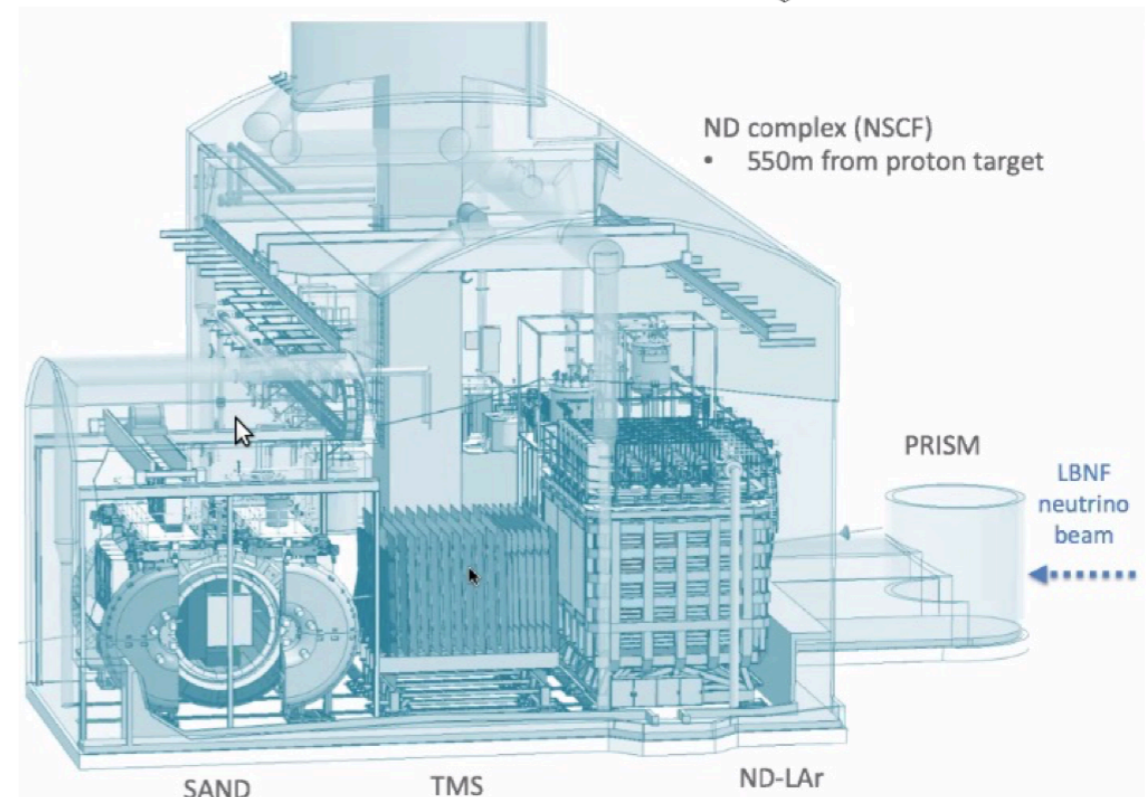
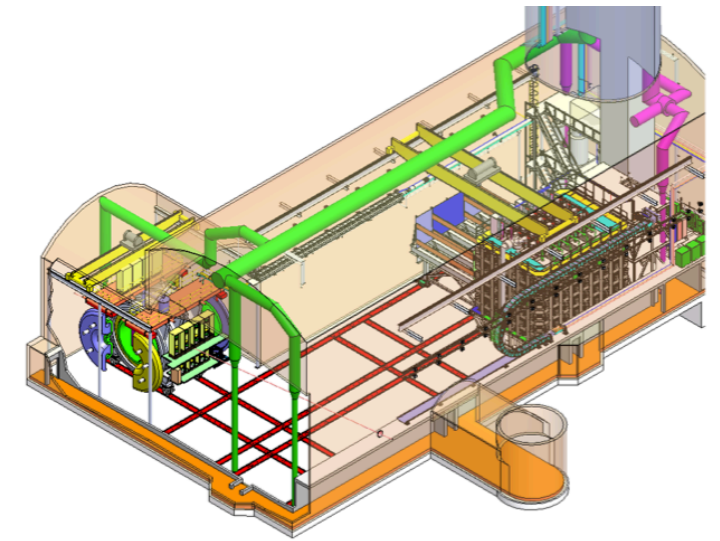


The deep underground neutrino experiment

Near Detector complex

DUNE ND Located 574 m from the proton beam target constitutes 3 essential detector systems:

- ND-LAr: A 67-ton Liquid Argon Time Projection Chamber (TPC).
 - LAr Target mass with high resolution imaging capability in high pileup environment
- TMS: Temporary Muon Spectrometer
 - Measurement of muons momentum and charge
 - To be replaced by the ND-GAr in a later phase
- SAND: System for on-Axis Neutrino Detection
 - Provides continuous on axis beam flux monitoring
- PRISM: A system to move ND-LAr and TMS off-axis
 - Moving up to 28.5 m (2.5°) off-axis, allows to probe different flux profiles

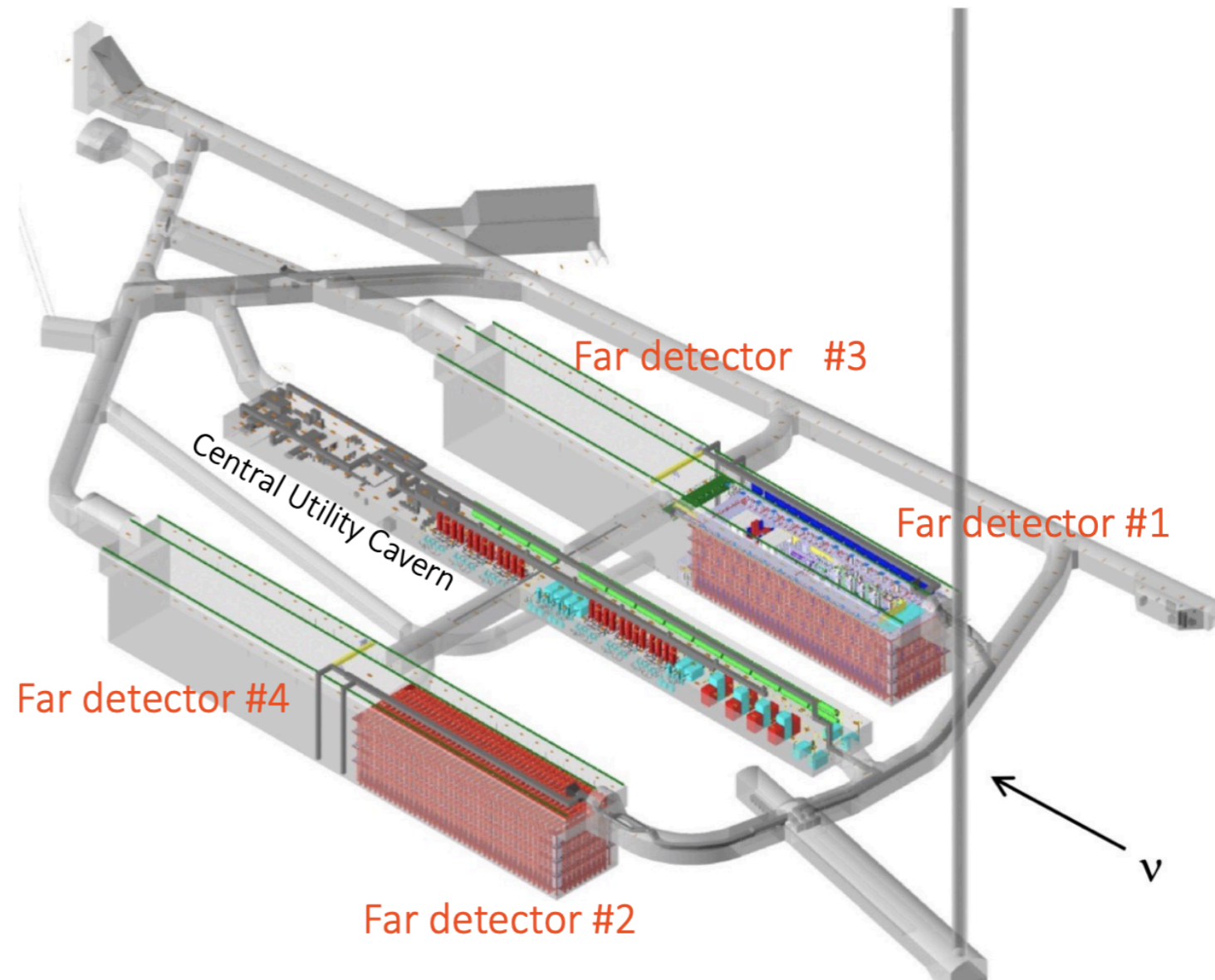


The deep underground neutrino experiment

Far Detector complex @SURF

- Constitutes 4 detector modules ~ 17.5 kton each
- Cryostat dimensions: 66 m x 19 m x 18 m
- Planned construction in stages

- FD #1: Horizontal drift LAr-TPC
 - FD #2: Vertical drift LAr-TPC
 - FD #3: ?
 - FD #4: ?
- From available or new technologies
Modules of Opportunity!



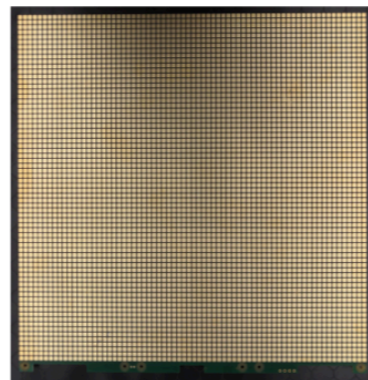
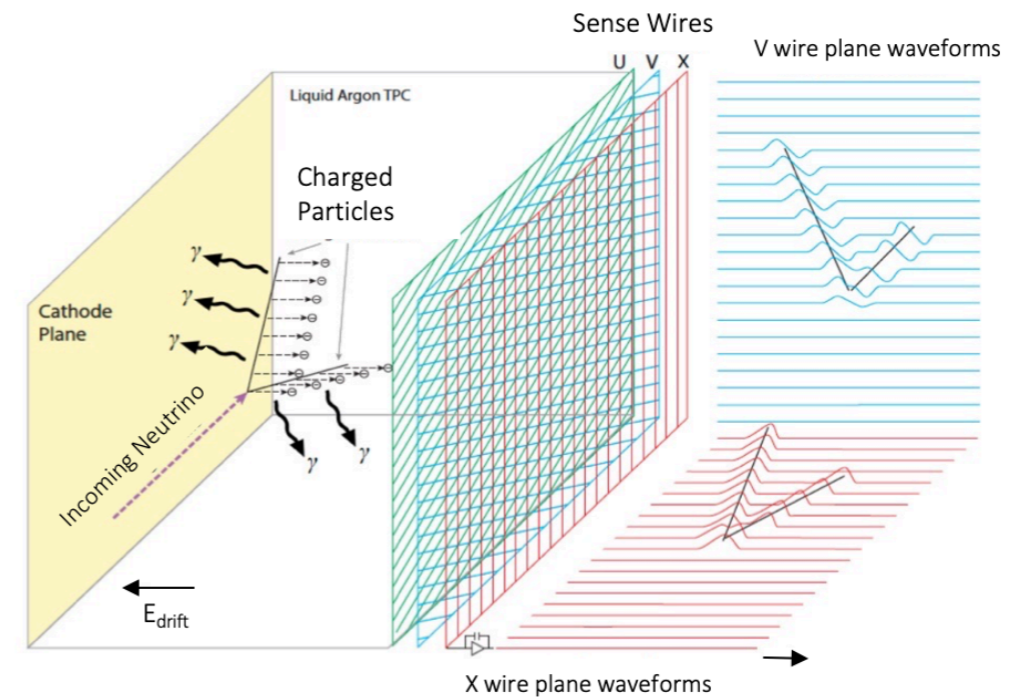
The deep underground neutrino experiment

LAr-TPC

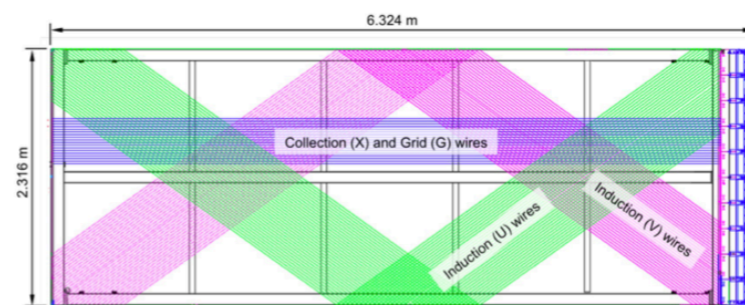
LAr-TPC working principle

- Charged particles ionize argon atoms, and cause flashes of scintillation light
- The ionized electrons record the location and the amount of energy deposited in LAr.
- By applying an electric field, the electrons drift toward the readout plane located at the Anode.
- There are different charge readout solutions:

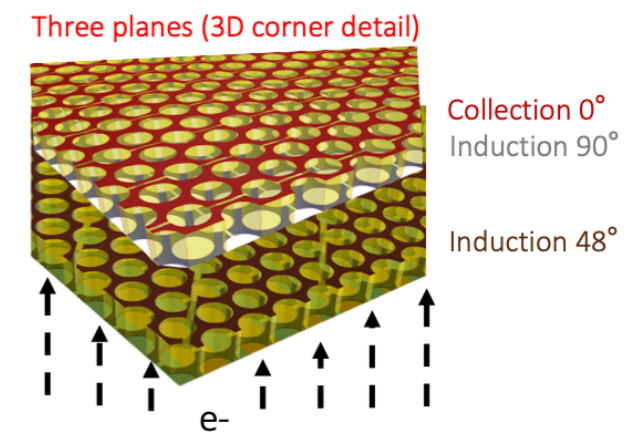
Liquid Argon TPC with wire readout



Pixelated readout (ArgonCube)



Wire readout (ICARUS, MicroBooNE)



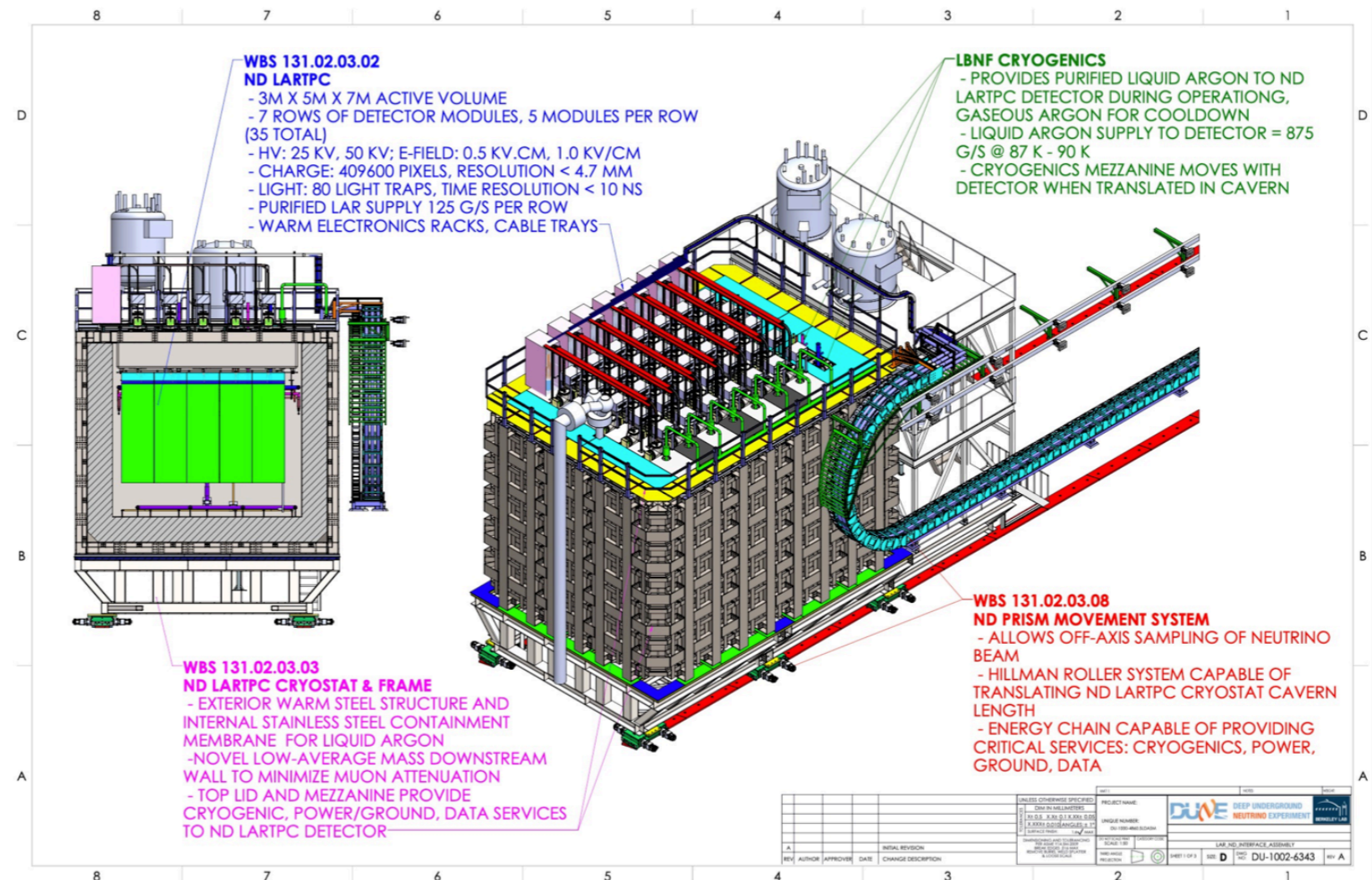
Perforated PCB (ProtoDUNE-DP)

The deep underground neutrino experiment

ND-LAr

<https://doi.org/10.3390/instruments5040031>

- Modular design: 35 modules of 1 x 1 x 3 m³ with two TPCs per module
- Dimensions are optimized to fully contain hadronic showers
- E-Drift 500V/cm, HV @ -30 kV
- Pixelated charge readout with unambiguous 3D imaging capabilities
- Optically isolated TPCs with ns scale Light readout time resolution



The deep underground neutrino experiment

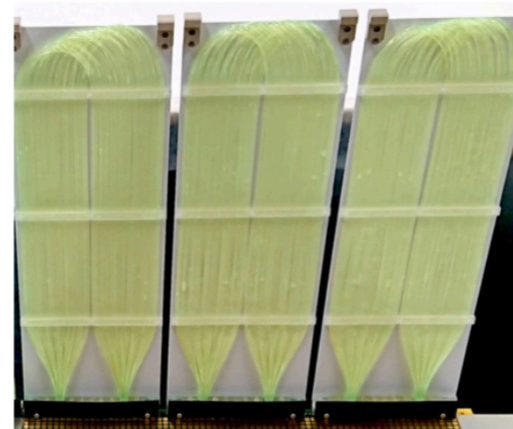
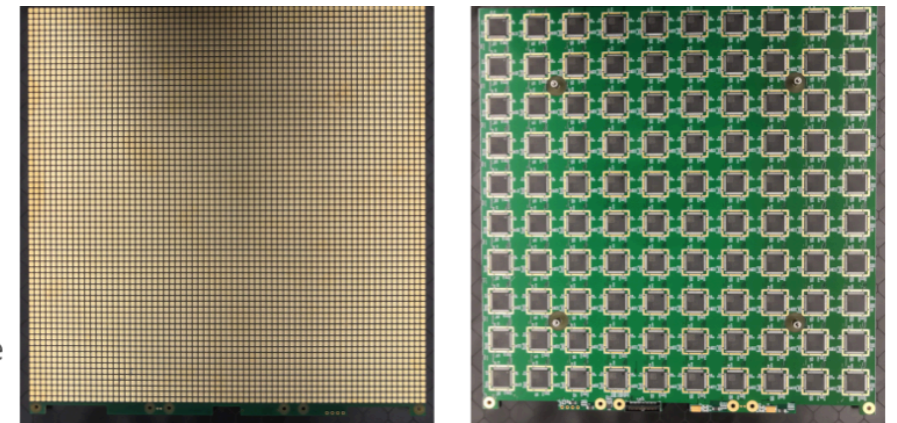
ND-LAr detector systems

Novel technologies developed to realize a modular design of LAr-TPC

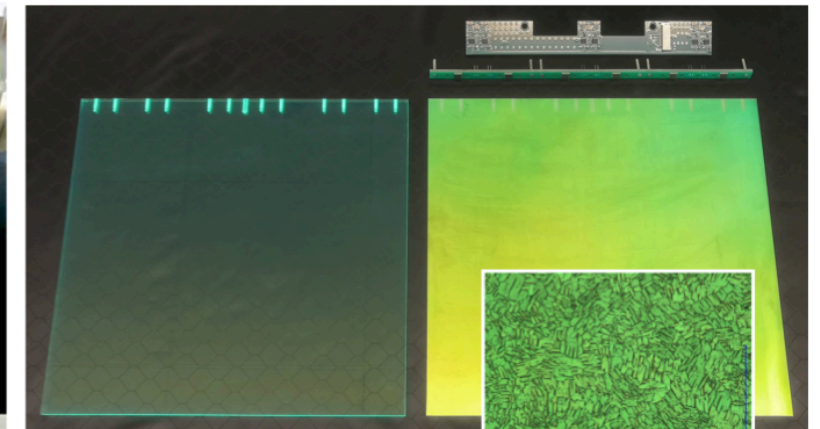
- Pixelated charge readout with LArPix chip
- Two complementary light collection modules + SiPM readout
 - ArCLight: WLS plastic + dichroic mirror + TPB
 - LCM: Bundle of WLS fibers painted with TPB
- Field structure with resistive shell (Kapton and DR8)

Challenge: Minimize dead volume between adjacent modules and allows back-to-back modules configuration

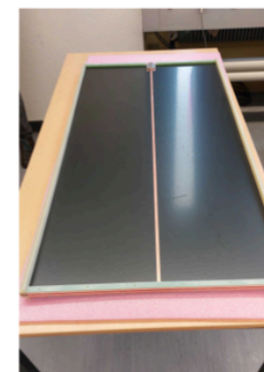
Pixelated anode tile
Front and back



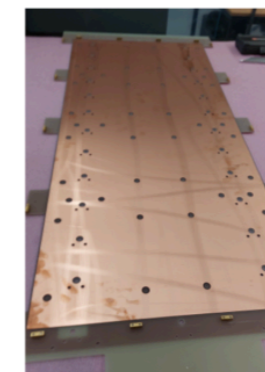
LCM



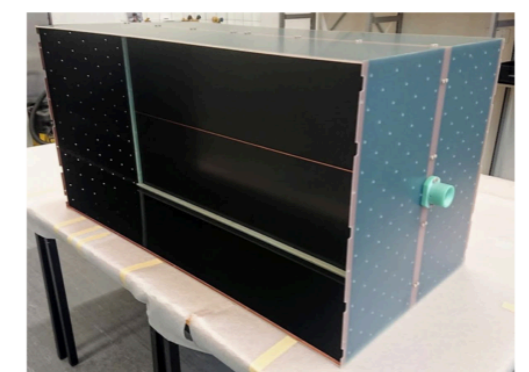
ArCLight



Cathode panel laminated



Anode panel supports

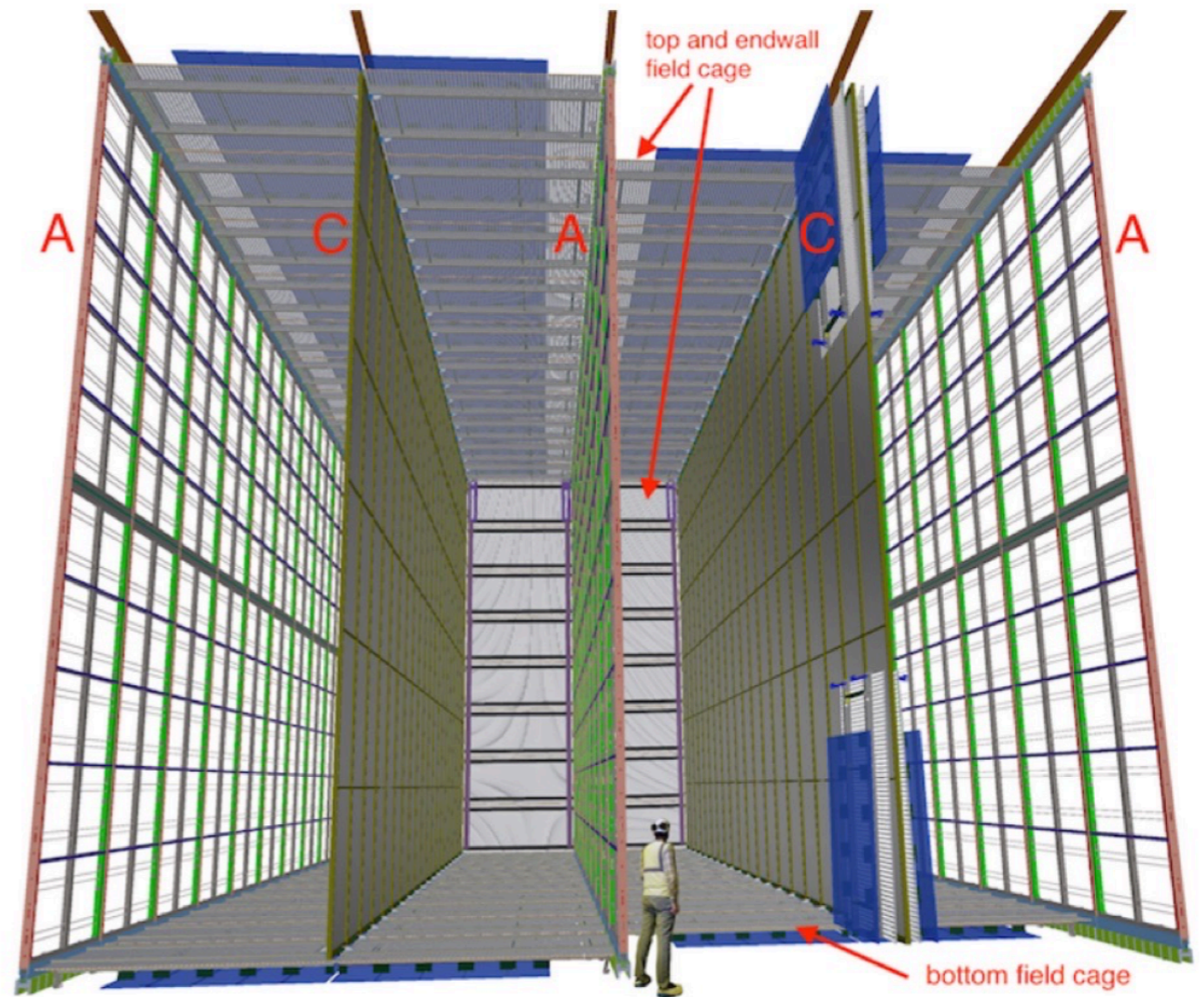


Filed shaping panels

The deep underground neutrino experiment

Far Detector #1 (Horizontal drift)

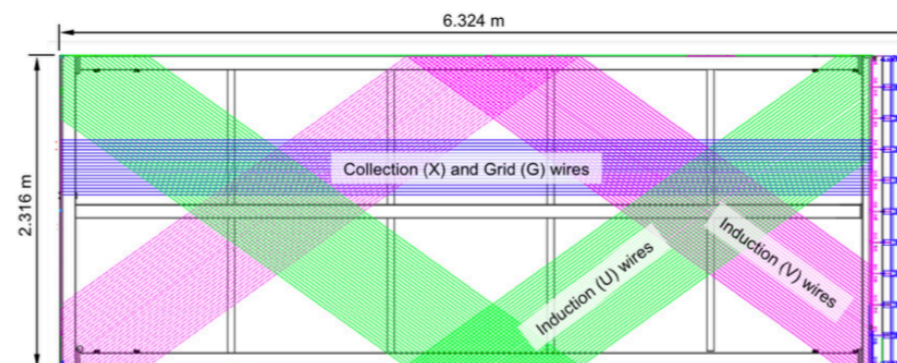
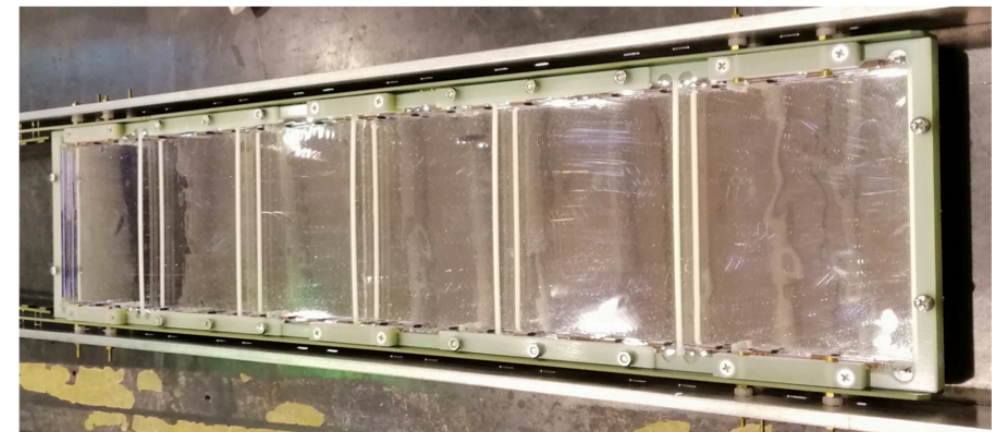
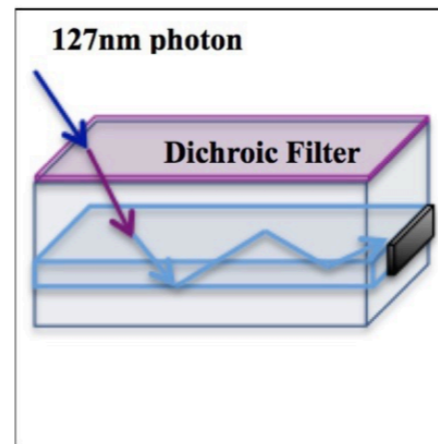
- Alternating Anode and Cathode planes
- Cathode Plane Assembly (CPA):
 - HV @ -180 kV for E-drift 500 V/cm with drift length of 3.6 m
 - High resistivity CPA for fast discharge prevention
- Anode Plane Assembly (APA):
 - 150 panels in total
- Photon Detectors: X-ARAPUCA light traps
 - 10 units per APA, located behind the wires
 - Provides timing and trigger



The deep underground neutrino experiment

Far Detector #1 (Horizontal drift)

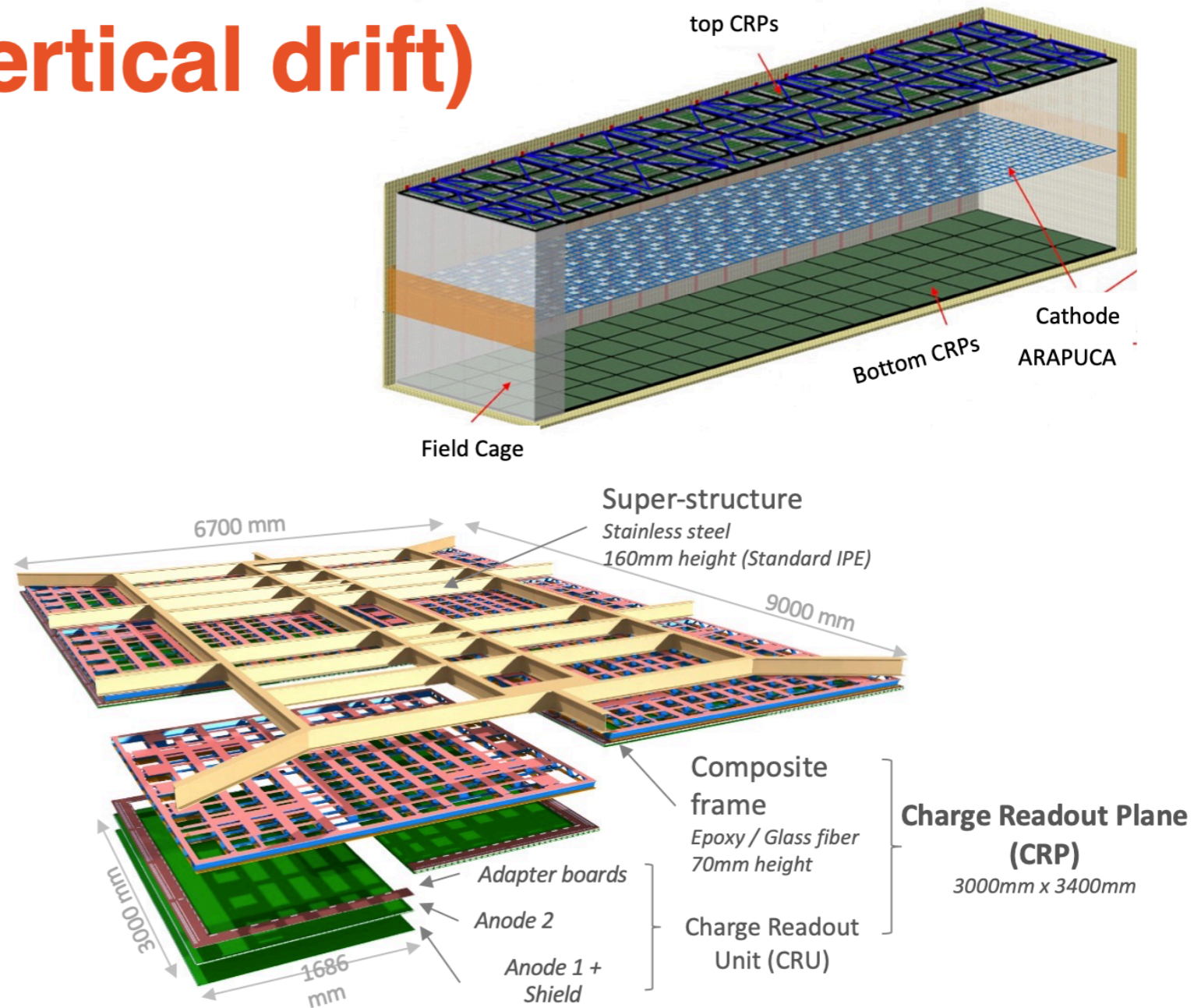
- X_ARAPUCA Light trap
 - Wavelength shifting + Dichroic filter + SiPM readout
- Anode plane Assembly (APA) unit
 - 4 wire planes (Grid, 2x induction, Collection)
 - 2560 wires per unit
 - Wire tension 5 N
 - Wire pitch 4.67 - 4.79 mm



The deep underground neutrino experiment

Far Detector #2 (Vertical drift)

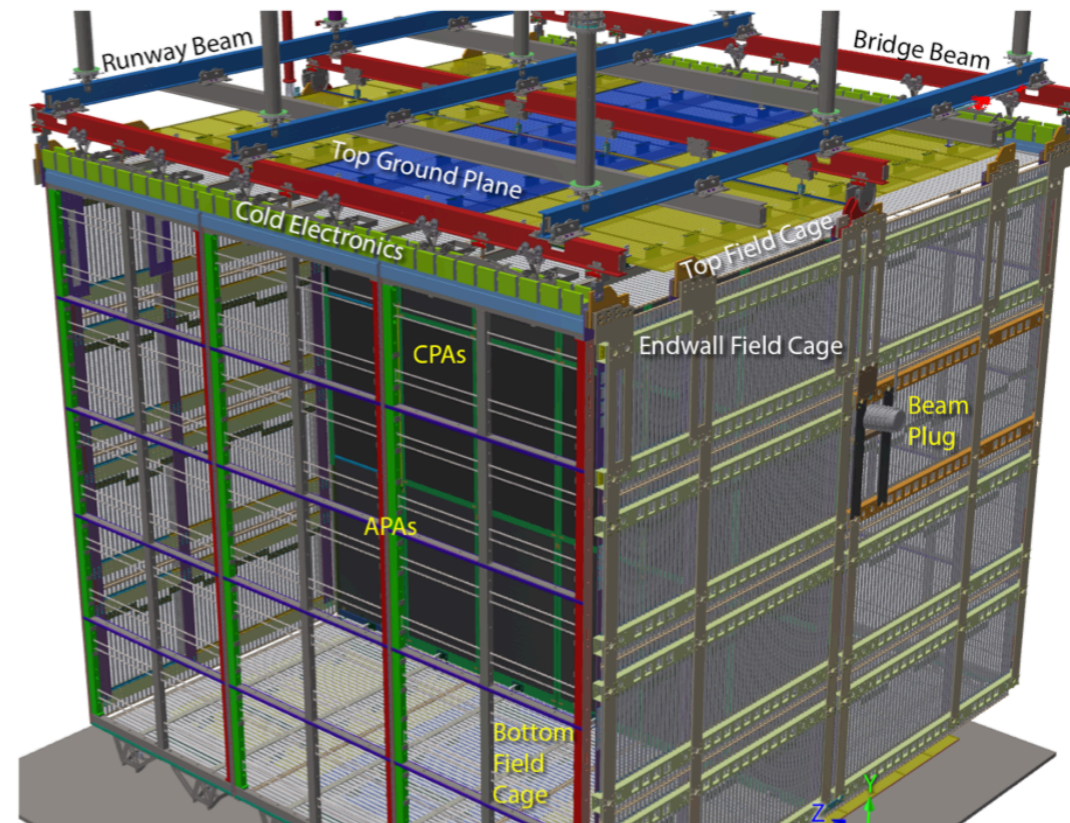
- Central Horizontal Cathode with readout on cryostat top and bottom
- HV: -300 kV, 6 m drift
- Photon Detectors: based on X-ARAPUCA light traps
 - 320 units on Cathode, analog readout (Power/Signal-over-Fiber)
 - 320 units on cryostat membrane behind field cage (70% transparency)
- Perforated PCB anode, fully immersed in LAr
- Promising first data from a 50L test setup @ CERN
 - Two 35 cm x 35 cm PCBs + shield



The deep underground neutrino experiment

ProtoDUNE_s

- Two ~1 ktons prototypes @ CERN
 - Inner dimensions ~ 6 m x 7 m x 7 m
- ProtoDUNE Single Phase (HD)
 - 2-month beam run in 2018 + cosmics
- ProtoDUNE-Dual Phase
 - Very High Voltage, large drift studies
 - Evolved into single phase Vertical Drift FD #2

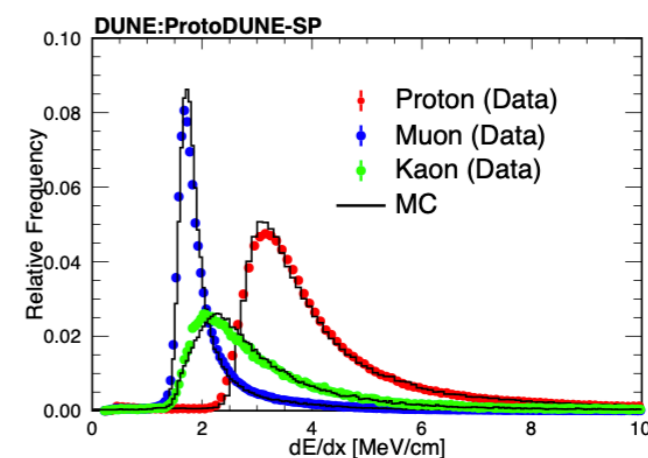
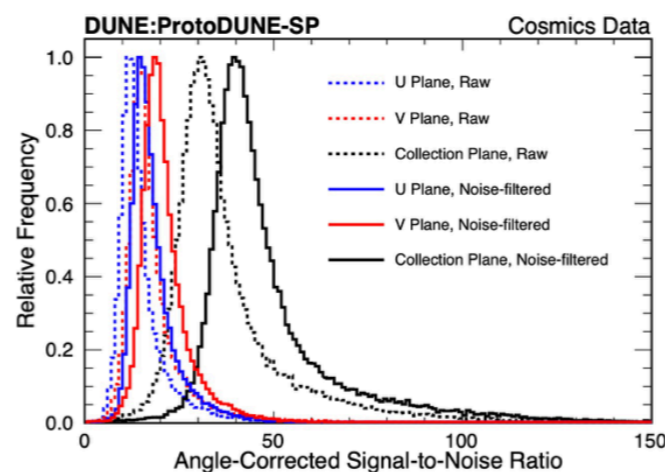
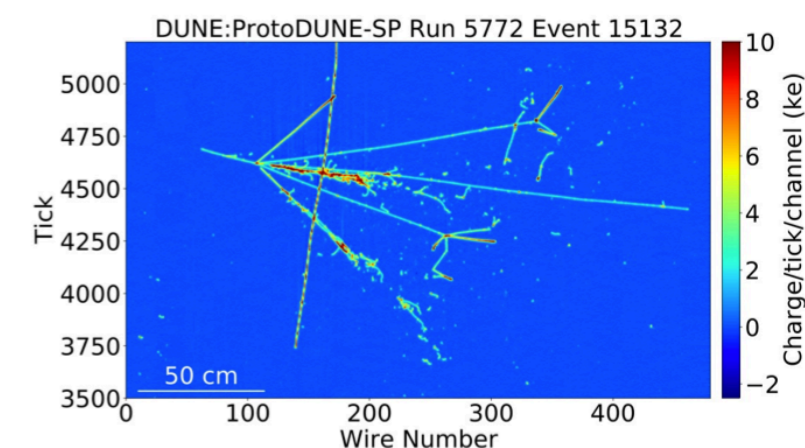
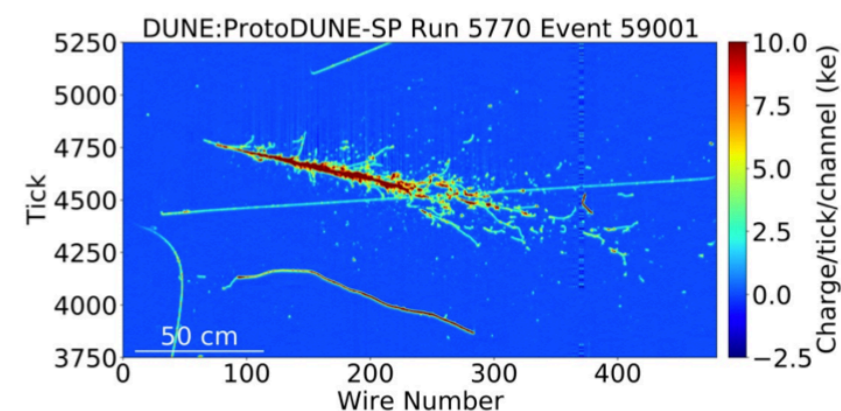


The deep underground neutrino experiment

ProtoDUNE-SP Performance

- ProtoDUNE-SP accumulated 4M events in the beam test at CERN.
 - Different momentum settings: 0.3, 0.5, 1, 2, 3, 6, 7 GeV/c.
 - Various beam particle species: e^+ , μ^+ , π^+ , K^+ , p
- Analysis work ongoing to measure hadron-argon cross sections over the full range 0.3 – 7 GeV/c.
- Study of detector response and measurement of the liquid argon properties with exquisite resolution

[JINST 15 P12004](#)



Summary

- Noble liquids: excellent properties for building large, homogeneous astroparticle physics detectors with ultra-low backgrounds at their cores (argon and xenon are predominantly employed in underground physics detectors)
- High light and charge yields, excellent energy and 3D position resolutions (in particular in detectors operated in TPC mode) allow for detectors with low-energy thresholds, good linearity and high-sensitivity searches for many beyond standard model physics channels (only dark matter and neutrino physics mentioned in this lecture)
- The fundamental properties of condensed noble gases for radiation detection have been studied for many decades, yet there is much room for improvement and new small-scale experiments
- To paraphrase the authors of the "Noble gas detectors" book (Aprile, Bolotnikov, Bolozdynya, Doke): I believe that the best pages of the history of noble liquid detectors in underground physics are yet to be written ;-)